TECHNICAL REPORT

ISO/TR 19222

First edition
2021-12

Road vehicles — Injury risk curves for the THOR dummy

Véhicules routiers — Courbe de risques de blessures pour mannequin THOR

Reference number
ISO/TR 19222:2021(E)

ISO copyright office
CP 401 • Ch. de Blandonnet 8
CH-1214 Vernier, Geneva
Phone: +41 22 749 01 11
Email: copyright@iso.org
Website: www.iso.org

Published in Switzerland

Contents

Page

Foreword

ISO (the International Organization for Standardization) is a worldwide federation of national standards bodies (ISO member bodies). The work of preparing International Standards is normally carried out through ISO technical committees. Each member body interested in a subject for which a technical committee has been established has the right to be represented on that committee. International organizations, governmental and non-governmental, in liaison with ISO, also take part in the work. ISO collaborates closely with the International Electrotechnical Commission (IEC) on all matters of electrotechnical standardization.

The procedures used to develop this document and those intended for its further maintenance are described in the ISO/IEC Directives, Part 1. In particular, the different approval criteria needed for the different types of ISO documents should be noted. This document was drafted in accordance with the editorial rules of the ISO/IEC Directives, Part 2 (see www.iso.org/directives).

Attention is drawn to the possibility that some of the elements of this document may be the subject of patent rights. ISO shall not be held responsible for identifying any or all such patent rights. Details of any patent rights identified during the development of the document will be in the Introduction and/or on the ISO list of patent declarations received (see www.iso.org/patents).

Any trade name used in this document is information given for the convenience of users and does not constitute an endorsement.

For an explanation of the voluntary nature of standards, the meaning of ISO specific terms and expressions related to conformity assessment, as well as information about ISO's adherence to the World Trade Organization (WTO) principles in the Technical Barriers to Trade (TBT), see www.iso.org/iso/foreword.html.

This document was prepared by Technical Committee ISO/TC 22, *Road vehicles*, Subcommittee SC 36, *Safety aspects and impact testing*.

Any feedback or questions on this document should be directed to the user's national standards body. A complete listing of these bodies can be found at www.iso.org/members.html.

Introduction

The THOR-M 50 dummy is in its final development phase and can be used to evaluate the occupant protection in frontal impact. US-NCAP and Euro-NCAP are currently developing test procedures using this dummy to evaluate car performances. However, injury risk curves (IRCs) are proposed by these organizations without a large consensus. Rules were established to develop IRCs (ISO/TS 18506). These rules were applied to the available data to evaluate IRCs for THOR-M 50. In addition to the quality evaluation as recommended in ISO/TS 18506, considerations on the repeatability and reproducibility of the criteria, as well as their performance with regard to field investigations will be proposed.

Road vehicles — Injury risk curves for the THOR dummy

1 Scope

This document provides injury risk curves to assess occupant protection in frontal impact using the 50th percentile THOR metric dummy (THOR-M 50).

Injury risk curves developed specifically for the THOR dummy are chosen preferably, however, when not available, the applicability of the PMHS injury risk curve is evaluated with regard to the dummy biofidelity.

Finally, when possible, a field evaluation is provided.

2 Normative references

There are no normative references in this document.

3 Terms and definitions and abbreviated terms

For the purposes of this document, the following terms and definitions apply.

ISO and IEC maintain terminology databases for use in standardization at the following addresses:

— ISO Online browsing platform: available at https://www.iso.org/obp

— IEC Electropedia: available at https://www.electropedia.org/

3.1 Terms and definitions

3.1.1
THOR-M 50
50th percentile metric dummy as defined in Reference [61]

3.1.2
injury criterion
physical parameter which correlates well with the severity of a specific injury or injuries of a body region under consideration

3.1.3
injury risk curve
IRC
curve giving the probability, for a defined population and for a given input, to sustain a specified severity of injury

3.1.4
injury risk function
IRF
mathematical function that relates a value of an *injury criterion* (3.1.2) and possible additional factors (variables) to a risk of sustaining an injury of a certain level

3.2 Abbreviated terms

AIS abbreviate injury score

BrIC	brain injury criterion
CI	confidence interval
CIBIC	convolution of impulse response for brain injury criterion
HIC	head injury criterion
KTH	knee-thigh-hip
MAIS	maximum abbreviate injury score
NFR	number of fractured ribs
NHP	non-human primate
NSFR	number of separated fractured ribs
PC-Score	principal component analysis score
PDB	partnership for dummy and biomechanics
PMHS	post mortem human subject
RVCI	rotational velocity change index
TBI	traumatic brain injury
THUMS	Toyota human body model
TIC	thoracic injury criterion
UBrIC	updated brain injury criterion

4 Methodology

The following steps were performed for each criterion:

— existing injury risk curves were collected;

— reference data were collected and verified;

— ISO/TS 18506 was applied;

— criteria quotation was calculated:

  — ISO/TS 18506 rules: from 1 for full application to 0 for a different method leading to different results, except if a rationale if provided;

  — ISO/TS 18506 quality index: relative size of the confidence interval for 5 %, 25 % and 50 % risks of injury. The relative size of the confidence interval is defined as the width of the 95 % confidence interval at a given injury risk, relative to the value of the stimulus at this same injury risk;

  — evaluation of the repeatability and reproducibility (R&R) of the THOR-M 50 for the considered criterion, when R&R data are available, this criterion is equal to 1-(standard deviation/mean):

    — R&R data in certification tests are provided in Annex H;

- R&R data in sled tests are provided in Annex I for the thorax;

- THOR applicability: this criterion has the following values:
  - THOR specific criterion: from 1 for full application to 0 for a different method leading to different results, except if a rationale is provided;
  - human IRC: biofidelity score;
  - transfer function between THOR and human: coefficient of correlation;
  - unknown: when the biofidelity score or the correlation coefficient are unknown;
- field data evaluation.

NHTSA is issuing a document on Injury Risk Curves for the THOR dummy (Reference [7]). This document was developed independently. Therefore, the readers can make their own comparisons and conclusions.

5 Injury risk curves

5.1 Head

5.1.1 HIC

5.1.1.1 HIC 15 ms / skull fracture – Mertz

- Injury target: skull fracture
- Source: ISO/TR 7861, Reference [51]
- Channels: linear accelerations (a_x, a_y, a_z) measured at the head centre of gravity
- Filtration: CFC1000
- Formula: $H_{15} = \max_{15}\left\{(t_2 - t_1)\left[\frac{1}{t_2 - t_1}\int_{t_1}^{t_2} a(t).\mathrm{d}t\right]^{2,5}\right\}$

where

H_{15} is the variable for the head injury criterion (HIC);

t_1 is the beginning of the time window;

t_2 is the end of the time window;

a is the resultant acceleration expressed in g;

t is the time expressed in milliseconds;

d is the derivative function;

$\max_{15}$ is the maximum of the function calculated between t_1 and t_2, with (t_2-t_1) not exceeding 15 ms.

- $P_{\text{skull\_fracture}} = \Phi(H_{15}; \mu = 1\ 500; \sigma = 488)$

where

$P_{skull\_fracture}$ is the injury probability for a skull fracture;

Φ is the cumulative distribution function of the normal distribution;

H_{15} Is the variable for the head injury criterion (HIC);

μ is the mean of the normal distribution;

σ is the standard deviation of the normal distribution.

— Data: 65 PMHS (References [20], [21], [82], [24], [25], [59]) provided in Table A.1 of Annex A

— Statistics: modified median rank method (Reference [50])

— Version of dummy: injury risk curve developed directly from PMHS data and is applicable to dummies with a biofidelic response to head impact response.

— Comments:

  — This curve is a human injury risk curve.

  — THOR biofidelity: in the corridors of head drop tests (Table 14 and Figure 4 in Reference [61]).

  — Reasons for not following ISO/TS 18506 rules: the modified median rank method has a better quality assessment than Eppinger's curve. Reference [51] points out that Hertz's log-normal curve predicts a 12 % risk of AIS ≥ 2 skull fracture at HIC=400, when no cases of skull fracture were observed at or below this value. This compares to 1 % risk predicted by Mertz's curve.

— Curves

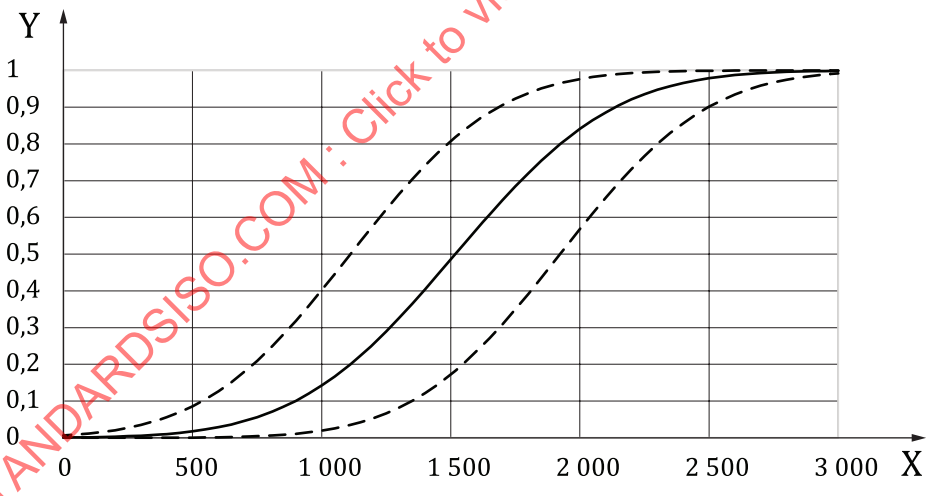

Key

X HIC

Y risk of skull fracture

——— IRF (skull fracture)

- - - - confidence interval

Figure 1 — Injury risk curves for Skull fracture as a function of HIC

— Quotation

  — ISO/TS 18506 rules: 0,5

- Quality assessment
  - CI at 5 % = 1,12 (marginal)
  - CI at 25 % = 0,68 (fair)
  - CI at 50 % = 0,54 (fair)

  NOTE The quality assessment at low levels of risk is relevant when assessing today's occupant restraint systems.
- R&R: 95 %
- THOR applicability: 1

5.1.1.2 HIC 15ms/skull fracture – Eppinger

- Injury target: skull fracture
- Source: Reference [12], Reference [23]
- Channels: linear accelerations (a_x, a_y, a_z) measured at the head centre of gravity
- Filtration: CFC1000
- Formula: $H_{15} = \max_{15}\left\{(t_2 - t_1)\left[\frac{1}{t_2 - t_1}\int_{t1}^{t2} a(t).\mathrm{d}t\right]^{2,5}\right\}$

where

H_{15} is the variable for the head injury criterion (HIC);

t_1 is the beginning of the time window;

t_2 is the end of the time window;

a is the resultant acceleration expressed in g;

d is the derivative function;

t is the time expressed in milliseconds;

$\max_{15}$ is the maximum of the function calculated between t_1 and t_2, with (t_2-t_1) not exceeding 15 ms.

- $P_{\text{skull\_fracture}} = \Phi(\ln(H_{15}); \mu = 6,96; \sigma = 0,847)$

where

$P_{\text{skull\_fracture}}$ is the injury probability for a skull fracture;

Φ is the cumulative distribution function of the normal distribution;

H_{15} is the variable for the head injury criterion (HIC);

μ is the mean of the normal distribution;

σ is the standard deviation of the normal distribution.

- Data: 54 PMHS (References [20], [21], [82], [24] and [25]) provided in Table A.2 of Annex A
- Statistics: maximum likelihood of log-normal

— Version of dummy: injury risk curve developed directly from PMHS data and is applicable to dummies with a biofidelic response to head impact response.

— Comments:

  — Human injury risk curve

  — THOR biofidelity: in the corridors of head drop tests (Table 14 and Figure 4 in Reference [61])

  — Risk curve close to the survival (log-normal) curve used in ISO/TS 18506

— Curves

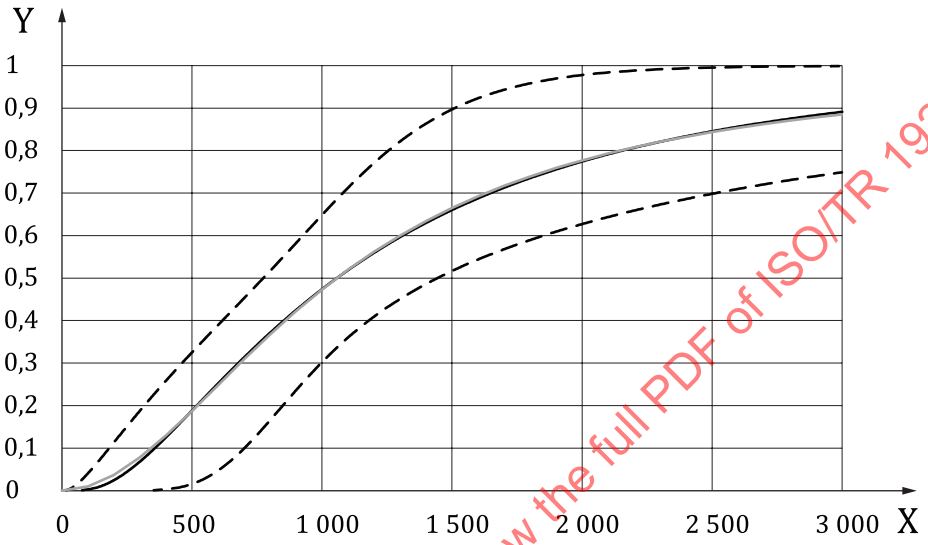

Key

X HIC
Y risk of skull fracture
——— IRF (skull fracture)
- - - - CI (skull fracture)
——— IRF (maximum likelihood of log-normal)

Figure 2 — Injury risk curves for Skull fracture as a function of HIC

— Quotation

  — ISO/TS 18506 rules: 1

  — Quality assessment

    — CI at 5 % = 1,88 (unacceptable)

    — CI at 25 % = 0,89 (fair)

    — CI at 50 % = 0,63 (fair)

  — R&R: 95 %

  — THOR applicability: 1

5.1.2 Rotational criterion

Numerous brain injury metrics have been proposed to predict diffuse-type traumatic brain injuries (TBIs) with the use of rotational response of head kinematics. Diffuse-type TBIs are hypothesized

to be caused by shear deformation of the brain tissue due to a rapid rotational motion of the head (Reference [26]). According to the hypothesis, the following five kinematics-based brain injury metrics derived from rotational head kinematic variables, BrIC (Reference [81]), CIBIC (Reference [80]), DAMAGE (Reference [18]), RVCI (Reference [91]), UBrIC (Reference [16]), were selected based on correlations with brain tissue strain response, as detailed in B.1.5.

As measurement channels for calculation of the kinematic-based brain injury metrics, angular velocities are obtained with gyro sensors fixed at the head centre of gravity of THOR. Angular velocities are filtered to channel frequency class (CFC) 60, and angular accelerations are obtained by differentiating the filtered angular velocity data.

Using survival analysis with Weibull distribution, injury risk curves (IRCs) for AIS 2 and AIS 4 traumatic brain injuries (TBIs), as given in Figure 3 to Figure 7, are formulated as the following function of the five kinematics-based brain injury metrics, DAMAGE, UBrIC, CIBIC, BrIC and RVCI, respectively.

$$P = 1 - e^{\left(-e^{\left(\frac{1}{b}\times\ln(dy+c)-\frac{a}{b}\right)}\right)}$$

Where a and b are coefficients corresponding to the shape ($1/b$) and scale (e^a) parameters in the Weibull distribution and y is the kinematics-based brain injury metric. The coefficients and quality indexes are provided in Table 1. P is the injury probability.

All IRCs given in this document for the THOR 50th percentile male were newly developed and are detailed in Annex B. Using survival analysis with Weibull distribution, original IRCs for AIS 2+ and AIS 4+ TBIs were developed based on the 95th percentile peak maximum principle strain of brain deformation (MPS95) in the finite element (FE) reconstruction simulations of human and Non-Human Primate (NHP) experiment data. The IRCs based on MPS95 were transferred to IRCs based on the kinematics-based brain injury metrics according to linear correlations between MPS95 and the kinematics-based brain injury metrics.

Table 1 — Coefficients and quality of the injury risk curves

Injury	Metrics	Scale (e^a)	Shape ($1/b$)	Intercept (c)	Slope (d)	5 % Risk (QI)	25 % Risk (QI)	50 % Risk (QI)
AIS2	DAMAGE	0,459	3,875	0,017	0,957	0,205 (0,41)	0,330 (0,25)	0,418 (0,25)
	UBrIC			-0,014	1,054	0,215 (0,36)	0,329 (0,22)	0,409 (0,23)
	CIBIC			0,016	0,505	0,390 (0,41)	0,627 (0,25)	0,794 (0,25)
	BrIC[a]			-0,103	0,600	0,527 (0,26)	0,726 (0,18)	0,867 (0,19)
	RVCI			0,012	0,012	16,75 (0,40)	26,70 (0,24)	33,76 (0,24)
AIS4	DAMAGE	0,646	6,051	0,017	0,957	0,395 (0,45)	0,531 (0,27)	0,617 (0,23)
	UBrIC			-0,014	1,054	0,388 (0,42)	0,512 (0,25)	0,590 (0,22)
	CIBIC			0,016	0,505	0,751 (0,45)	1,009 (0,27)	1,172 (0,23)
	BrIC[a]			-0,103	0,600	0,830 (0,35)	1,048 (0,22)	1,185 (0,19)

QI: Quality index and its categories based on (Reference [64]), the quality of injury risk functions can be categorized into 'good' (0,0 – 0,5); 'fair' (0,5 – 1,0); 'marginal' (1,0 – 1,5); and 'unacceptable' (> 1,5).

[a] BrIC: caution should be used with the IRCs for BrIC presented here from the original injury risk curves provided in Reference [81].

Table 1 *(continued)*

Injury	Metrics	Scale (e^a)	Shape ($1/b$)	Intercept (c)	Slope (d)	5 % Risk (QI)	25 % Risk (QI)	50 % Risk (QI)
	RVCI			0,012	0,012	31,93 (0,45)	42,79 (0,27)	49,64 (0,23)

QI: Quality index and its categories based on (Reference [64]), the quality of injury risk functions can be categorized into 'good' (0,0 – 0,5); 'fair' (0,5 – 1,0); 'marginal' (1,0 – 1,5); and 'unacceptable' (> 1,5).

[a] BrIC: caution should be used with the IRCs for BrIC presented here from the original injury risk curves provided in Reference [81].

5.1.2.1 DAMAGE

$$\begin{bmatrix} m_x & 0 & 0 \\ 0 & m_y & 0 \\ 0 & 0 & m_z \end{bmatrix} \begin{Bmatrix} \ddot{\delta}_x \\ \ddot{\delta}_y \\ \ddot{\delta}_z \end{Bmatrix} + \begin{bmatrix} c_{xx}+c_{xy}+c_{xz} & -c_{xy} & -c_{xz} \\ -c_{xy} & c_{xy}+c_{yy}+c_{yz} & -c_{yz} \\ -c_{xz} & -c_{yz} & c_{xz}+c_{yz}+c_{zz} \end{bmatrix} \begin{Bmatrix} \dot{\delta}_x \\ \dot{\delta}_y \\ \dot{\delta}_z \end{Bmatrix}$$

$$+ \begin{bmatrix} k_{xx}+k_{xy}+k_{xz} & -k_{xy} & -k_{xz} \\ -k_{xy} & k_{xy}+k_{yy}+k_{yz} & -k_{yz} \\ -k_{xz} & -k_{yz} & k_{xz}+k_{yz}+k_{zz} \end{bmatrix} \begin{Bmatrix} \delta_x \\ \delta_y \\ \delta_z \end{Bmatrix} = \begin{bmatrix} m_x & 0 & 0 \\ 0 & m_y & 0 \\ 0 & 0 & m_z \end{bmatrix} \begin{Bmatrix} \ddot{u}_x \\ \ddot{u}_y \\ \ddot{u}_z \end{Bmatrix}$$

— Formula: $B_{\mathrm{DAMAGE}} = \beta \times t_{\max}\left\{\left|\vec{\delta}(t)\right|\right\}$

where

$\vec{\delta}(t) = \left[\delta_x(t) \quad \delta_y(t) \quad \delta_z(t)\right]^T$

β is the scale factor;

m is the mass expressed in kg;

c_{ij} is the damping expressed in Ns/m;

k_{ij} is the stiffness expressed in N/m;

$\ddot{\delta}, \dot{\delta}, \delta$ are the acceleration, velocity and displacement respectively;

$\ddot{u}$ is the applied angular acceleration;

and the following variables have the following values:

$m_x = 1$; $m_y = 1$; $m_z = 1$;

$k_{xx} = 32\,142$; $k_{yy} = 23\,493$; $k_{zz} = 16\,935$;

$k_{xy} = 0$; $k_{yz} = 0$; $k_{xz} = 1\,636{,}3$;

$\lambda = 5{,}914\,8$; $\beta = 2{,}990\,31$;

$[c] = \lambda \times [k]$

— Curves

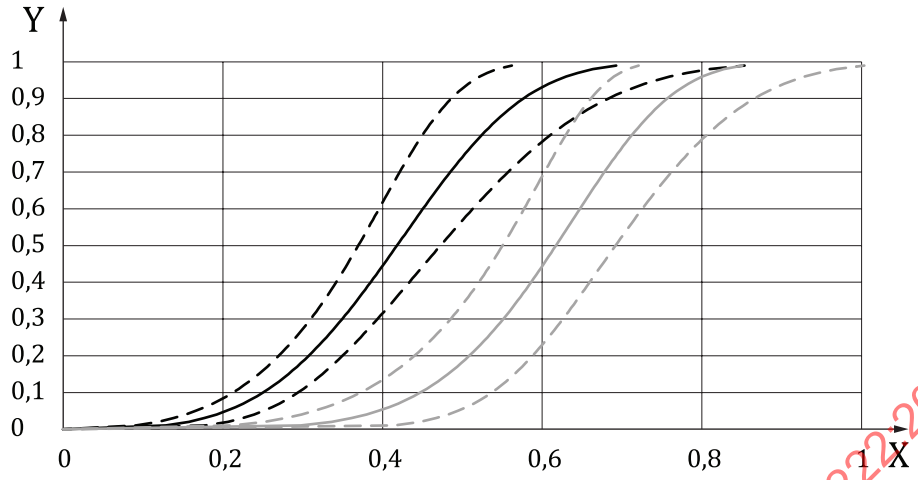

Key

X	DAMAGE
Y	risk of injury
———	IRF (AIS2)
- - - -	CI (AIS2)
———	IRF (AIS4)
- - - -	CI (AIS4)

Figure 3 — Injury risk curves for AIS 2 and AIS 4 as a function of DAMAGE

— Quotation

  — ISO/TS 18506 rules: 1

  — R&R: 97 % (mean of head angular rates in flexion, extension, lateral flexion and torsion neck tests)

  — THOR applicability: unknown

5.1.2.2 UBrIC

— Formula: $B_{\mathrm{UBrIC}} = \left\{ \sum_i \left[\omega_i^* + \left(\alpha_i^* - \omega_i^* \right) e^{-\frac{\alpha_i^*}{\omega_i^*}} \right]^2 \right\}^{\frac{1}{2}}$

where

B_{UBrIC} is the variable for the brain injury criterion UBrIC;

ω_i^* and α_i^* ($i = x, y, z$) are directionally dependent maximum magnitudes of the head angular velocity and angular acceleration which are each normalized by a critical value (*cr*); $\omega_i^* = \omega_i / \omega_{\mathrm{icr}}$ and $\alpha_i^* = \alpha_i / \alpha_{\mathrm{icr}}$. ω_i^* are expressed in rad/s and α_i^* are expressed in rad/s^2:

$$\omega_{\mathrm{xcr}} = 211;\ \alpha_{\mathrm{xcr}} = 20{,}0 \times 10^3;$$

$$\omega_{\mathrm{ycr}} = 171;\ \alpha_{\mathrm{ycr}} = 10{,}3 \times 10^3;$$

$\omega_{zcr} = 115;\ \alpha_{zcr} = 7{,}76 \times 10^3$.

— Curves

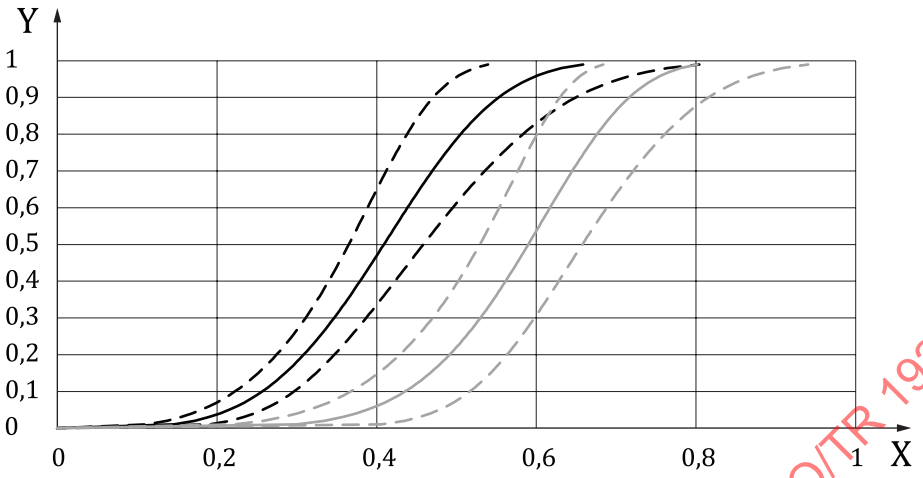

Key

X UBrIC
Y risk of injury
IRF (AIS2)
CI (AIS2)
IRF (AIS4)
CI (AIS4)

Figure 4 — Injury risk curves for AIS 2 and AIS 4 as a function of UBrIC

— Quotation

  — ISO/TS 18506 rules: 1

  — R&R: 97 % (mean of head angular rates in flexion, extension, lateral flexion and torsion neck tests)

  — THOR applicability: unknown

5.1.2.3 CIBIC

— Formula: $B_{CIBIC} = \max\left\{\sqrt{\sum_{i=1}^{3}\left\{\beta_i \int_0^t x_i(t-\tau)\alpha_i(\tau)\,\mathrm{d}\tau\right\}^2}\right\}$

where

B_{CIBIC} is the variable for the brain injury criterion CIBIC;

i=1, 2, 3 are x, y and z axes;

α_i is an angular acceleration;

d is the derivative function;

$x_i(t) = E_{1i}e^{-A_{1i}t} - e^{-A_{2i}t}\{E_{1i}\cos(B_i t) + E_{2i}\sin(B_i t)\}$

$A_{1i} = -s_i$, s_i: real root of $s_i^3 + \frac{k_{2i}}{c_i} s_i^2 + \frac{k_{1i} + k_{2i}}{m} s_i + \frac{k_{1i} k_{2i}}{c_i m} = 0$;

$$A_{2i} = \frac{k_{2i} / c_i - A_{1i}}{2};$$

$$B_i = \frac{1}{2} \sqrt{\frac{4(k_{1i} + k_{2i})}{m} - 2A_{1i} \frac{k_{2i}}{c_i} + 3A_{1i}^2 - \frac{k_{2i}^2}{c_i^2}};$$

$$E_{1i} = \frac{A_1 - \frac{k_{2i}}{c_i}}{\left(2A_{1i} \frac{k_{2i}}{c_i} - 3A_{1i}^2 - \frac{(k_{1i} + k_{2i})}{m}\right)};$$

$$E_{2i} = \frac{2A_{1i}^2 - A_{1i} \frac{k_{2i}}{c_i} + A_{1i} A_{2i} - A_{2i} \frac{k_{2i}}{c_i} + \frac{(k_{1i} + k_{2i})}{m}}{\left(2A_{1i} \frac{k_{2i}}{c_i} - 3A_{1i}^2 - \frac{(k_{1i} + k_{2i})}{m}\right) B_i};$$

m is the mass, expressed in kg;

c_i is the damping expressed in Ns/m;

k_i is the stiffness expressed in N/m;

β_i is the scaling factor expressed in 1/m;

$k_{1x} = 12\,760$; $k_{1y} = 16\,390$; $k_{1z} = 17\,040$;

$k_{2x} = 22\,670$; $k_{2y} = 3\,163\,170$; $k_{2z} = 4\,751\,890$;

$c_x = 129{,}1$; $c_y = 120{,}4$; $c_z = 74{,}4$;

$m = 1$;

$\beta_x = 0{,}003\,13$, $\beta_y = 0{,}003\,95$, $\beta_z = 0{,}004\,94$.

— Curves

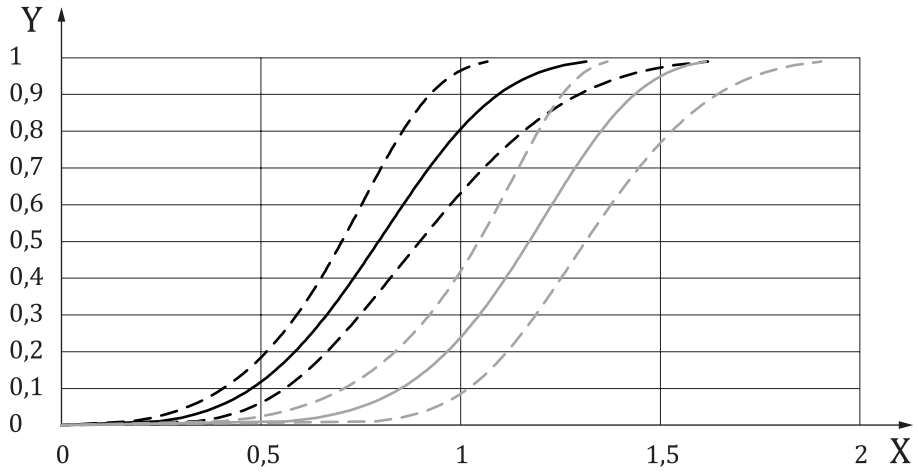

Key

X CIBIC
Y risk of injury
IRF (AIS2)
CI (AIS2)
IRF (AIS4)
CI (AIS4)

Figure 5 — Injury risk curves for AIS 2 and AIS 4 as a function of CIBIC

— Quotation

  — ISO/TS 18506 rules: 1

  — R&R: 97 % (mean of head angular rates in flexion, extension, lateral flexion and torsion neck tests)

  — THOR applicability: unknown

5.1.2.4 BrIC

— Formula: $B_{\mathrm{BrIC}} = \sqrt{\left(\frac{\omega_{\mathrm{x}}}{\omega_{\mathrm{xcr}}}\right)^2 + \left(\frac{\omega_{\mathrm{y}}}{\omega_{\mathrm{ycr}}}\right)^2 + \left(\frac{\omega_{\mathrm{z}}}{\omega_{\mathrm{zcr}}}\right)^2}$

where

B_{BrIC} is the variable for the brain injury criterion BrIC;

$\omega_i \ (i = \mathrm{x,y,z})$ are directionally dependent maximum magnitudes of the head angular expressed in rad/s;

$\omega_{i\mathrm{cr}} \ (i = \mathrm{x,y,z})$ are critical values expressed in rad/s;

$\omega_{\mathrm{xcr}} = 66{,}25$, $\omega_{\mathrm{ycr}} = 56{,}45$, $\omega_{\mathrm{zcr}} = 42{,}87$.

— Curves

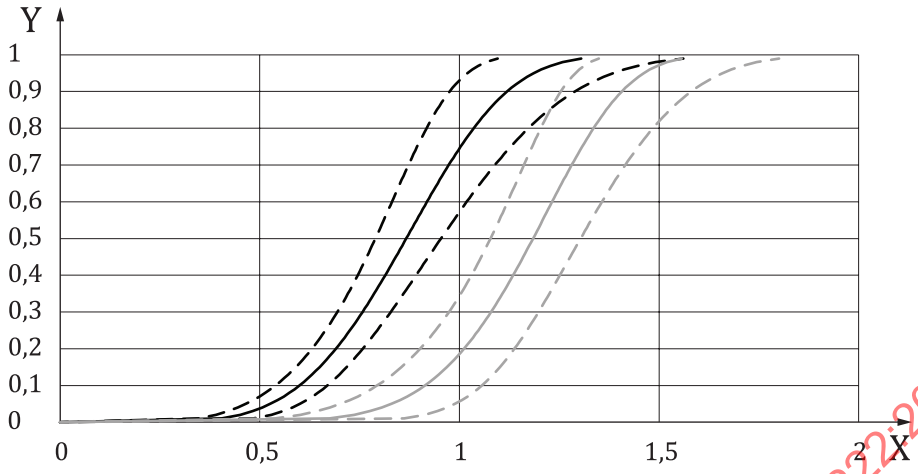

Key

X BrIC
Y risk of injury
IRF (AIS2)
CI (AIS2)
IRF (AIS4)
CI (AIS4)

Figure 6 — Injury risk curves for AIS 2 and AIS 4 as a function of BrIC

— Quotation

  — ISO/TS 18506 rules: 1

  — R&R: 97 % (mean of head angular rates in flexion, extension, lateral flexion and torsion neck tests)

  — THOR applicability: unknown

5.1.2.5 RVCI

— Formula: $B_{\mathrm{RVCI}} = \max(t_1, t_2)\sqrt{W_{\mathrm{x}}\left(\int_{t_1}^{t_2}\alpha_{\mathrm{x}}.\mathrm{d}t\right)^2 + W_{\mathrm{y}}\left(\int_{t_1}^{t_2}\alpha_{\mathrm{y}}.\mathrm{d}t\right)^2 + W_{\mathrm{z}}\left(\int_{t_1}^{t_2}\alpha_{\mathrm{z}}.\mathrm{d}t\right)^2}$

where

B_{RVCI} is the variable for the brain injury criterion RVCI;

W_i are weighting factors about each orthogonal axis;

α_i (i = x, y, z) are directionally dependent maximum magnitudes of the head angular acceleration expressed in rad/s^2;

d is the derivative function;

$W_{\mathrm{x}} = 1{,}00$, $W_{\mathrm{y}} = 1{,}00$, $W_{\mathrm{z}} = 1{,}17$.

— Curves

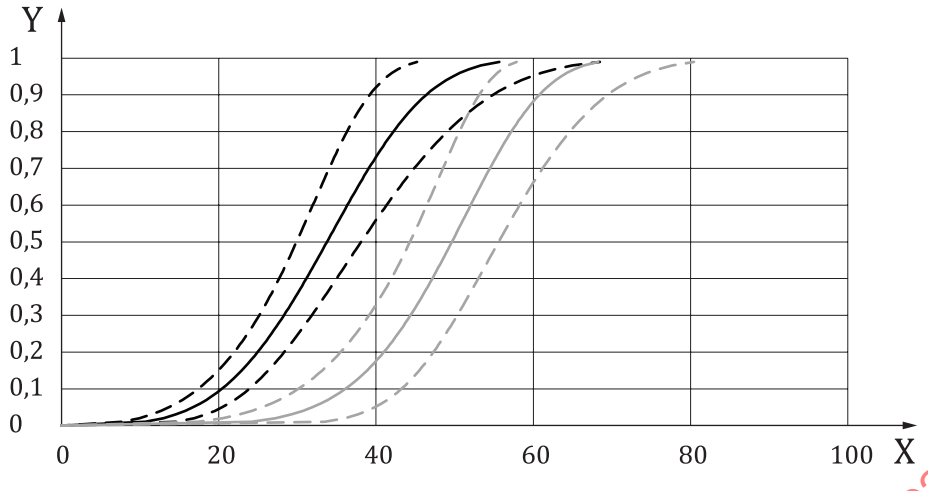

Key

X RVCI
Y risk of injury
IRF (AIS2)
CI (AIS2)
IRF (AIS4)
CI (AIS4)

Figure 7 — Injury risk curves for AIS 2 and AIS 4 as a function of RVCI

— Quotation
  — ISO/TS 18506 rules: 1
  — R&R: 97 % (mean of head angular rates in flexion, extension, lateral flexion and torsion neck tests)
  — THOR applicability: unknown

5.2 Neck

5.2.1 N_{ij} – Eppinger

— Injury target: AIS3+ neck injury
— Source: Reference [12]
— Channels: upper neck force F_z and moment M_y
— Filtration: forces CFC600 ; moments CFC600
— Formula: $N_{ij} = \frac{F_z}{F_{zc}} + \frac{M_y}{M_{yc}}$

where

F_z is the upper neck force in the z direction expressed in N;

M_y is the upper neck moment in the y direction expressed in Nm;

F_{zc} (tension/compression) = 2 520/-3 640 N;

M_{yc} (flexion/extension) = 48/-72 Nm.

— NHTSA Eppinger curve: $P_{AIS \geq 3} = \frac{1}{1+e^{3,227-1,969 N_{ij}}}$

— Survival with Weibull: $P_{AIS \geq 3} = 1 - \exp\left(-\left[\frac{N_{ij}}{1,936\ 4}\right]^{2,142\ 4}\right)$

where

$P_{AIS \geq 3}$ is the injury probability for an AIS3+ neck injury;

N_{ij} is the neck injury criterion.

— Data: 43 piglet tests and associated 3 years old airbag dummy (Reference [52]) provided in Table C.1 of Annex C

— Statistics: logistic for Eppinger curve; survival with Weibull for ISO curve

— Comments:

  — Original curve for 3 years old airbag dummy transferred to HIII M50

  — The THOR intercepts were proposed in Reference [10] and the SAE THOR evaluation task group based on the human tolerance and the THOR biofidelity.

    — PMHS critical values from literature (References [4], [56], [57] and [65]): F_{zc} (tension/compression) = (2 100/-3 030) N; M_{yc} (flexion/extension) = (40/-60) Nm

    — Scale for age (References [31], [44], [56]): factor of 1,2

    — The biofidelity of the THOR was not accounted for and it is assumed that PMHS values are conservative when used for the THOR.

    — Paired sled tests were performed with HIII and THOR head neck complex. The sled acceleration was the same for the two dummies. The results are provided in Annex G. Both in flexion and extension, the N_{ij} were much higher for the THOR compared to the HIII (0,68 versus 0,29 in flexion; 0,55 versus 0,27 in extension). A factor of about 2,2 on the THOR intercepts is needed to get the same risk with the THOR and the HIII in these simple and controlled configurations. However, this comment just intends to demonstrate that the proposed intercepts are not consistent with intercepts on HIII, not to propose alternative intercepts. In addition, for extension tests, THOR exhibited neck compression, while Hybrid III exhibited neck tension, therefore a simple scaling of the intercepts is not adequate.

  — Further investigations are needed, and it is not recommended to use these curves as provided.

— Curves

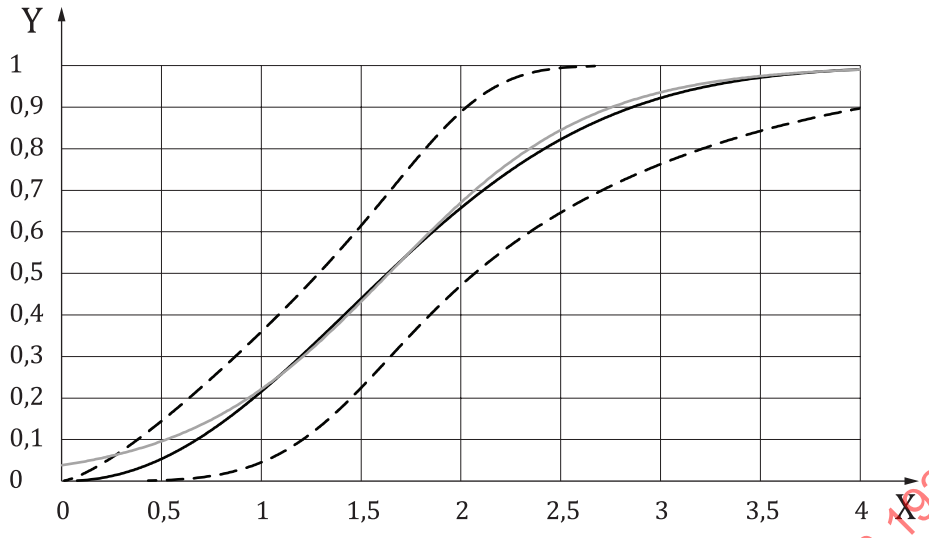

Key

X	N_{ij}
Y	risk of neck AIS3+
———	IRF (survival Weibull)
- - - -	CI (survival Weibull)
———	IRF (Eppinger logistic)

Figure 8 — Injury risk curves for AIS 3+ as a function of N_{ij}

— Quotation

  — ISO/TS 18506 rules: 0,7

  — Quality assessment

    — CI at 5 % = 1,64 (unacceptable)

    — CI at 25 % = 0,73 (fair)

    — CI at 50 % = 0,48 (good)

  — R&R: 96 % (mean of upper neck forces and moments in flexion, extension, lateral flexion and torsion neck calibration tests)

  — THOR applicability: 0

5.2.2 N_{te} – Mertz

— Injury target: AIS3+ neck injury

— Source: Reference [53]

— Channels: Upper neck force F_z and moment M_y

— Filtration: Forces CFC600 ; Moments CFC600

— Formula: $N_{te} = \frac{F_t}{F_{tc}} + \frac{M_e}{M_{ec}}$

where

F_z is the upper neck force in the z direction expressed in N;

M_y is the upper neck moment in the y direction expressed in Nm;

F_t is the portion of F_z when the neck is in tension (positive values);

M_e is the portion of M_y when the neck is in extension (negative values);

F_{tc} (tension) = 6 200 N;

M_{ec} (extension) = -122 Nm.

— $P_{AIS \geq 3} = \varphi(N_{te};\ \mu = 1{,}480;\ \sigma = 0{,}235)$

where

$P_{AIS \geq 3}$ is the injury probability for an AIS3+ neck injury;

Φ is the cumulative distribution function of the normal distribution;

N_{te} is the neck injury criterion;

μ is the mean of the normal distribution;

σ is the standard deviation of the normal distribution.

— Data: 43 piglet tests and associated 3 years old airbag dummy (Reference [53]) provided in Table C.2 of Annex C

— Statistics: Modified median rank method (Reference [50])

— Comments:

  — Original curve for 3 years old airbag dummy transferred to HIII M50

  — The THOR intercepts were proposed by Reference [10] and the SAE THOR evaluation task group based on the human tolerance and the THOR biofidelity.

    — PMHS Critical values from literature (References [4], [56], [57] and [65]): F_{zc} (tension/compression) = (2100/-3030) N; M_{yc} (flexion/extension) = (40/-60) Nm

    — Scale for age (References [31], [44], [56]): factor of 1,2

    — The biofidelity of the THOR was not accounted for and it is assumed that PMHS values are conservative when used for the THOR

    — Paired sled tests were performed with HIII and THOR head neck complex. The sled acceleration was the same for the two dummies. The results are provided in Annex G. Both in flexion and extension, the N_{ij} were much higher for the THOR compared to the HIII (0,68 versus 0,29 in flexion; 0,55 versus 0,27 in extension). A factor of about 2,2 on the THOR intercepts is needed to get the same risk with the THOR and the HIII in these simple and controlled configurations.

  — Further investigations are needed, and it is not recommended to use these curves as provided.

— Curves

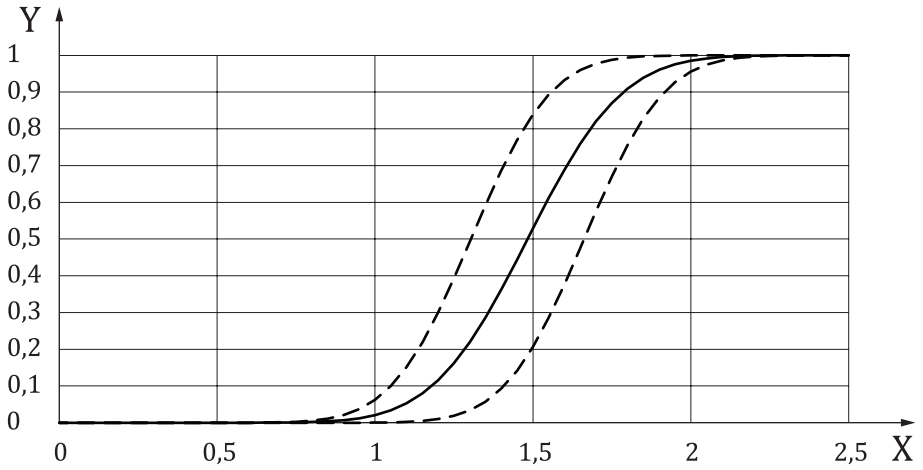

Key

X N_{te}
Y risk of neck AIS3+
——— IRF (Mertz-Weber)
- - - - CI (Mertz-Weber)

Figure 9 — Injury risk curves for AIS 3+ as a function of Nte

— Quotation
  — ISO/TS 18506 rules: 0
  — Quality assessment
    — CI at 5 % = 0,33 (good)
    — CI at 25 % = 0,27 (good)
    — CI at 50 % = 0,24 (good)
  — R&R: 95 % (mean of upper neck forces and moments in extension neck calibration tests)
  — THOR applicability: 0

5.3 Thorax

According to the AIS definition, several rib fractures NFS (Non-Further Specified) correspond to AIS2. The definition of an AIS3 in the thorax corresponds to 3 fractured ribs. Nevertheless, several studies have shown that this definition cannot be applied directly to the PMHS. On the one hand they are more fragile than living subjects of the same age, and on the other hand there is a detection bias. On living subjects, the detection is performed by X-ray, which only detects displaced fractures with a gap between the fractured edges. Non-displaced fractures cannot be detected and are therefore not counted. If a practitioner detects several rib fractures without being able to identify them with X-rays, he will therefore indicate NFS and rate AIS2. On a PMHS, the detection is usually performed by autopsy and all fractures can be detected, whether displaced or not. To take this bias into account, Reference [87] defined AIS3 as 6 fractured ribs, Reference [40] as 7 fractured ribs. More recently, Reference [85] recommended to count only displaced fractured ribs to assess the clinical risk. The following curves are defined for 3 and 7 fractured ribs for deflection, PC-score and TIC_NFR and for 3 separate fractured ribs for TIC_NSFR.

5.3.1 Maximum resultant deflexion

— Injury target: AIS3+ chest injury (3 fractured ribs)

— Source: Reference [66]

— Channels: 4 3D rib deflections (D_{ulx}, D_{uly}, D_{ulz}, D_{urx}, D_{ury}, D_{urz}, D_{llx}, D_{lly}, D_{llz}, D_{lrx}, D_{lry}, D_{lrz})

— Data: 40 PMHS sled— Filtration: CFC180

— Formula:

$$R_{max} = \max(D_{ulmax}, D_{urmax}, D_{llmax}, D_{lrmax})$$

where

$$D_{ulmax} = \max\left(\sqrt{D_{ulx}^2 + D_{uly}^2 + D_{ulz}^2}\right);$$

$$D_{urmax} = \max\left(\sqrt{D_{urx}^2 + D_{ury}^2 + D_{urz}^2}\right);$$

$$D_{llmax} = \max\left(\sqrt{D_{llx}^2 + D_{lly}^2 + D_{llz}^2}\right);$$

$$D_{lrmax} = \max\left(\sqrt{D_{lrx}^2 + D_{lry}^2 + D_{lrz}^2}\right);$$

D_{ijk} is the deflection measured at the *ij* position in the *k* direction and expressed in mm:

i = (u, l) for upper and lower positions;

j = (l, r) for left and right positions;

k = (x, y, z) for the direction.

— $$P_{NFR \geq 3|\dot{A},R_{max}} = 1 - \exp\left(-\left[\frac{R_{max}}{\exp(4,477\ 75 - 0,017\ 1\dot{A})}\right]^{3,356}\right)$$

— $$P_{NFR \geq 7|\dot{A},R_{max}} = 1 - \exp\left(-\left[\frac{R_{max}}{\exp(4,470\ 1 - 0,007\ 6\dot{A})}\right]^{2,547\ 6}\right)$$

where

P is the injury probability;

$\dot{A}$ is the age;

R_{max} is the chest injury criterion.

tests (28 belt only; 7 3-point belt+AB; 2 lap belt+AB; 3 inflatable belt) provided in Table D.1 of Annex D

— Statistics: Survival (Weibull)

— Dummy version: THOR mod-kit 2013

— Comments:

— No impactor tests

— Curves

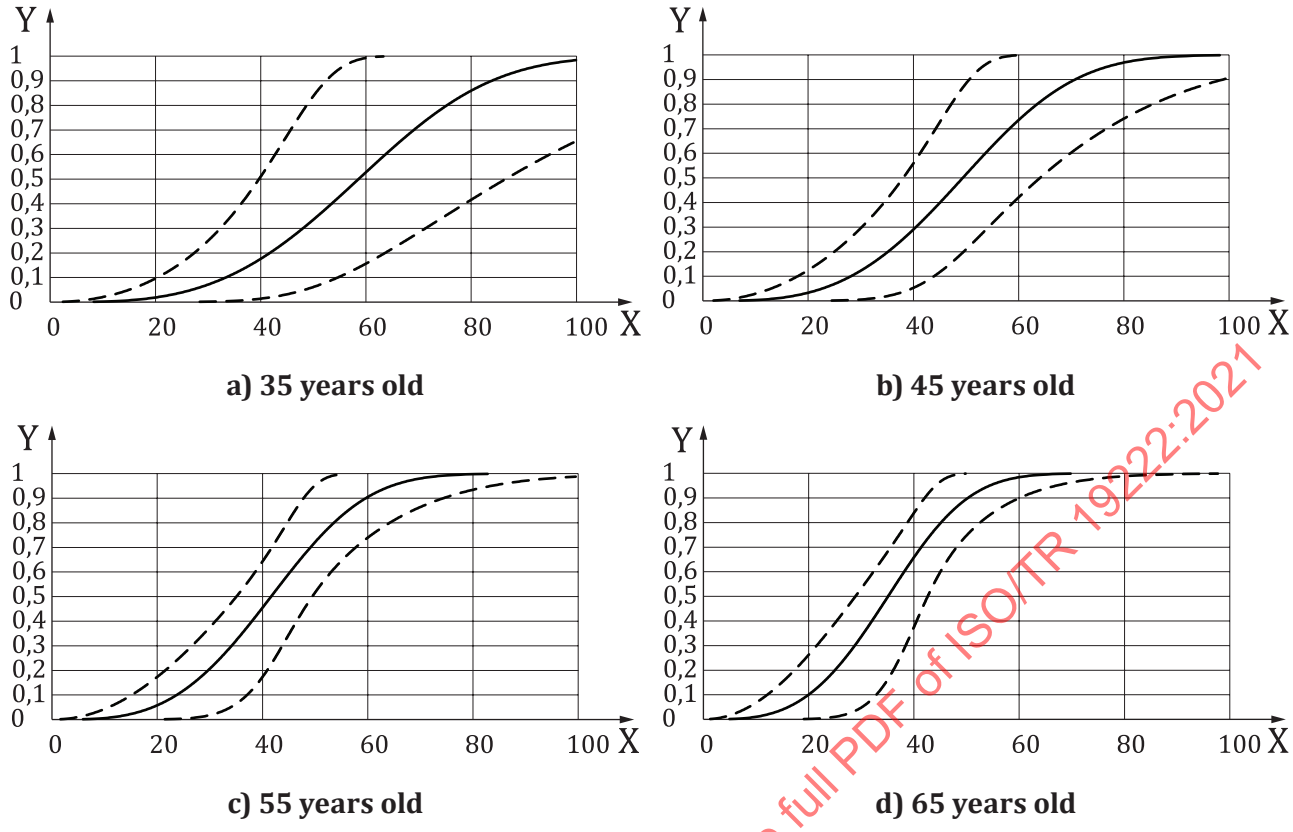

a) 35 years old

b) 45 years old

c) 55 years old

d) 65 years old

Key

X	R_{max} (mm)
Y	risk of NFR3+
———	IRF (NFR3+)
- - - -	CI (NFR3+)

Figure 10 — Injury risk curves for NFR3+ as a function of Rmax

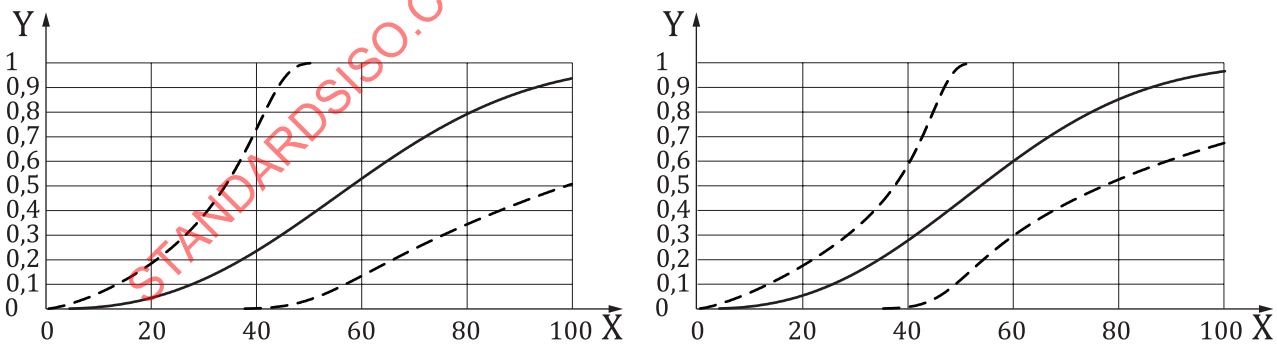

a) 35 years old

b) 45 years old

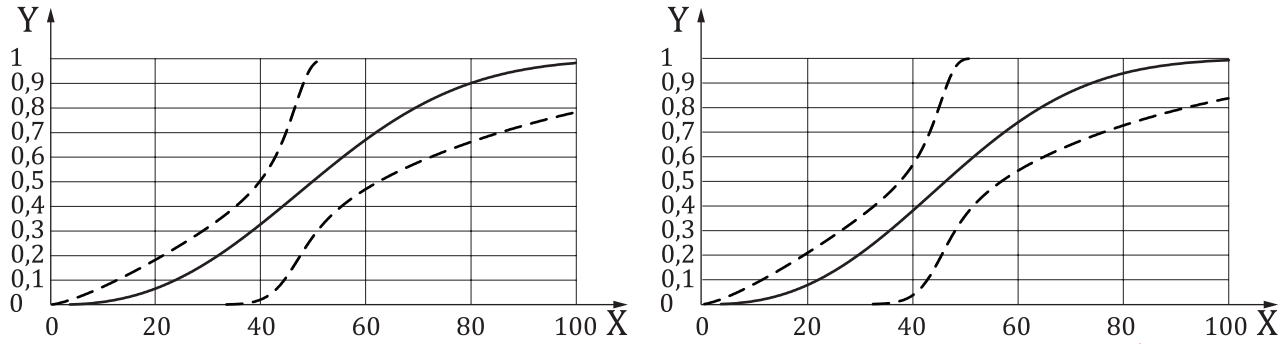

c) 55 years old **d) 65 years old**

Key

X R_{max} (mm)
Y risk of NFR7+
——— IRF (NFR7+)
- - - - CI (NFR7+)

Figure 11 — Injury risk curves for NFR7+ as a function of R_{max}

— Quotation

  — ISO/TS 18506 rules: 1

  — Quality assessment (Table 2)

Table 2 — Quality assessment of R_{max}

Age	35 years old	45 years old	55 years old	years old
NFR3+				
5 % CI	1,24	1,18	1,21	1,34
25 % CI	0,83	0,64	0,57	0,66
50 % CI	0,80	0,53	0,35	0,39
NFR7+				
5 % CI	2,07	1,94	1,94	2,04
25 % CI	1,13	0,83	0,67	0,73
50 % CI	1,12	0,74	0,45	0,42
NFR3+ calculated with enlarged database of TIC				
5 % CI	1,75	1,85	2,02	2,24
25 % CI	0,90	0,83	0,87	1,01
50 % CI	0,80	0,59	0,48	0,53
Quotation: 0 ≤ good ≤ 0,5 < fair ≤ 1,0 < marginal ≤ 1,5 < unacceptable.				

  — R&R: 94 %

  — THOR applicability: 1

5.3.2 PC-Score

— Injury target: AIS3+ chest injury (3 fractured ribs)

— Source: Reference [66]

— Channels: 4 3D rib deflections (D_{ulx}, D_{uly}, D_{ulz}, D_{urx}, D_{ury}, D_{urz}, D_{llx}, D_{lly}, D_{llz}, D_{lrx}, D_{lry}, D_{lrz})

— Filtration: CFC180

— Formula: $S_{pca} = 0,486\left(\frac{D_{uptot}}{17,439}\right) + 0,492\left(\frac{D_{lowtot}}{14,735}\right) + 0,496\left(\frac{D_{updif}}{9,672}\right) + 0,526\left(\frac{D_{lowdif}}{12,384}\right)$

where

$$D_{uptot} = \max\left(\sqrt{D_{ulx}^{2} + D_{uly}^{2} + D_{ulz}^{2}}\right) + \max\left(\sqrt{D_{urx}^{2} + D_{ury}^{2} + D_{urz}^{2}}\right);$$

$$D_{updif} = \max\left(\left|\sqrt{D_{ulx}^{2} + D_{uly}^{2} + D_{ulz}^{2}} - \sqrt{D_{urx}^{2} + D_{ury}^{2} + D_{urz}^{2}}\right|\right);$$

$$D_{lowtot} = \max\left(\sqrt{D_{llx}^{2} + D_{lly}^{2} + D_{llz}^{2}}\right) + \max\left(\sqrt{D_{lrx}^{2} + D_{lry}^{2} + D_{lrz}^{2}}\right);$$

$$D_{lowdif} = \max\left(\left|\sqrt{D_{llx}^{2} + D_{lly}^{2} + D_{llz}^{2}} - \sqrt{D_{lrx}^{2} + D_{lry}^{2} + D_{lrz}^{2}}\right|\right);$$

D_{ijk} is the deflection measured at the *ij* position in the *k* direction and expressed in mm:

i = (u, l) for upper and lower positions;

j = (l, r) for left and right positions;

k = (x, y, z) for the direction;

S_{pca} is the variable for chest injury criterion PC-Score.

— $P_{NFR \geq 3|\dot{A},S_{pca}} = 1 - \exp\left(-\left[\frac{S_{pca}}{\exp\left(2,867\ 7 - 0,018\ 1\dot{A}\right)}\right]^{3,311\ 8}\right)$

— $P_{NFR \geq 7|\dot{A},S_{pca}} = 1 - \exp\left(-\left[\frac{S_{pca}}{\exp\left(2,533\ 7 - 0,007\ 9\dot{A}\right)}\right]^{2,470\ 8}\right)$

where

P is the injury probability;

$\dot{A}$ is the age;

S_{pca} is the variable for the chest injury criterion PC-Score.

— Data: 40 PMHS sled tests (28 belt only; 7 3-point belt+AB; 2 lap belt+AB; 3 inflatable belt) provided in Table D.1 of Annex D

— Statistics: PCA then survival (Weibull)

— Dummy version: THOR mod-kit 2013

— Comments:

  — No impactor tests

— Curves

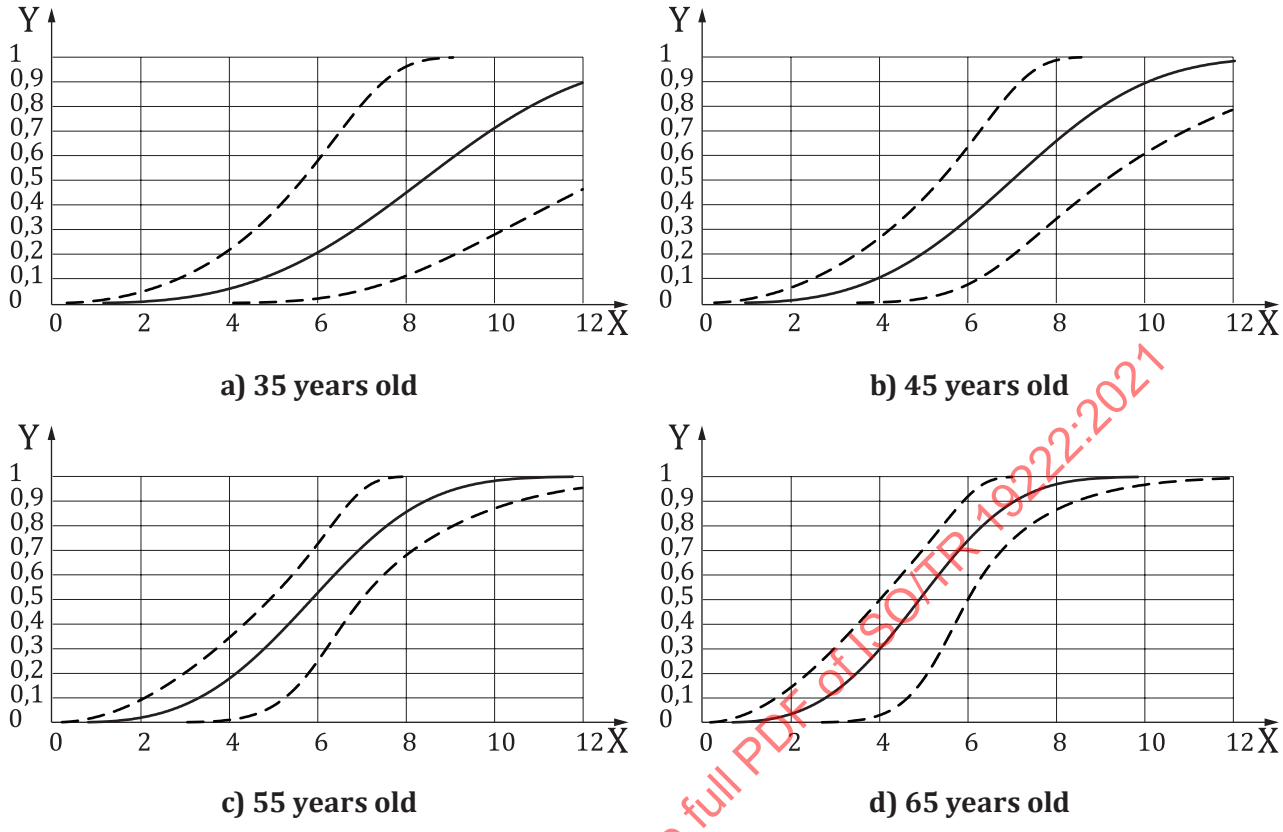

a) 35 years old

b) 45 years old

c) 55 years old

d) 65 years old

Key

X	PC-Score
Y	risk of NFR3+
———	IRF (NFR3+)
- - - -	CI (NFR3+)

Figure 12 — Injury risk curves for NFR3+ as a function of PC-Score

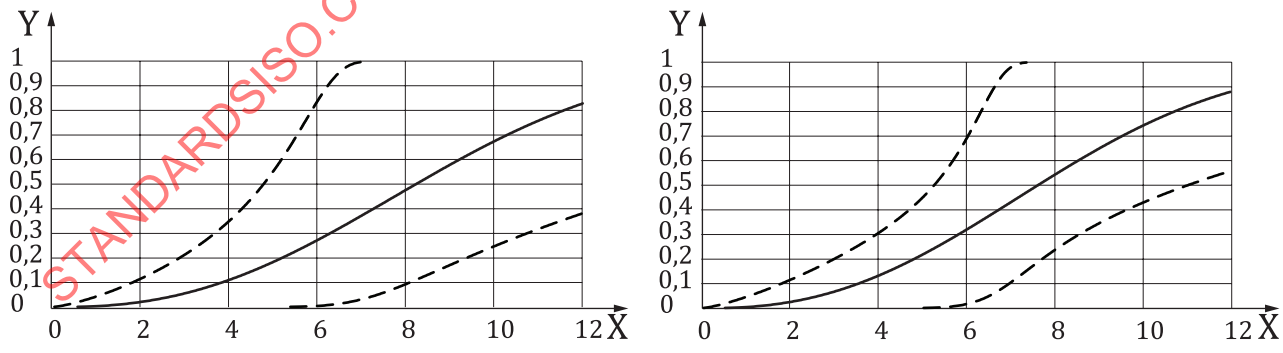

a) 35 years old

b) 45 years old

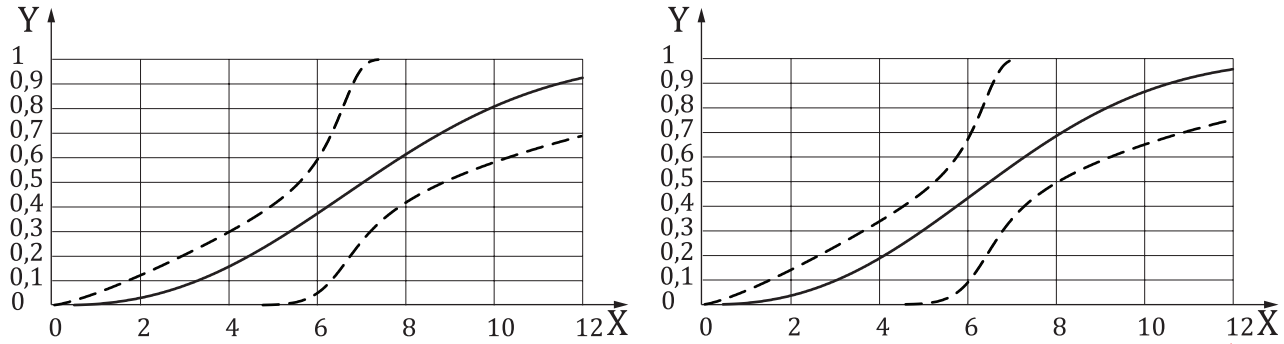

c) 55 years old

d) 65 years old

Key

X PC-Score

Y risk of NFR7+

——— IRF (NFR7+)

- - - - CI (NFR7+)

Figure 13 — Injury risk curves for NFR7+ as a function of PC-Score

— Quotation

  — ISO/TS 18506 rules: 1

  — Quality assessment (Table 3)

Table 3 — Quality assessment of PC-Score

Age	35 years old	45 years old	55 years old	65 years old
NFR3+				
5 % CI	1,28	1,22	1,26	1,39
25 % CI	0,85	0,65	0,59	0,69
50 % CI	0,81	0,53	0,35	0,41
NFR7+				
5 % CI	2,17	2,05	2,04	2,15
25 % CI	1,17	0,86	0,70	0,76
50 % CI	1,14	0,75	0,46	0,43
NFR3+ calculated with enlarged database of TIC				
5 % CI	1,26	1,30	1,37	1,48
25 % CI	0,70	0,64	0,64	0,71
50 % CI	0,61	0,46	0,38	0,40
Quotation: 0 ≤ good ≤ 0,5<fair ≤ 1,0<marginal ≤ 1,5<unacceptable.				

  — R&R: 94 %

  — THOR applicability: 1

5.3.3 TIC

— Injury target: AIS3+ chest injury (3 fractured ribs or 3 displaced fractured ribs)

— Source: Reference [85]

— Channels: 4 3D rib deflections (D_{ulx}, D_{uly}, D_{ulz}, D_{urx}, D_{ury}, D_{urz}, D_{llx}, D_{lly}, D_{llz}, D_{lrx}, D_{lry}, D_{lrz})

— Filtration: CFC180

— Formula:

$$T_{NRF} = R_{max} + 1{,}66\ D_{updif}$$

$$T_{NSRF} = R_{max} + 3\ D_{updif}$$

where

$$R_{max} = \max(D_{ulmax}, D_{urmax}, D_{llmax}, D_{lrmax});$$

$$D_{ulmax} = \max\left(\sqrt{D_{ulx}^2 + D_{uly}^2 + D_{ulz}^2}\right);$$

$$D_{urmax} = \max\left(\sqrt{D_{urx}^2 + D_{ury}^2 + D_{urz}^2}\right);$$

$$D_{llmax} = \max\left(\sqrt{D_{llx}^2 + D_{lly}^2 + D_{llz}^2}\right);$$

$$D_{lrmax} = \max\left(\sqrt{D_{lrx}^2 + D_{lry}^2 + D_{lrz}^2}\right);$$

$$D_{updif} = \max\left(\left|\sqrt{D_{ulx}^2 + D_{uly}^2 + D_{ulz}^2} - \sqrt{D_{urx}^2 + D_{ury}^2 + D_{urz}^2}\right|\right);$$

D_{ijk} is the deflection measured at the ij position in the k direction and expressed in mm:

i = (u, l) for upper and lower positions;

j = (l, r) for left and right positions;

k = (x, y, z) for the direction;

T_{NFR} is the variable for the chest injury criterion TIC_{NFR};

T_{NSFR} is the variable for the chest injury criterion TIC_{NSFR}.

— $$P_{NFR \geq 3|\dot{A},T_{NFR}} = 1 - \exp\left(-\left[\frac{T_{NFR}}{\exp(5{,}2675 - 0{,}0135\dot{A})}\right]^{\gamma}\right)$$

— With

— $$\gamma = \frac{1}{(0{,}093\ 25 + 0{,}004\ 75\ \dot{A})}$$

— $$P_{NSFR \geq 3|\dot{A},T_{NSFR}} = 1 - \exp\left(-\left[\frac{T_{NSFR}}{\exp(6{,}125 - 0{,}015\dot{A})}\right]^{\gamma}\right)$$

— With

— $$\gamma = \frac{1}{(0{,}025\ 25 + 0{,}004\ 15\ \dot{A})}$$

— Data: 71PMHS sled tests (58 belt only; 7 3-point belt+AB; 3 lap belt+AB; 3 inflatable belt and 9 PMHS static AB tests) provided in Table D.2 of Annex D

— Statistics: survival (Weibull)

— Dummy version: THOR mod-kit 2013

— Comments:

  — No impactor tests

  — Enlarged test sample including airbag only loading and a larger range of deflections. Tests consisting of the deployment of unfolded airbags were included because they were carried out in such a way as to generate only a membrane effect close to the loading of a subject in a crash test

  — Meaningful gauss like distribution of age (median 68,5 years), mass (median 70,5 kg) and height (median 175 cm)

  — A principal component analysis of this sample indicated that a good criterion describing the chest deflection needs two components: one describing the extent of the deflection; one describing the left-right asymmetry of the deflection

  — For the development of TIC, different THORs have been used and it is unclear if some effects (e.g. belted vs. only airbag) seen in the development of TIC are real effects or just dummy artefacts

— Curves

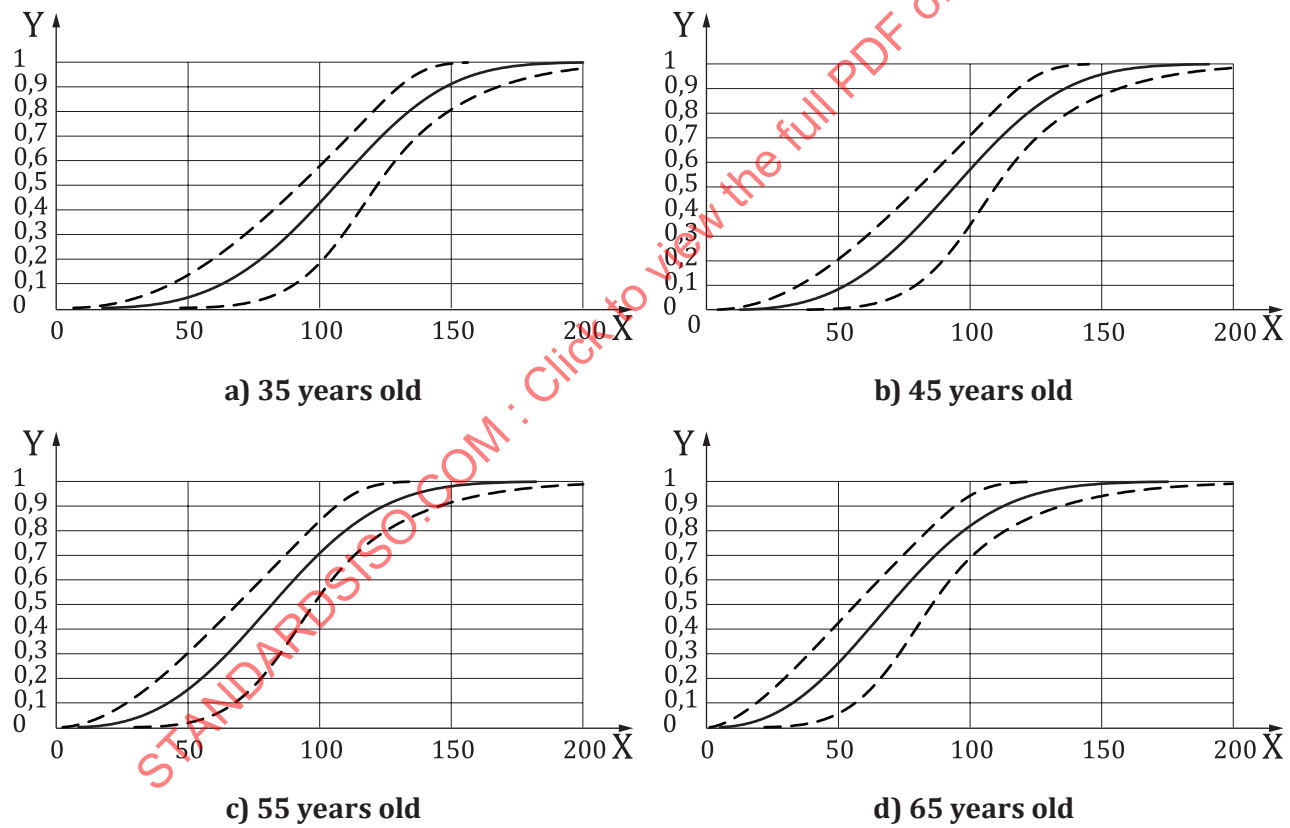

a) 35 years old

b) 45 years old

c) 55 years old

d) 65 years old

Key

X TIC_NFR (mm)

Y risk of NFR3+

——— IRF (NFR3+)

– – – – CI (NFR3+)

Figure 14 — Injury risk curves for NFR3+ as a function of TIC_NFR

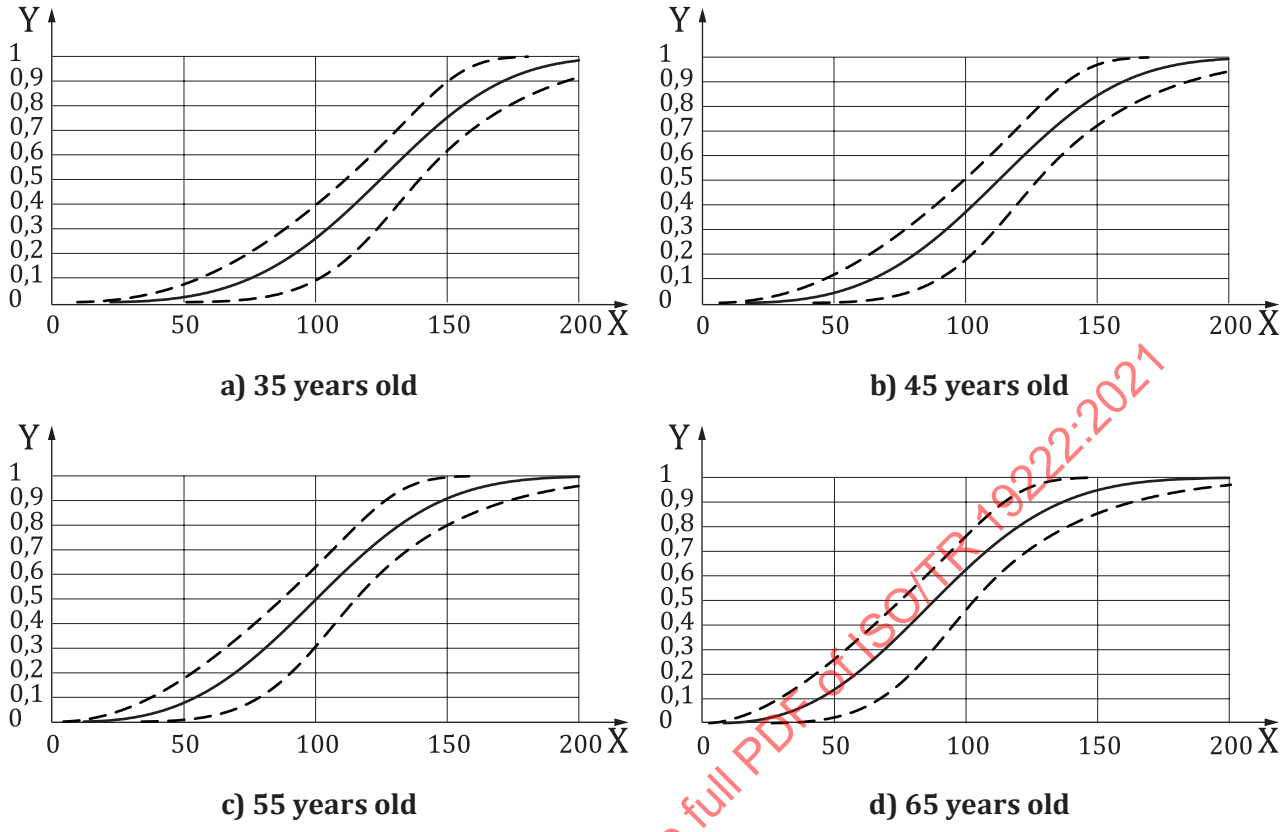

a) 35 years old

b) 45 years old

c) 55 years old

d) 65 years old

Key

X	TIC_NFR (mm)
Y	risk of NFR7+
———	IRF (NFR7+)
- - - -	CI (NFR7+)

Figure 15 — Injury risk curves for NFR7+ as a function of TIC_NFR

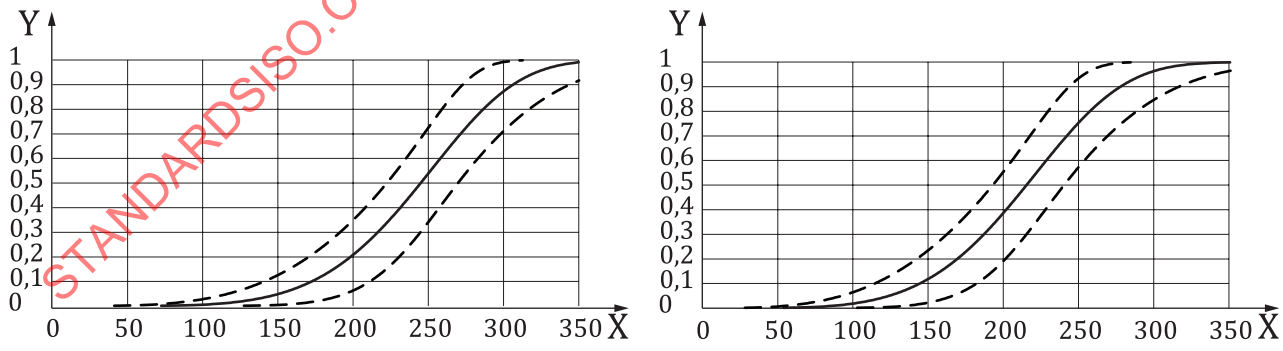

a) 35 years old

b) 45 years old

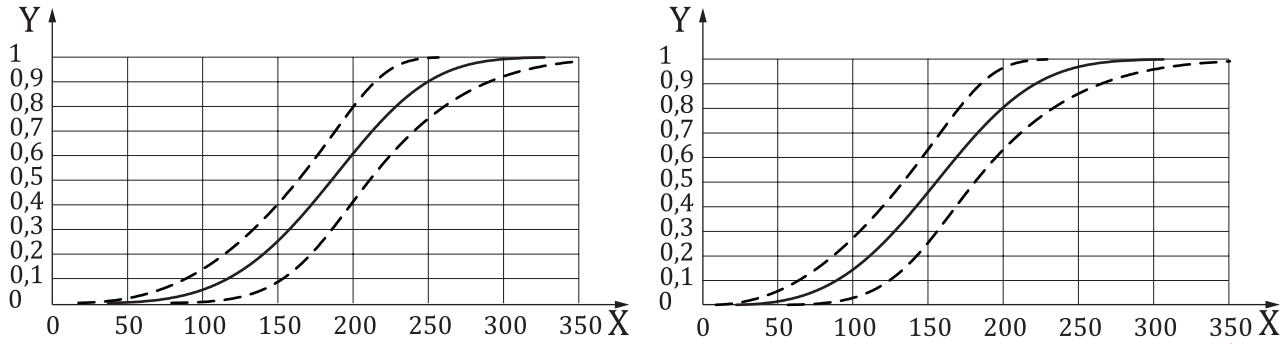

c) 55 years old **d) 65 years old**

Key

X TIC_NSFR (mm)
Y risk of NSFR3+
——— IRF (NSFR3+)
- - - - CI (NSFR3+)

Figure 16 — Injury risk curves for NSFR3+ as a function of TIC_NSFR

— Quotation

  — ISO/TS 18506 rules: 1

  — Quality assessment (Table 4)

Table 4 — Quality assessment of TIC

Age	35 years old	45 years old	55 years old	65 years old
TIC_NFR3+				
5 % CI	0,95	1,07	1,24	1,49
25 % CI	0,47	0,53	0,61	0,72
50 % CI	0,28	0,31	0,36	0,42
TIC_NFR7+				
5 % CI	0,77	0,86	0,98	1,13
25 % CI	0,38	0,42	0,47	0,54
50 % CI	0,23	0,25	0,28	0,32
TIC_NSFR3+				
5 % CI	0,52	0,60	0,70	0,87
25 % CI	0,27	0,31	0,37	0,45
50 % CI	0,19	0,22	0,26	0,31
Quotation: 0 ≤ good ≤ 0,5<fair ≤ 1,0<marginal ≤ 1,5<unacceptable.				

  — R&R: 81 %

  — THOR applicability: 1

5.4 Abdomen

5.4.1 Penetration

— Injury target: AIS3+

— Source: Reference [32]

— Channels: 2 3D rib deflections (D_{alx}, D_{aly}, D_{alz}, D_{arx}, D_{ary}, D_{arz})

— Filtration: CFC180

— Formula:

$C_{abdomen} = D_{abdomen}/238,5$ (Normalized penetration)

where

$D_{abdomen} = \max(D_{alx}, D_{arx})$;

D_{alx} is the left deflection in the x direction expressed in mm;

D_{arx} is the right deflection in the x direction expressed in mm.

— $$P_{AIS \geq 3|C_{abdomen}} = 1 - \exp\left(-\left[\frac{C_{abdomen}}{0,424\ 7}\right]^{3,67}\right)$$

— $$P_{AIS \geq 3|D_{abdomen}} = 1 - \exp\left(-\left[\frac{D_{abdomen}}{101,3}\right]^{3,67}\right)$$

where

P is the injury probability;

$C_{abdomen}$ is the variable for the abdomen injury criterion normalized penetration;

$D_{abdomen}$ is the variable for the abdomen injury criterion penetration.

— Data: 33 porcine ramp release tests (model of 6 y/o human) provided in Table E.1 of Annex E

— Statistics: Survival (Weibull)

— Comments:

  — Porcine IRCs. Transferred to human through a scaling by abdomen depth

  — Only ramp-release tests were considered because ramp-hold tests generated more severe injuries during the hold portion of the waveform.

  — THOR biofidelity: in the corridors of belt abdomen tests up to 75 mm, i.e. 31 % (Reference[61])

— Curves

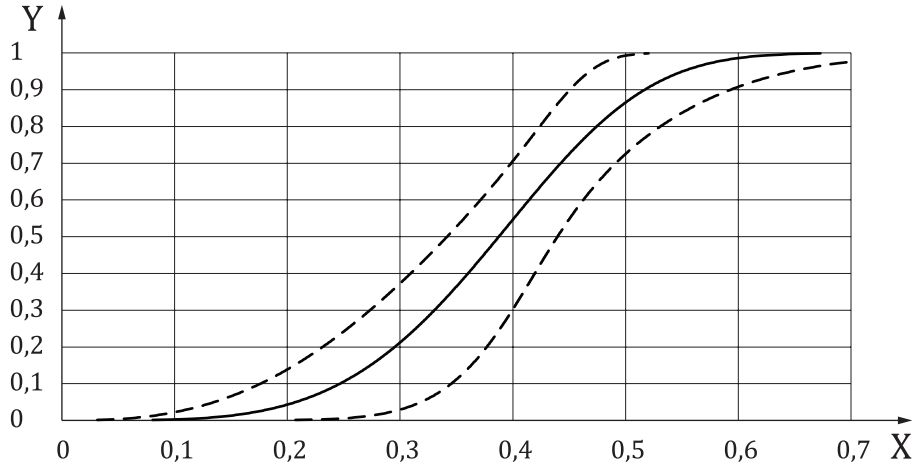

Key

X $C_{abdomen}$
Y risk of abdomen AIS3+
——— IRF (Abdomen MAIS3+)
- - - - CI (Abdomen MAIS3+)

Figure 17 — Injury risk curves for MAIS3+ as a function of $C_{abdomen}$

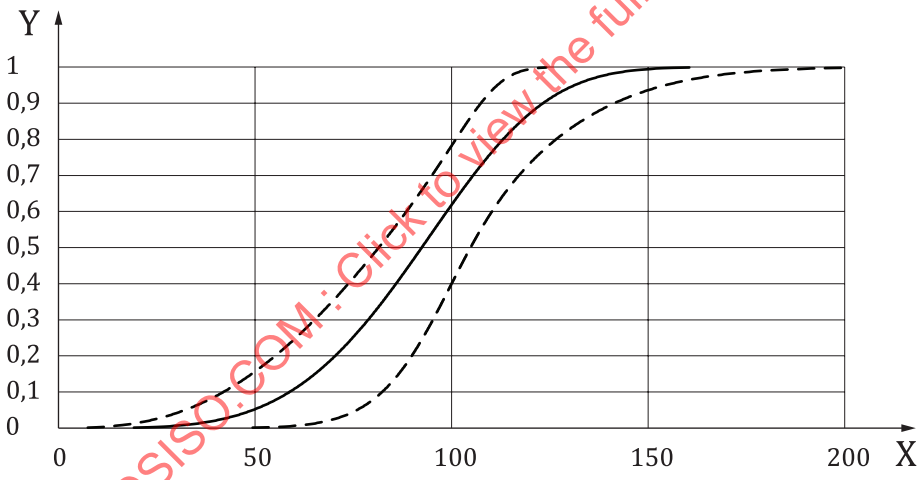

Key

X $D_{abdomen}$ (mm)
Y risk of abdomen AIS3+
——— IRF (Abdomen MAIS3+)
- - - - CI (Abdomen MAIS3+)

Figure 18 — Injury risk curves for MAIS3+ as a function of δ_{max}

— Quotation
  — ISO/TS 18506 rules: 1
  — Quality assessment
    — CI at 5 % = 0,88 fair
    — CI at 25 % = 0,43 good

— CI at 50 % = 0,25 good

— R&R: 96 % (mean of left and right abdomen displacements in abdomen certification tests)

— THOR applicability: 0,5 (attributed based on Reference [61] paper, although no biofidelity target was validated by ISO TC22/SC36/WG5)

5.5 Knee-thigh-hip

5.5.1 Femur z-force

— Injury target: Femur fracture

— Source: Annex F

— Channels: Femur compressive force (F_z)

— Filtration: CFC600

— Formula: $F_{femur} = \max(F_z)$

where

F_z is the femur compressive force expressed in N.

— $$P_{\text{Fracture}|\dot{A},\text{rigid},F_{femur}} = \Phi\left[\frac{\ln(1{,}3\ F_{femur}) - (10{,}8 - 0{,}016\ \dot{A} - 0{,}14\ \text{rigid})}{0{,}671}\right]$$

where

P is the injury probability;

$\dot{A}$ is the age;

Φ is the cumulative distribution function of the standard normal distribution;

F_{femur} is the variable for the femur injury criterion femur force.

— Data: 175 unembalmed PMHS tests from References [48], [27], [88], [58], [5], [6], [41], [11], [55] and [92] provided in Table F.7 of Annex F

— Statistics: Survival (log-normal)

— Comments:

The THOR 50th percentile male dummy does not have a force sensor to measure the knee impact force. That is, the injury risk function developed for the human cannot be used directly with THOR. But under some assumptions the injury risk function for impact force can be used with THOR:

— THOR produces the same force at the knee as a human;

— 77 % of knee force of Hybrid III is transmitted to the femur load cell (Reference [70]);

— THOR has the same behaviour as the Hybrid III regarding the knee impact (Reference [43]).

Assuming the assumptions are valid the force measured at the femur load cell of the THOR must be multiplied by 1:0,77 (about 1,3) to be used with the injury risk function based on impact force measured on PMHS.

— Curves (padded impact)

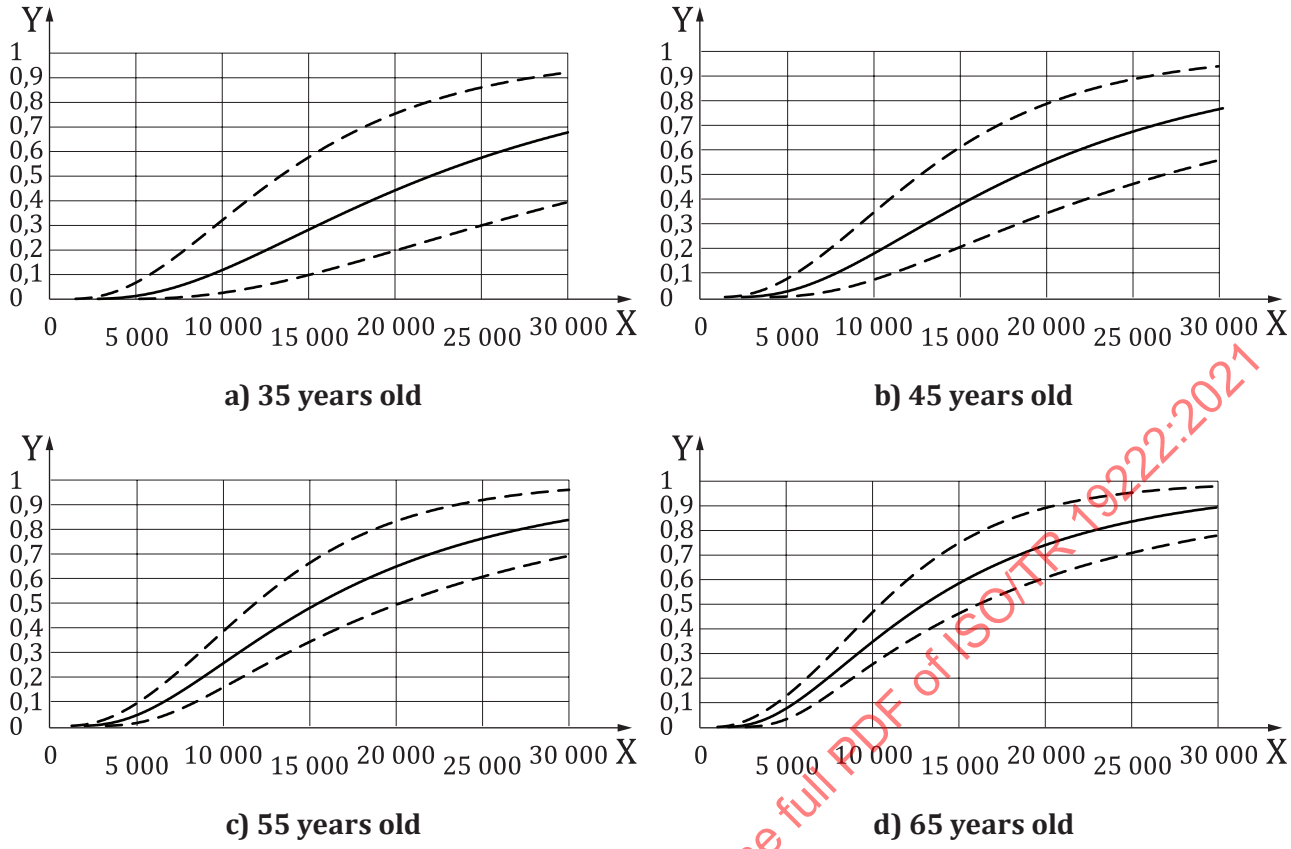

a) 35 years old

b) 45 years old

c) 55 years old

d) 65 years old

Key

X femur force (N)

Y risk of fracture

_____ IRF (fracture) - padded

- - - - CI (fracture) - padded

Figure 19 — Injury risk curves for femur fractures as a function of THOR Femur force

— Quotation

  — ISO/TS 18506 rules: 1

  — Quality assessment (Table 5)

Table 5 — Quality assessment of Femur force

Age	35 years old	45 years old	55 years old	65 years old
Femur fracture				
5 % CI	1,02	0,76	0,57	0,50
25 % CI	0,98	0,70	0,46	0,35
50 % CI	1,04	0,76	0,54	0,44
Quotation: 0 ≤ good ≤ 0,5<fair ≤ 1,0<marginal ≤ 1,5<unacceptable.				

  — R&R: 95 % (femur force in upper leg certification tests)

  — THOR applicability: 1

5.5.2 Acetabulum force

— Injury target: AIS3+

— Source: References [70] and [71]

— Channels: acetabulum forces (F_x, F_y, F_z)

— Filtration: CFC600

— Formula: Maximum resultant acetabulum force in compression

  — $F_{acetabulum}(t) = F_{resultant}(F_x, F_y, F_z)$ when

    — left acetabulum $F_x > 0$ (compression)

    — right acetabulum $F_x < 0$(compression)

  — $F_{acetabulum}(t) = 0$ when

    — left acetabulum $F_x \leq 0$ (tension)

    — right acetabulum $F_x \geq 0$ (tension)

— $$P_{\text{hip fracture}|F_{acetabulum}} = \Phi\left[\frac{\ln\left(\frac{F_{acetabulum}}{0{,}72}\right) - 1{,}652\ 6}{0{,}199\ 1}\right]$$

where

P is the injury probability;

Φ is the cumulative distribution function of the standard normal distribution;

$F_{acetabulum}$ is the acetabulum force expressed in kN.

— Data: 27 PMHS impactor tests (exact data) provided in Table F.8 of Annex F

— Statistics: Survival (log-normal)

— Comments:

The assumptions used to derive the above injury risk curves from Rupp experiments where investigated based on simulation results (THOR and THUMS v5 models), PMHS test results from the literature and THOR sled experiments (see F.2 acetabulum/transfer function between PMHS and THOR).

  — Hip joint angle

    — An average hip flexion angle of 11° (co-driver) and 16° (driver) was found for a typical sitting posture of the dummy. This value is overestimated (<10°) (see F.2 acetabulum/transfer function between PMHS and THOR).

    — There is currently no data available to tell if the abduction angle used in the injury risk function is plausible.

  — Force transfer

    — The factor T_{hip} is used to transfer the acetabulum force of the THOR to PMHS. To calculate the value of T_{hip} (1,429), Reference [7] uses four assumptions:

      — r_K(THORtoPMHS) is assumed to be 1,

- r_{KtoA}(PMHS) is assumed to be 0,55,
- r_{KtoF}(THOR) is assumed to be 0,77 for THOR (Reference [70] for HIII),
- r_{FtoA}(THOR) is assumed to be 0,50 for THOR (Reference [43]).

— These assumptions were investigated based on simulation results (THOR and THUMS v5 models), PMHS test results from the literature and THOR sled experiments (see F.2 acetabulum/transfer function between PMHS and THOR).

— Based on these results, only one assumption could be validated and the value of should be significantly lower (≈0,8).

— The value of T_{hip} has a significant influence on the injury risk.

— Compression/tensile force:

— tests with THOR can lead to tensile force at the acetabulum,

— the injury risk curve is only meaningful for compressive forces,

— acetabulum force criterion should only be used with compressive forces.

— Curves

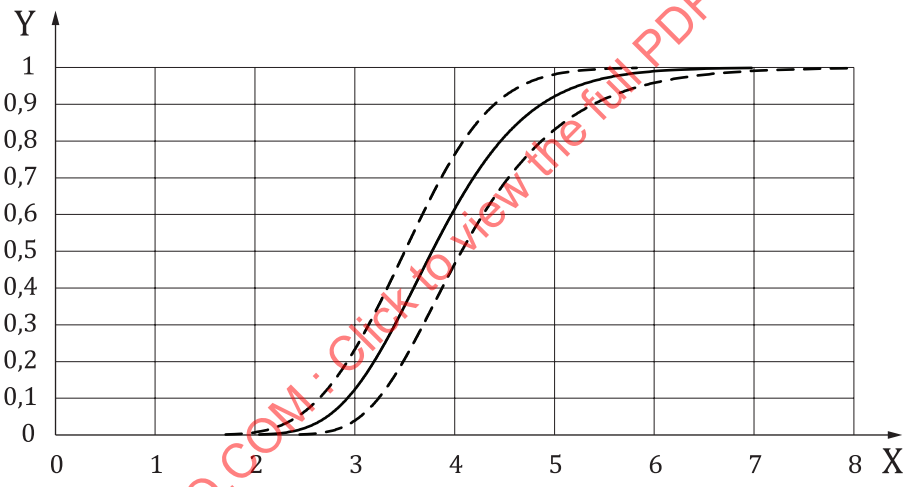

Key

X acetabulum force (kN)
Y risk of AIS3+
_____ IRF (Acetabulum AIS3+)
- - - - CI (Acetabulum AIS3+)

Figure 20 — Injury risk curves for AIS3+ as a function of THOR acetabulum force with T_{hip}=1,429

— Quotation

— ISO/TS 18506 rules: 1

— Quality assessment

— CI at 5 % = 0,23 (good)

— CI at 25 % = 0,17 (good)

— CI at 50 % = 0,15 (good)

— R&R: 95 % (acetabulum force in upper leg certification tests)

— THOR applicability: 1 (depending on the value of T_{hip})

5.5.3 Femur force versus acetabulum force

Both injury risk functions proposed above deal with an impact to the knee of a vehicle occupant (frontal impact situation), both functions predict the risk of injuries to the knee-thigh-hip body region. In both test series used for the two injury risk functions the acetabulum is loaded via the knee and femur, i.e. for both injury risk functions the load path is equal.

However, acetabulum tests and femur tests were performed with different test setups. The main difference is that in the acetabulum tests the pelvis of the specimens was fixed.

Annex A
(informative)

HIC data

A.1 HIC 15ms / Skull fracture - Mertz

Data : References [20], [21], [82], [24], [25] and [59]

Only the weakest subject (H1805R at HIC=450, j=1), the strongest subject (H2439 at HIC=2585, j=51) and the number of tests between these two subjects (N=51) are considered.

$P(HIC(j)) = (j-0,3)/(N+0,4)$

Table A.1 — Mertz data

PMHS number	HIC	Skull fracture
H1805R	450	Yes
H2358	509	Yes
APR107	516	Yes
H2448	554	No
H1747R	640	Yes
APR61	650	No
APR165	692	No
H2219	731	Yes
APR163	750	No
APR18-2	770	No
APR110	781	Yes
APR143	839	No
H1873R	870	Yes
H2418	892	No
APR144	900	No
H2321	913	No
ONO4	997	Yes
H2440	1 000	Yes
APR172	1 042	No
H2212	1 050	No
H1699R	1 070	Yes
APR159	1 078	No
APR251	1 085	Yes
H1857R	1 130	Yes
APR174	1 156	No
APR175	1 200	No
APR166	1 270	Yes
H2205	1 305	Yes
APR162	1 334	No

Table A.1 *(continued)*

PMHS number	HIC	Skull fracture
ONO3	1 405	Yes
APR160	1 411	No
APR176	1 416	Yes
ONO2	1 423	Yes
APR250	1 460	Yes
APR102	1 483	Yes
H2415	1 520	No
APR126-2	1 600	No
H1701R	1 600	Yes
H2220	1 716	Yes
APR108	1 720	Yes
H2247	1 804	Yes
APR355	1 927	No
H2298	1 955	No
ONO1	1 989	Yes
H2412	1 998	Yes
ONO6	2 019	Yes
H2214	2 038	Yes
APR177	2 138	No
APR103	2 351	No
APR135-2	2 510	No
H2439	2 585	No
ONO5	2 598	Yes

A.2 HIC 15ms/Skull fracture – Eppinger

Data: References [20], [21], [82], [24] and [25]

When a subject is tested twice, only the test with injury is considered.

Table A.2 — Eppinger data

Test number	HIC	Skull fracture
13	175	No
4	278	No
2	291	No
10	326	No
17	384	No
9	411	No
1	413	No
DOT6	450	Yes
3	461	No
APR107	516	Yes
11	531	No
8	554	No

Table A.2 *(continued)*

Test number	HIC	Skull fracture
12	554	No
19	611	No
DOT2	640	Yes
APR165	692	No
7	711	No
APR163	750	No
APR110	781	Yes
14	791	No
APR143	839	No
16	845	No
DOT22	850	Yes
DOT29	870	Yes
6	892	No
APR144	900	No
DOT24	965	Yes
APR172	1 042	No
15	1 050	No
DOT4	1 070	Yes
APR159	1 078	No
APR251	1 085	Yes
DOT30	1 130	Yes
APR174	1 156	Yes
APR175	1 200	No
APR166	1 270	Yes
APR162	1 334	No
DOT26	1 410	Yes
APR160	1 411	No
APR176	1 416	Yes
APR250	1 460	Yes
APR102	1 483	Yes
18	1 520	No
DOT3	1 600	Yes
APR108	1 720	Yes
DOT17	1 930	Yes
DOT23	2 000	Yes
APR177	2 138	No
DOT20	2 220	Yes
APR103	2 351	No
DOT18	2 380	Yes
DOT19	2 550	Yes
DOT30	2 780	Yes
DOT21	3 400	Yes

Annex B
(informative)

Brain

B.1 General

This annex describes the steps used in the construction of the injury risk curves for diffuse-type traumatic brain injuries.

B.2 Tissue-level and kinematics-based brain injury risk curves for head rotational kinematics

B.2.1 Introduction

Traumatic brain injuries (TBIs) are one of many serious issues which occur in motor vehicle crashes. Diffuse-type brain injuries, including concussions and diffuse axonal injuries (DAIs), are the most common types of TBIs (References [80] and [2]). Diffuse-type TBIs are hypothesized to be caused by shear deformation of brain tissue due to the rapid rotational motion of the head (Reference [26]). According to the hypothesis, injury risk curves (IRCs) based on tissue-level brain deformation quantified by brain tissue strain (tissue-level brain injury metric) were developed to estimate injury risks of sustaining diffuse-type TBIs. Thereafter, the IRCs based on the tissue-level brain injury metric were transferred to IRCs based on existing brain injury metrics derived from rotational rigid body motion of the head (kinematics-based brain injury metrics) for practical application to the THOR dummy. In compliance with AIS coding for concussion (AIS 2~3) and DAI (AIS 4~5), AIS 2 and AIS 4 IRCs were developed.

B.2.2 TBI data collection for developing tissue-level brain injury risk curves

TBI data with known 6-degree-of-freedom head kinematic time histories and clinical outcomes were collected from sub-injurious volunteer tests (Reference [13]), laboratory reconstruction tests of professional football (References [62] and [73]) and non-human primate (NHP) tests (References [35], [83] and [77]). Test cases collected contain no injury or diffuse-type brain injuries (concussion and DAI). A TBI data set consisting of these test data is summarized in B.3.1. The TBI data set excluded test cases containing only focal injuries in nature (skull fracture, contusion, epidural hemorrhage, subdural hemorrhage).

B.2.3 Data preparation for developing tissue-level brain injury risk curves: Species-specific brain finite element models and reconstruction simulations

To reconstruct tissue-level brain deformation of the test cases in the TBI data set (B.3.1), harmonized species-specific brain finite element (FE) models shown in Figure B.1 were used. For the human volunteer test cases, the brain FE model extracted from the Global Human Body Models Consortium 50th percentile male detailed seated occupant (GHBMC M50-O v4.3) was used (Figure B.1 a). Brain model responses of the GHBMC brain FE model, including tissue-level brain deformation, were previously validated with experimental post mortem human subjects (PMHS) test data (Reference [45]). For NHP test cases, NHP brain FE models, which were prepared by modifying previously developed rhesus macaque and baboon brain FE models were used (Figure B.1 b). The NHP brain FE models have harmonized numerical definitions (mesh type, mesh density, hourglass control etc.) and brain tissue model structures with the human brain FE model. Brain material properties used in the human brain FE model were applied to the NHP brain FE models.

Using the human and NHP brain FE models, the head impacts in the TBI data set (B.3.1) were simulated by applying the 6 degree-of-freedom head kinematics data obtained from the data set, directly to the centre of gravity of the rigid dura. All the FE simulations were conducted using LS-DYNA (v971 R9.2.0, double precision; LSTC).

In each FE simulation case, the following tissue-level brain injury metrics were extracted to evaluate brain deformation. The tissue-level injury metrics concerned here were: maximum principle strain represented based on the 95th (MPS95) (References [15] and [60]), 99th (MPS99) and 100th (MPS100) (References [80] and [81]) percentile peak responses and the Cumulative Strain Damage Measure (CSDM) with maximum principle strain thresholds of 15 % (CSDM15) (Reference [72]) and 25 % (CSDM25) (Reference [81]).

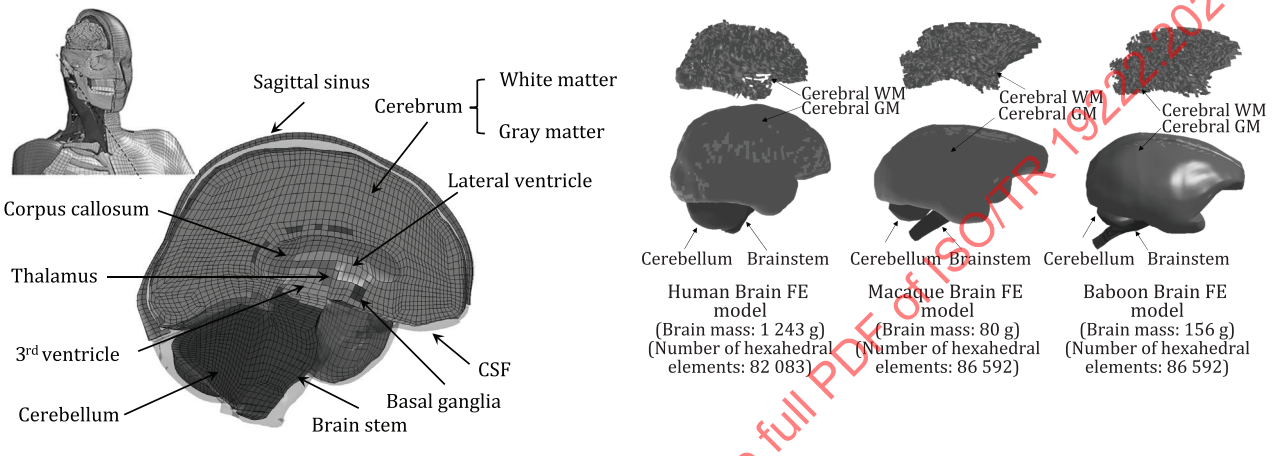

a) GHBMC v4.3 brain FE model

b) Human brain FE model and harmonized NHP brain FE models

Figure B.1 — Brain FE models used in the construction of IRCs

B.2.4 Statistical modelling: development of tissue-level brain injury risk curves

According to ISO/TS 18506:2014, tissue-level IRCs based on the tissue-level brain injury metrics were developed using survival analyses. All of the statistical analyses mentioned below were conducted using the RStudio software[1)], version 1.1.456.

Distribution assumption: Weibull, log-logistic and log-normal distributions were evaluated based on the Akaike information criterion (AIC) in order to choose the distribution with the best fit. The three distributions were plotted with nonparametric maximum likelihood estimation (NPMLE), as illustrated in Figure B.2. Weibull distribution had the lowest AIC. In addition, as Weibull distribution ensures zero risks of injury for zero stimuli, subsequent processes in this document considered Weibull distribution.

Influential observations: the overly influential cases were identified using the DFBETA statistics. However, these cases did not significantly change the IRCs, as shown in Figure B.3 a). Therefore, these cases remained in the construction of the IRCs.

Check on the distribution assumption: the assumed distribution was verified graphically using a Q-Q plot ("Q" stands for quantile). The percentiles of the distribution were plotted against the corresponding percentiles of the biomechanical samples, as illustrated in Figure B.3 b). The plots seem to fall about a straight line; thus, the chosen distribution is appropriate. Another way is to graphically plot the cumulative risk calculated with the survival analysis with a given distribution against the cumulative risk calculated with an NPMLE, as illustrated in Figure B.3 c). The cumulative risks lie close to one another, indicating that the chosen distribution is appropriate.

1) RStudio is the trade name of a product supplied by R Studio, Inc. This information is given for the convenience of users of this document and does not constitute an endorsement by ISO of the product named. Equivalent products may be used if they can be shown to lead to the same results.

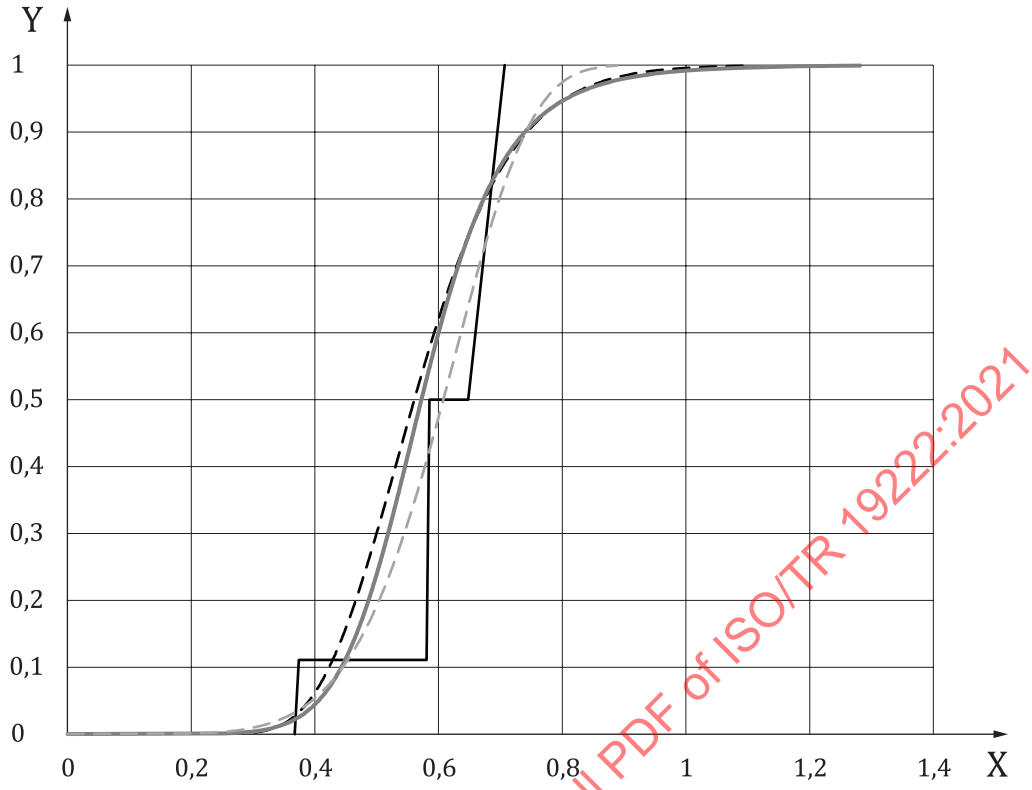

Key

X	MPS95
Y	injury risk
———	IRF (NPMLE)
- - - -	IRF (log-normal - AIC = 34,73)
———	IRF (log-logistic - AIC = 34,89)
- - - -	IRF (Weibull - AIC = 30,99)

Figure B.2 — Comparison of tissue-level IRCs between distribution assumptions

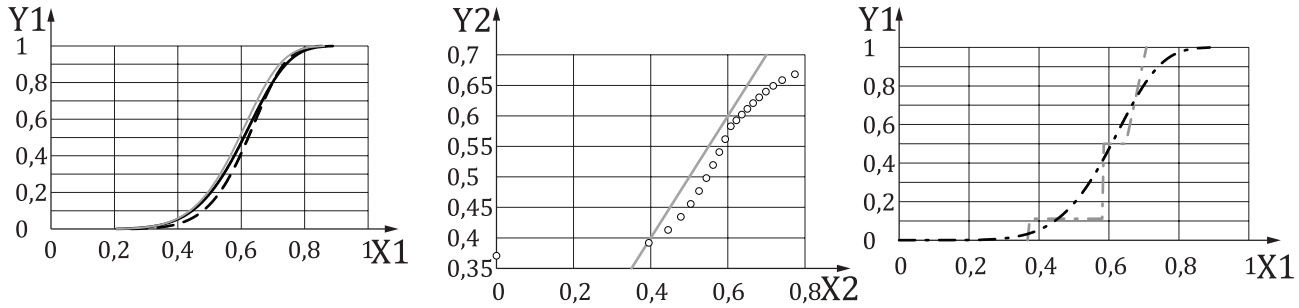

a) Effects of overly influential observations (number of critical DFBETAS: 4)

b) Q-Q plot to check distribution assumptions (0 % - 100 %; step size: 5 %)

c) Model fit verified with non-parametric method (NPMLE LogLik=-13,5 AIC=30,99)

Key

X1	MPS95
Y1	injury risk
X2	theoretical quantiles
Y2	samples quantiles
———	IRF (original)
- - - -	IRF (without influential observations on shape)
———	IRF (without influential observations on scale)
-.-.-.	IRF (NPMLE)
-.-.-.	IRF (Weibull)

Figure B.3 — Tissue-level IRCs based on MPS95

Tissue-level IRCs: the developed tissue-level IRCs for AIS2 and AIS4 diffuse-type TBIs are as illustrated in Figure B.4. The IRCs are formulated as shown below according to Weibull distribution.

$$P_{\text{injury}} = 1 - e^{\left(-e^{\left(\frac{1}{b}\times\ln(x)-\frac{a}{b}\right)}\right)}$$

Where x is the tissue-level brain injury metric. a and b are coefficients corresponding the shape ($1/b$) and scale (e^a) parameters for the Weibull distribution. The coefficients of each IRC are summarized in Table B.1.

95 % confidence intervals and quality index: the 95 % confidence intervals of the tissue-level IRCs were calculated, as illustrated in Figure B.4. The relative sizes of the 95 % confidence intervals at the 5 %, 25 % and 50 % with the quality index are also summarized in Table B.1.

Metric selection: AICs of the tissue-level IRCs are summarized in Table B.1. According to ISO/TS 18506:2014, the difference of AIC between an IRC and the IRC with the lowest AIC was calculated, as shown in Figure B.5. If the relative AIC between two IRCs is lower than two, they can essentially be considered to have no difference between the two IRCs. Therefore, MPS99 was recommended as the first candidate for the tissue-level brain injury metrics, with MPS95 and MPS100 as the second candidates.

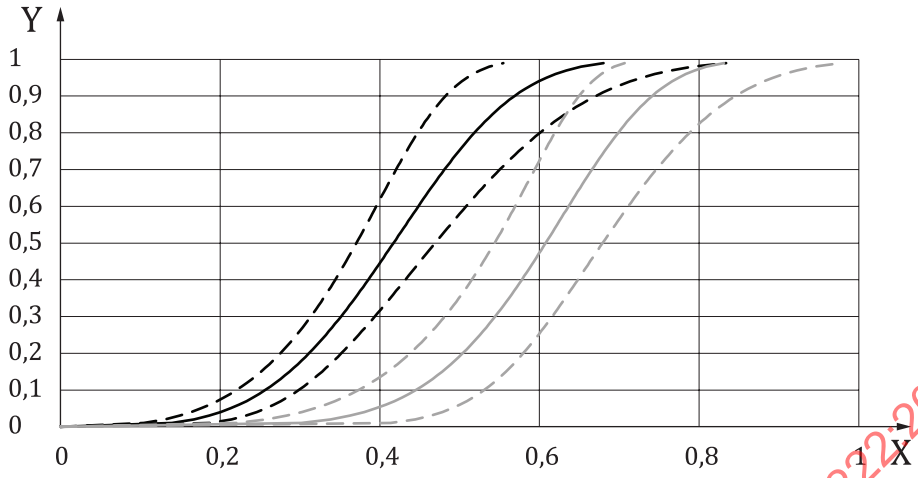

Key

X	DAMAGE
Y	risk of injury
———	IRF (AIS2)
- - - -	CI (AIS2)
———	IRF (AIS4)
- - - -	CI (AIS4)

Figure B.4 — Tissue-level IRCs based on MPS95

Table B.1 — Coefficients and quality index of the tissue-level IRCs

Injury	Metrics	Scale (e^a)	Shape ($1/b$)	5 % Risk (QI)	25 % Risk (QI)	50 % Risk (QI)	AIC
AIS2	MPS95	0,459	3,875	0,213 (0,38)	0,332 (0,23)	0,417 (0,24)	83,21
	MPS99	0,584	4,030	0,279 (0,37)	0,428 (0,23)	0,533 (0,23)	80,11
	MPS100	0,890	4,218	0,440 (0,37)	0,663 (0,22)	0,816 (0,19)	81,03
	CSDM15	0,622	3,061	0,236 (0,63)	0,414 (0,34)	0,552 (0,23)	97,56
	CSDM25	0,270	1,238	0,025 (1,61)	0,099 (0,85)	0,201 (0,59)	90,83
AIS4	MPS95	0,646	6,051	0,395 (0,43)	0,526 (0,26)	0,608 (0,22)	30,99
	MPS99	0,809	7,133	0,534 (0,41)	0,680 (0,24)	0,769 (0,18)	30,40
	MPS100	1,125	8,681	0,799 (0,34)	0,974 (0,19)	1,078 (0,13)	34,18
	CSDM15	0,820	11,485	0,633 (0,27)	0,736 (0,15)	0,794 (0,11)	37,95
	CSDM25	0,553	3,873	0,257 (0,81)	0,401 (0,47)	0,503 (0,33)	34,57

QI: quality index and its categories based on (Reference [64]), the quality of injury risk functions can be categorized into 'good' (0,0 – 0,5); 'fair' (0,5 – 1,0); 'marginal' (1,0 – 1,5); 'Unacceptable' (> 1,5).

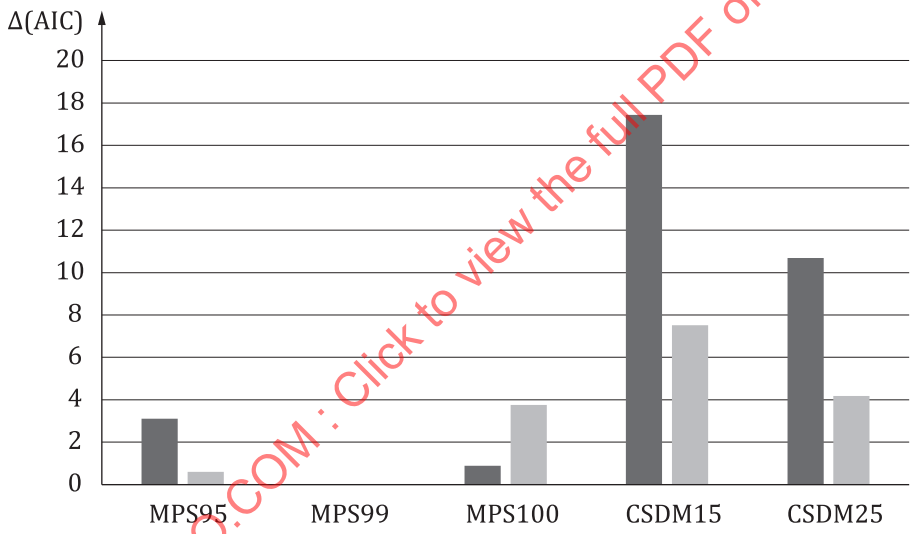

For each candidate IRC, the differences of AICs were calculated as: Δ_i (AIC) = AIC_i - min(AIC), where AIC_i is the AIC value for the candidate IRC, and min(AIC) is the minimum of the AIC values among all the IRCs.

Figure B.5 — Difference of AIC to measure the goodness of fit

B.2.5 Linear correlation between tissue-level and kinematics-based brain injury metrics

The tissue-level brain injury metrics cannot be measured directly by the THOR dummy. Based on its high correlation with the tissue-level brain injury metrics, previously proposed kinematics-based brain injury metrics can be used as alternative metrics for the practical application of the developed tissue-level IRCs to the THOR dummy.

Identifying correlations between the tissue-level injury metrics and existing kinematics-based brain injury metrics, the capability of the kinematics-based brain injury metrics for predicting brain tissue

strain was evaluated under diverse human head impact loading conditions. For this, a human head kinematics data set previously developed (Reference [17]) was used. The data set comprises 1,595 head motion and head impact tests, as summarized in B.2.2. Using the human brain FE model shown in Figure B.1, each test in the data set were reconstructed by providing the 6 degree-of-freedom head kinematics data obtained from the data set, directly to the centre of gravity of the rigid dura. Then, tissue-level brain injury metrics including MPS95, MPS99, MPS100, CSDM15 and CSDM25 were extracted. All the FE simulations were conducted using LS-DYNA (v971 R9.2.0. double precision; LSTC). Also, previously proposed kinematics-based brain injury metrics were calculated with the head kinematic data. Here, the following 10 head kinematics-based brain injury criteria recently published after 2010 were considered, BITS (Reference [1]), BrIC (Reference [81]), CIBIC (Reference [80]), DAMAGE (Reference [18]), NBIC (Reference [36]), PRHIC (Reference [37]), RBIC (Reference [54]), RIC (Reference [38]), RVCI (Reference [91]), UBrIC (Reference [16]). Applying linear regression analysis using least squares, correlations between tissue-level brain injury metrics and the kinematics-based brain injury metrics were assessed based on the coefficient of determination, as summarized in Figure B.6. The five kinematics-based brain injury metrics with greater coefficient of determination, DAMAGE, UBrIC, CIBIC, BrIC and RVCI shown in Figure B.7, were selected. For tissue-level brain injury metrics, DAMAGE, UBrIC, BrIC and RVCI have the best correlation with MPS95, and CIBIC with MPS99.

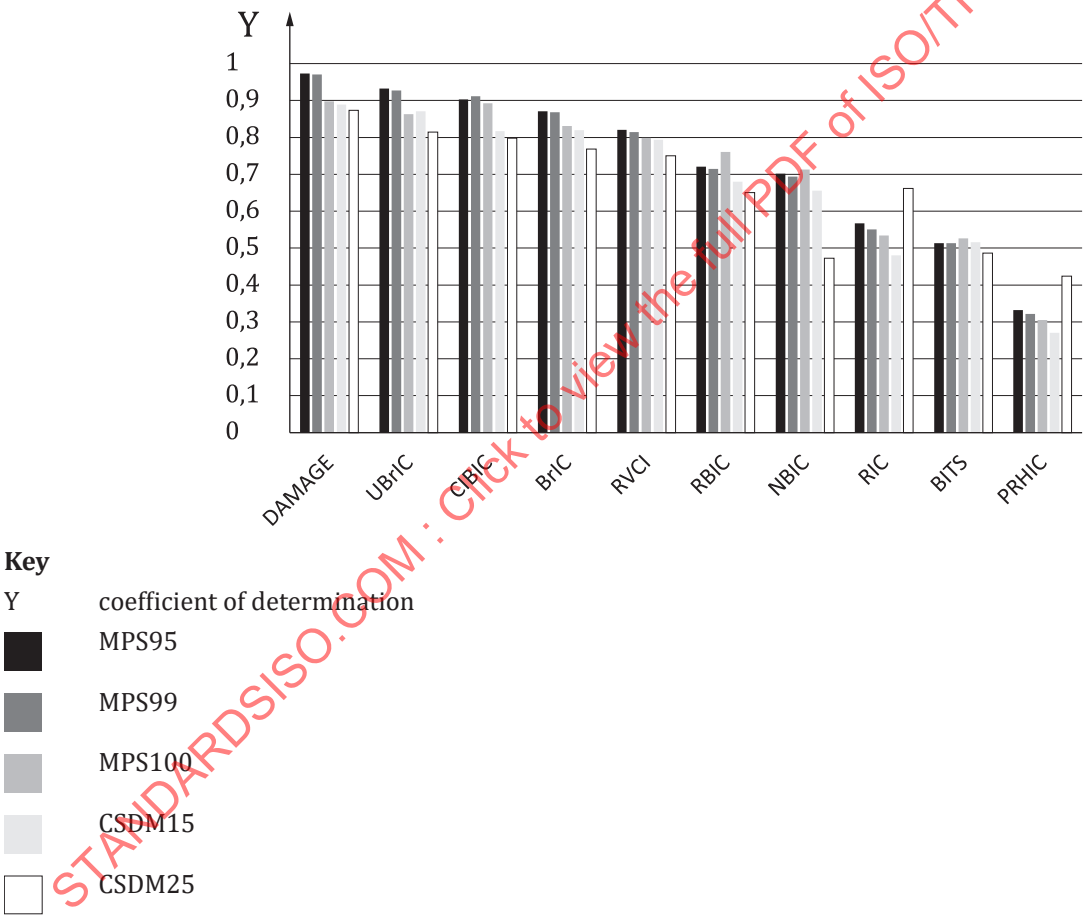

Figure B.6 — Coefficients of determination of different kinematics-based brain injury metrics based on their correlation with tissue-level brain injury metrics

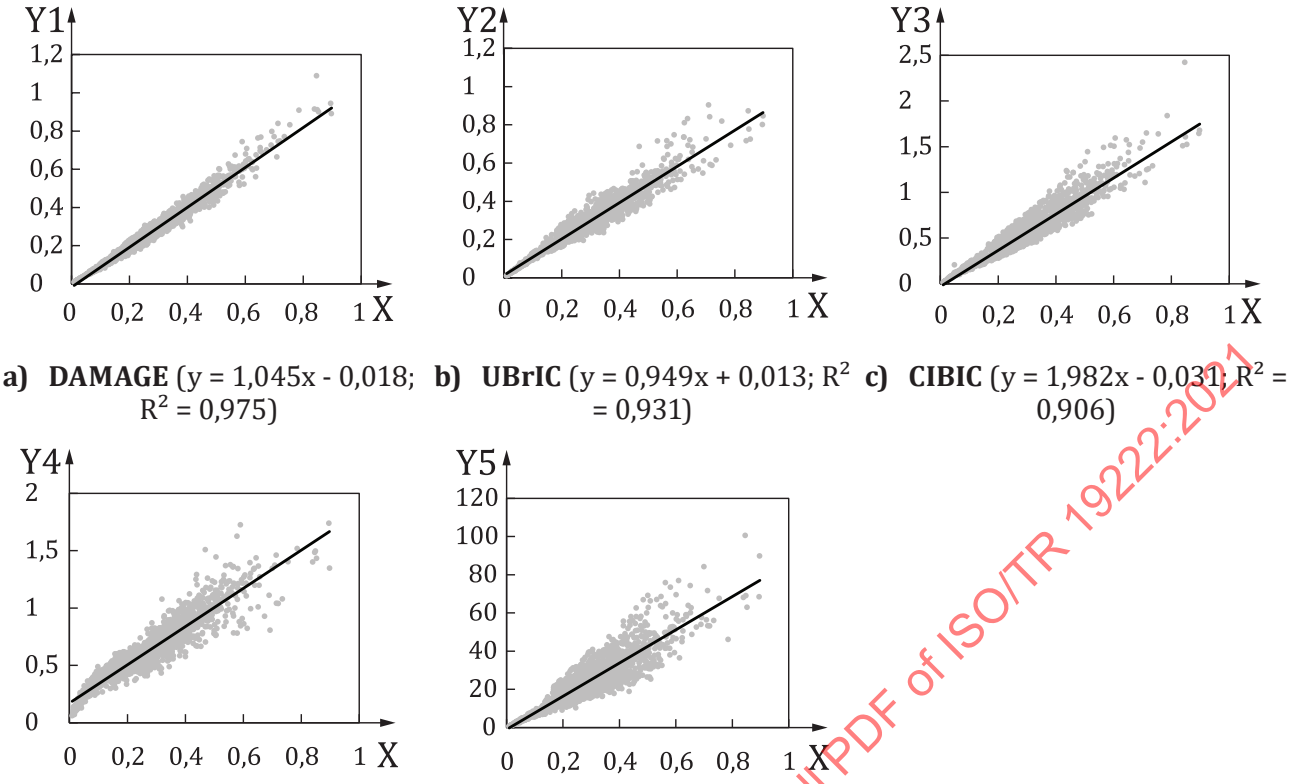

a) DAMAGE (y = 1,045x - 0,018; R^2 = 0,975) **b) UBrIC** (y = 0,949x + 0,013; R^2 = 0,931) **c) CIBIC** (y = 1,982x - 0,031; R^2 = 0,906)

d) BrIC (y = 1,666x + 0,171; R^2 = 0,873) **e) RVCI** (y = 86,938x - 1,017; R^2 = 0,820)

Key

X MPS95
Y1 DAMAGE
Y2 UBrlc
Y3 CIBIC
Y4 Brlc
Y5 RVCI

Figure B.7 — Linear regression model between MPS95 and the top five best kinematics-based brain injury metrics

B.2.6 Development of kinematics-based brain injury risk curves

Previous studies have used MPS95 to avoid having the responses of a few elements characterise the simulation results of the whole brain (References [15] and [60]). Considering both the AIC and R2 evaluations, the MPS95 IRCs were also used in this document to develop kinematics-based IRCs. Using the linear regression equations in Figure B.7, IRCs for the five kinematics-based brain injury metrics were transferred from MPS95 IRCs, as shown in Figure B.8. The IRCs for kinematics-based injury metrics can be obtained based on the formula in B.2.4 and the linear regression ($x = dy + c$) between the tissue-level brain injury metrics x and the kinematics-based brain injury metrics y, as formulated below. The coefficients and quality index of each IRC are summarized in Table B.2.

$$P_{\text{injury}} = 1 - e^{\left(-e^{\left(\frac{1}{b}\times\ln(dy+c)-\frac{a}{b}\right)}\right)}$$

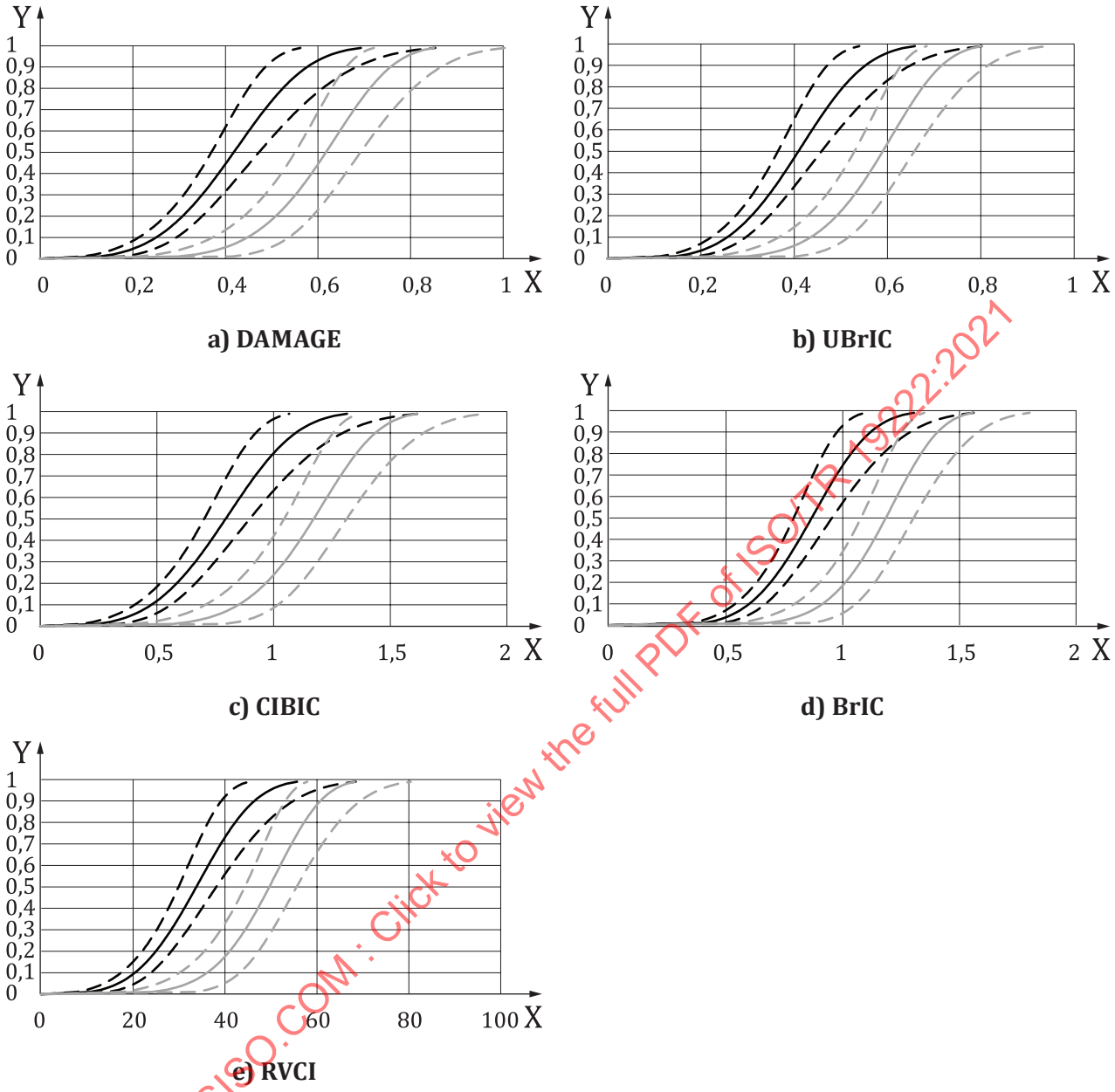

a) DAMAGE

b) UBrIC

c) CIBIC

d) BrIC

e) RVCI

Key

X brain injury metric

Y risk of injury

——— IRF (AIS2)

– – – CI (AIS2)

——— IRF (AIS4)

– – – CI (AIS4)

Figure B.8 — IRCs for the kinematics-based brain injury metrics developed based on MPS 95 IRCs.

Table B.2 — Model coefficients and quality index of the kinematics-based IRCs

Injury	Metrics	Scale (e^a)	Shape ($1/b$)	Intercept (c)	Slope (d)	5 % Risk (QI)	25 % Risk (QI)	50 % Risk (QI)
AIS2	DAMAGE	0,459	3,875	0,017	0,957	0,205 (0,41)	0,330 (0,25)	0,418 (0,25)
	UBrIC			-0,014	1,054	0,215 (0,36)	0,329 (0,22)	0,409 (0,23)
	CIBIC			0,016	0,505	0,390 (0,41)	0,627 (0,25)	0,794 (0,25)
	BrIC			-0,103	0,600	0,527 (0,26)	0,726 (0,18)	0,867 (0,19)
	RVCI			0,012	0,012	16,75 (0,40)	26,70 (0,24)	33,76 (0,24)
AIS4	DAMAGE	0,646	6,051	0,017	0,957	0,395 (0,45)	0,531 (0,27)	0,617 (0,23)
	UBrIC			-0,014	1,054	0,388 (0,42)	0,512 (0,25)	0,590 (0,22)
	CIBIC			0,016	0,505	0,751 (0,45)	1,009 (0,27)	1,172 (0,23)
	BrIC			-0,103	0,600	0,830 (0,35)	1,048 (0,22)	1,185 (0,19)
	RVCI			0,012	0,012	31,93 (0,45)	42,79 (0,27)	49,64 (0,23)

QI: quality index and its categories based on (Reference [64]), the quality of injury risk functions can be categorized into 'good' (0,0 – 0,5); 'fair' (0,5 – 1,0); 'marginal' (1,0 – 1,5); 'Unacceptable' (> 1,5).

B.2.7 Field data evaluation

The developed tissue-level IRCs were evaluated by comparing the predicted injury risk with real-world accident analysis. The real-world accident analysis was conducted on the National Automotive Sampling System Crashworthiness Data System (NASS-CDS) in a manner previously used (Reference [67]).

Since the direct measures of the head kinematics were not available in the NASS-CDS, 534 crash tests conducted by the National Highway Traffic Safety Administration (NHTSA), the Insurance Institute for Highway Safety (IIHS) and Transport Canada (TC) were used to predict the risk of brain injury. The crash test data set comprises full engagement, moderate overlap, small overlap, and oblique crash tests, as summarized in B.3.3. Using the human brain FE model shown in Figure B.1, crash tests in the data set were reconstructed by giving the 6 degree-of-freedom head kinematics data taken from ATDs, directly to the centre of gravity of the rigid dura. The tissue-level brain injury metric MPS95 was extracted from the computational reconstructions and applied to the MPS95 IRCs. All the FE simulations were conducted using LS-DYNA[2)] (v971 R9.2.0. double precision; LSTC).

To analyse the field injury incident rates of diffuse-type TBIs in similar crash configurations to the above collected crash tests, accident cases that satisfy the following inclusion criteria in the NASS-CDS were selected:

— crash year 2001-2015,

— vehicle model year 2001-2016,

— passenger cars (including SUV and wagons, excluding minivan and truck),

— seat position: driver or front passenger,

— non-ejected, airbag-deployed and belted occupant,

2) LS-DYNA is the trademark of a product supplied by LST. This information is given for the convenience of users of this document and does not constitute an endorsement by ISO of the product named. Equivalent products may be used if they can be shown to lead to the same results.

— no rollover,

— age 15 or higher,

— occupants with known injury outcomes.

After obtaining the NASS-CDS cases meeting the inclusion criteria, diffuse-type TBIs sustained were categorized into AIS2+ and AIS4+ injuries based on the AIS codes (1998 version). Corresponding to the crash tests, four crash configurations were identified based on principle direction of deformation (PDOF), general area of damage (GAD), deformation location - specific longitudinal or lateral location (SHL) and extent of deformation (EXTENT):

— full engagement (PDOFs: 11, 12 and 1 o'clock, GAD: F, SHL: D, EXTENT: 3-6);

— moderate overlap (PDOFs: 11, 12 and 1 o'clock, GAD: F, SHL: Y, EXTENT: 3-6);

— small overlap (PDOFs: 11, 12 and 1 o'clock, GAD: F, SHL: L, EXTENT: 3-6);

— oblique (PDOFs: 11 and 12o'clock, GAD: F, SHL: Y, EXTENT: 3-6).

The real-world injury incident rates were calculated as the weighted number of occupants with a certain diffuse-type TBI divided by the weighted number of occupants with known injury status for each crash configuration. The real-world injury incident rates were used as the representative real-world injury risks of sustaining diffuse-type TBIs for certain crash configurations.

The median injury risks predicted using the MPS 95 IRCs were compared with the AIS2+ and AIS4+ injury incident rates in the NASS-CDS, as shown in Figure B.9. For the full engagement crash configuration, the absolute errors of injury risk were smaller than 0,1.

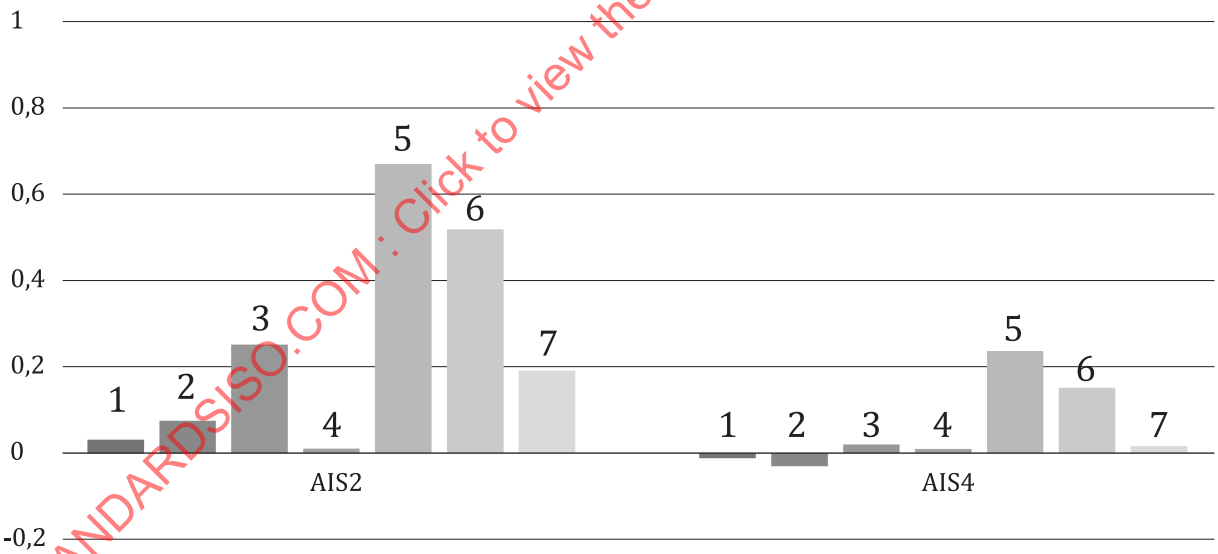

Key

1 driver, full engagement
2 passenger, full engagement
3 driver, moderate
4 passenger, moderate
5 driver, oblique
6 passenger, oblique
7 driver, small overlap

Error was calculated by subtracting the weighted field injury incident rate from median of the predicted injury risks. Positive values indicated over predicting injury.

Figure B.9 — Errors between the predicted injury risks (MPS95) and field injury incident rates

B.2.8 Limitations

The kinematics-based brain injury metrics and the associated IRCs described in this document were proposed as the predictors of diffuse-type TBIs based on MPS95 obtained from the GHBMC brain FE model (v4.3) and the harmonised NHP brain FE models. Many studies related to TBIs, including diffuse-type injuries, are still in progress. Addressing the following limitations would provide more accurate brain injury metrics and IRCs in future.

Definitions of concussion in the TBI data set: there were several limitations related to diagnosing concussion in the subjects included in the TBI data set. Historically, the clinical and theoretical definitions of concussion and corresponding AIS codes have varied (References [42]; [63]). Subsequent revisions of the AIS may have introduced changes in coding the severity of equivalent traumatic brain injuries. The volunteer and NHP tests used for developing the IRC in this document were conducted when the concussion was defined by a loss of consciousness. The definition of concussion has changed since then. Modern definitions have a wider range of symptoms and do not require the loss of consciousness. The diagnoses of concussion for the professional football players were more consistent with the contemporary definition of concussion and were established after play and verified with follow-up medical testing and treatment of the players. However, there were still some variations in symptoms compared with current concussion diagnosis techniques (Reference [62]). In addition, cognitive dysfunction in the NHP subjects was difficult to detect, and the diagnosis of concussion or no injury could be erroneous. Future studies to acquire and investigate concussion data would improve the ASI2 IRCs in this work.

Football data in the TBI data set: the fidelity of the football reconstruction data used to develop the IRCs was dependent on the biofidelity of ATDs (Anthropomorphic Test Devices) (Hybrid-III). The biofidelity of the Hybrid-III was previously evaluated for sports injury scenarios. The Hybrid-III produced similar peak head accelerations for concussive impacts but generated higher head rotational velocities under blunt impact (Reference [75]). Also, the ATDs were designed to replicate PMHS responses. The axial rotation of the ATD head might not be realistic for human volunteers because of the lack of muscle activity (Reference [84]). The head motion would be affected by the condition of the brain, and the difference between human volunteers and PMHSs needs to be considered. Further on, the head kinematics of different ATDs in similar conditions were also discordant. For the Hybrid-III and THOR dummies, experimental studies demonstrated the differences of head kinematics between these two dummies in controlled laboratory tests (References [22]; [61]).

Brain FE models and tissue-level and kinematics-based brain injury metrics: the IRCs provided in this document depend on the accuracy of the FE models. Although the brain FE model of GHBMC v4.3 has been validated for brain deformation (Reference [45]), the head kinematics and brain strain responses for some cases used to develop the IRCs were observed beyond the range of the experimental data for validation of the brain FE model. For the NHP brain FE models, the absence of or validation is also a limitation due to lack of NHP experiment data. In addition, the IRCs in this document rely on the capability of the FE-derived tissue-level brain injury metrics. The tissue-level brain injury metrics used in this document are derived from maximum principle strain of the brain tissue. As other brain injury predictors, strain rate (Reference [39]), the product of strain and strain rate (References [39]; [79]), fibre-oriented (Reference [79]) and region-specific strain (Reference [39]) have been proposed. Furthermore, kinematics-based brain injury metrics, such as BrIC, CIBIC, DAMAGE and UBRIC, were developed based on brain strain responses of the GHBMC brain FE model. These kinematics-based brain injury metrics contain limitations that are inherent in the GHBMC brain FE model and tissue-level brain injury metrics.

Human head kinematic data set: selection bias was a concern with the human head kinematic data set. The human head kinematic data set used to analyse correlations between the tissue-level and kinematics-based brain injury metrics comprises various test configurations and test subjects including frontal, side, pedestrian impacts etc. with ATDs, PMHSs and human volunteers, as summarized in B.2.2. Experimental investigations have demonstrated that head kinematics responses depended on the type of test subjects even in similar impact conditions (References [22]; [61]). The selection bias in the human head kinematic data set might have some effect on values of the coefficient of determination.

B.3 Data

B.3.1 TBI data set for the construction of the tissue-level IRCs.

In order to develop IRCs for AIS2 and AIS4, in vivo human and NHP experiment data with known 6-degree-of-freedom head kinematic time histories and clinical outcomes were collected, as summarized in Table B.3. Detailed information for each case is provided in Tables B.4 and B.5. The AIS 98 version was used for classification of TBI severities. The main limitation of the human data is that it provides information on concussion. Hence, the NHP were used to span clinical outcomes from no injury to DAI.

Table B.3 — Summary of the TBI data set

Data source (reference)	Sample size (n=466)	Surrogate	Impact category (direction)	Severity (sample size)
NBDL volunteers (Reference [13])	335	Human (male)	Sled (oblique, lateral and frontal)	Sub-injurious (50)
Pellman football reconstructions (References [62], [89], [73])	53	H-III, 50TH	Real-world impact (complex)	Sub-injurious (33), AIS1 (9), AIS2 (11)
JARI blunt impacts (Reference [35])	5	Macaque	Impactor tests (lateral)	Sub-injurious (5)
Penn non-impact rotational tests (Reference [83])	56	Baboon	Rotation (axial and coronal)	AIS4-5 (56)
UMTRI blunt impacts (Reference [77])	17	Macaque	Impactor tests (lateral and occipital)	Sub-injurious (4), AIS2-3 (8), AIS4-6 (5)

Human data

1) NBDL volunteers: this data set contains in total 335 sled tests with 22 human volunteers, conducted at the Naval Biodynamics Laboratory (NBDL) (Reference [13]). The human volunteers were subjected to frontal, lateral, and oblique sled conditions up to 16*g* peak sled acceleration.

2) Pellman football reconstructions: this data set contains 53 head kinematic data with known clinical outcomes (20 concussed and 33 non-concussed), obtained from 31 National Football League (NFL) head impacts reconstruction experiments. The data was originally published by Reference [62] and re-evaluated by Reference [73]. The clinical information for the concussed players was detailed by Reference [89].

NHP data

1) JARI blunt impacts: this data set was selected from a series of NHP experiments conducted at the Japan Automobile Research Institute (JARI) (Reference [35]). The original series of the experiments contains a total of 193 head impacts with 89 macaque subjects under various loading conditions. As most of the macaques were subjected to impact tests several times, the injury outcomes were ambiguous. Only five sub-injurious macaque data were usable to develop the injury risk curve in this document.

2) Penn non-impact rotational tests: this data set consists of 56 baboon tests with DAI, conducted at the University of Pennsylvania (UPenn). The baboons were subjected to controlled non-impact biphasic rotational acceleration-deceleration to the head. The original time scale of the angular acceleration was incorrectly documented (References [19]; [46]), and collected by Reference [49]. For developing the IRCs in this document, all of the collected data for 56 baboon tests were used.

3) UMTRI blunt impacts: this data set was selected from a series of NHP experiments conducted at the University of Michigan Transportation Research Institute (UMTRI) (Reference [77]). Macaques were subjected to padded and rigid impacts to the heads using a pneumatic impacting device. For developing the IRCs in this document, 17 macaque test data containing 4 no injuries, 8 AIS2-3 injuries and 5 AIS4+ injuries were used.

Table B.4 — TBI data set – non-human primate data (n=78)

Source	Species	ID	Sex	Age	Brain mass [g]	Injury description	AIS coding	Symptoms
UMTRI	rhesus[c]	2-004	N/A	N/A	88	no injury	0	No
		3-012	N/A	N/A	81	concussion	2	Unconscious < 15 min
		2-013	N/A	N/A	88	no injury	0	Slightly dazed[a]
		2-014	N/A	N/A	86	dead, ICH	6	Dead
		2-015	N/A	N/A	88	no injury	0	No[a]
	cynomolgus[c]	2-019	N/A	N/A	64	no injury	0	No[a]
		2-020	N/A	N/A	54	concussion	2	Unconscious < 15 min
	Rhesus[c]	2-024	N/A	N/A	111	concussion	2-3	Dazed 2 min
		2-025	N/A	N/A	105	concussion, skull fracture	2-3	Unconscious < 15 min
		2-027	N/A	N/A	100	contusion, DAI	4	Unconscious > 15 min
		2-030	N/A	N/A	112	concussion, skull fracture	2	Dazed 1 min
		2-031	N/A	N/A	112	concussion, skull fracture	2	Unconscious < 15 min
	Cynomolgus[c]	2-089	N/A	N/A	57	DAI, ICH	5	Unconscious > 15 min
		2-090	N/A	N/A	57	concussion, skull fracture	3	Unconscious < 15 min
		2-092	N/A	N/A	67	ICH	3	Unconscious < 15 min
		2-093	N/A	N/A	78	fracture, ICH	5-6	Unconscious < 15 min
	baboon	2-096	N/A	N/A	163	fracture, ICH	5	Unconscious > 15 min

[a] No symptoms, or very minor symptoms, which may be caused by invasive instrumentations instead of the impact.

[b] The histopathological identification of DAI was dependent upon the visualization of abnormal axonal profiles, but individual information is unavailable.

[c] Macaques (Genus Macaca): rhesus macaque (Macaca mulatta), cynomolgus macaque (Macaca fascicularis), Japanese macaque (Macaca fuscata).

Table B.4 *(continued)*

Source	Species	ID	Sex	Age	Brain mass [g]	Injury description	AIS coding	Symptoms
JARI	Japanese macaque[c]	402	Female	4	107	no injury	0	No[a]
		542	Male	N/A	110	no injury	0	No[a]
		541	Male	N/A	110	no injury	0	No[a]
		529	Male	N/A	130	no injury	0	No[a]
	Cynomolgus[c]	539	Male	N/A	71	no injury	0	No*
UPenn	baboon	B01	Female	N/A	143	DAI	4-5	N/A[b]
		B10	Female	N/A	160	DAI	4-5	N/A[b]
		B100	Female	N/A	134	DAI	4-5	N/A[b]
		B101	Female	N/A	130	DAI	4-5	N/A[b]
		B11	Female	N/A	153	DAI	4-5	N/A[b]
		B20	Female	N/A	112	DAI	4-5	N/A[b]
		B23	Female	N/A	139	DAI	4-5	N/A[b]
		B30	Female	N/A	169	DAI	4-5	N/A[b]
		B32	Female	N/A	124	DAI	4-5	N/A[b]
		B33	Female	N/A	149	DAI	4-5	N/A[b]
		B35	Female	N/A	125	DAI	4-5	N/A[b]
		B37	Female	N/A	150	DAI	4-5	N/A[b]
		B92	Female	N/A	156	DAI	4-5	N/A[b]
		BB2	N/A	N/A	116	DAI	4-5	N/A[b]
		BB3	N/A	N/A	105	DAI	4-5	N/A[b]
		BB6	Female	N/A	128	DAI	4-5	N/A[b]
		BB7	Female	N/A	139	DAI	4-5	N/A[b]
		BB8	Female	N/A	136	DAI	4-5	N/A[b]
		BB9	Female	N/A	126	DAI	4-5	N/A[b]
		RR18	N/A	N/A	81	DAI	4-5	N/A[b]
		RR21	Female	N/A	101	DAI	4-5	N/A[b]
		RR22	Female	N/A	96	DAI	4-5	N/A[b]
		1098	N/A	N/A	80	DAI	4-5	N/A[b]
		1106	N/A	N/A	115	DAI	4-5	N/A[b]
		1108	N/A	N/A	140	DAI	4-5	N/A[b]
		1109	N/A	N/A	160	DAI	4-5	N/A[b]
		1112	N/A	N/A	155	DAI	4-5	N/A[b]
		1114	N/A	N/A	170	DAI	4-5	N/A[b]
		1115	N/A	N/A	160	DAI	4-5	N/A[b]
		1116	N/A	N/A	140	DAI	4-5	N/A[b]
		1121	N/A	N/A	152	DAI	4-5	N/A[b]
		1125	N/A	N/A	124	DAI	4-5	N/A[b]
		1126	N/A	N/A	149	DAI	4-5	N/A[b]
		1127	N/A	N/A	129	DAI	4-5	N/A[b]

[a] No symptoms, or very minor symptoms, which may be caused by invasive instrumentations instead of the impact.

[b] The histopathological identification of DAI was dependent upon the visualization of abnormal axonal profiles, but individual information is unavailable.

[c] Macaques (Genus Macaca): rhesus macaque (Macaca mulatta), cynomolgus macaque (Macaca fascicularis), Japanese macaque (Macaca fuscata).

Table B.4 *(continued)*

Source	Species	ID	Sex	Age	Brain mass [g]	Injury description	AIS coding	Symptoms
		1131	N/A	N/A	140	DAI	4-5	N/A[b]
		1135	N/A	N/A	135	DAI	4-5	N/A[b]
		1136	N/A	N/A	138	DAI	4-5	N/A[b]
		1137	N/A	N/A	140	DAI	4-5	N/A[b]
		1139	N/A	N/A	149	DAI	4-5	N/A[b]
		1140	N/A	N/A	147	DAI	4-5	N/A[b]
		1141	N/A	N/A	152	DAI	4-5	N/A[b]
		1142	N/A	N/A	140	DAI	4-5	N/A[b]
		1143	N/A	N/A	163	DAI	4-5	N/A[b]
		1144	N/A	N/A	140	DAI	4-5	N/A[b]
		1145	N/A	N/A	140	DAI	4-5	N/A[b]
		1149	N/A	N/A	148	DAI	4-5	N/A[b]
		1154	N/A	N/A	126	DAI	4-5	N/A[b]
		1156	N/A	N/A	140	DAI	4-5	N/A[b]
		1157	N/A	N/A	140	DAI	4-5	N/A[b]
		1158	N/A	N/A	130	DAI	4-5	N/A[b]
		1159	N/A	N/A	134	DAI	4-5	N/A[b]
		1160	N/A	N/A	140	DAI	4-5	N/A[b]
		1161	N/A	N/A	140	DAI	4-5	N/A[b]
		1162	N/A	N/A	140	DAI	4-5	N/A[b]
		1163	N/A	N/A	140	DAI	4-5	N/A[b]
		1164	N/A	N/A	140	DAI	4-5	N/A[b]

[a] No symptoms, or very minor symptoms, which may be caused by invasive instrumentations instead of the impact.

[b] The histopathological identification of DAI was dependent upon the visualization of abnormal axonal profiles, but individual information is unavailable.

[c] Macaques (Genus Macaca): rhesus macaque (Macaca mulatta), cynomolgus macaque (Macaca fascicularis), Japanese macaque (Macaca fuscata).

Table B.5 — TBI data set – human data (n=388)

Source	Surrogate	ID	Sex	Age	Brain mass [g]	Injury description[b]	AIS Coding	Symptoms
		7 Striking	Male	N/A	N/A	no injury	0	N/A
		7 Struck	Male	N/A	N/A	MTBI	1	Dizziness

[a] Detailed information of the NDBL are listed in B.2.2.

[b] In the Sanchez's NFL data, the reconstructed concussion cases in the laboratory were independently verified as mild traumatic brain injuries (MTBIs) by two members of the MTBI committee (NFL team physicians) who reviewed the clinical information. The clinical information reviewed originated from three sources, i.e. team physician forms, athletic trainer forms, and through a direct contact with the member of the MTBI committee along with the medical staff of the injured player (independent verification).

[c] In the NBDL volunteer data, original medical reports were reviewed (non-blinded) by a clinician (JSM) specifically looking for evidence related to the current state of concussion and mild traumatic brain injury symptomatology. Pre- and post-test medical evaluations showed no clinical evidence of injury for any of the volunteers. Some volunteers had minor pre-existing orthopaedic issues identified during the entrance examination, none of which were affected by their participation in the research study. Following testing, participants returned to their daily jobs and did not seem to be affected by participation in the study.

Table B.5 *(continued)*

Source	Surrogate	ID	Sex	Age	Brain mass [g]	Injury description[b]	AIS Coding	Symptoms
		9 Striking	Male	N/A	N/A	no injury	0	N/A
		9 Struck	Male	N/A	N/A	MTBI	1	N/A
		38 Striking	Male	N/A	N/A	no injury	0	N/A
		38 Struck	Male	N/A	N/A	MTBI	2	Memory problem
		39 Striking	Male	N/A	N/A	no injury	0	N/A
		48 Striking	Male	N/A	N/A	no injury	0	N/A
		48 Striking	Male	N/A	N/A	no injury	0	N/A
		57 Striking	Male	N/A	N/A	no injury	0	N/A
		59 Striking	Male	N/A	N/A	no injury	0	N/A
		59 Striking	Male	N/A	N/A	no injury	0	N/A
		69 Striking	Male	N/A	N/A	no injury	0	N/A
		69 Struck	Male	N/A	N/A	MTBI	2	Loss of consciousness Memory problem
		71 Striking	Male	N/A	N/A	no injury	0	N/A
		71 Struck	Male	N/A	N/A	MTBI	1	Headache, dizziness
		77 Striking	Male	N/A	N/A	no injury	0	N/A
		77 Struck	Male	N/A	N/A	MTBI	2	Memory problem
		84 Striking	Male	N/A	N/A	no injury	0	N/A
		84 Struck	Male	N/A	N/A	MTBI	2	Memory problem
		92 Striking	Male	N/A	N/A	no injury	0	N/A
		92 Struck	Male	N/A	N/A	MTBI	2	Memory problem
Sanchez	H-III	98 Striking	Male	N/A	N/A	no injury	0	N/A
		98 Struck	Male	N/A	N/A	MTBI	1	Headache
		113 Striking	Male	N/A	N/A	no injury	0	N/A
		113 Struck	Male	N/A	N/A	MTBI	2	Memory problem
		118 Striking	Male	N/A	N/A	no injury	0	N/A
		118 Struck	Male	N/A	N/A	MTBI	1	Headache
		124 Striking	Male	N/A	N/A	no injury	0	N/A
		124 Struck	Male	N/A	N/A	MTBI	2	Loss of consciousness
		125 Striking	Male	N/A	N/A	no injury	0	N/A
		125 Struck	Male	N/A	N/A	MTBI	2	Memory problem

[a] Detailed information of the NDBL are listed in B.2.2.

[b] In the Sanchez's NFL data, the reconstructed concussion cases in the laboratory were independently verified as mild traumatic brain injuries (MTBIs) by two members of the MTBI committee (NFL team physicians) who reviewed the clinical information. The clinical information reviewed originated from three sources, i.e. team physician forms, athletic trainer forms, and through a direct contact with the member of the MTBI committee along with the medical staff of the injured player (independent verification).

[c] In the NBDL volunteer data, original medical reports were reviewed (non-blinded) by a clinician (JSM) specifically looking for evidence related to the current state of concussion and mild traumatic brain injury symptomatology. Pre- and post-test medical evaluations showed no clinical evidence of injury for any of the volunteers. Some volunteers had minor pre-existing orthopaedic issues identified during the entrance examination, none of which were affected by their participation in the research study. Following testing, participants returned to their daily jobs and did not seem to be affected by participation in the study.

Table B.5 *(continued)*

Source	Surrogate	ID	Sex	Age	Brain mass [g]	Injury description[b]	AIS Coding	Symptoms
		135 Striking	Male	N/A	N/A	no injury	0	N/A
		135 Struck	Male	N/A	N/A	MTBI	1	Headache
		142 Striking	Male	N/A	N/A	no injury	0	N/A
		148 Striking	Male	N/A	N/A	no injury	0	N/A
		148 Struck	Male	N/A	N/A	MTBI	1	Headache, dizziness
		154 Striking	Male	N/A	N/A	no injury	0	N/A
		154 Striking	Male	N/A	N/A	no injury	0	N/A
		155 Striking	Male	N/A	N/A	no injury	0	N/A
		155 Struck	Male	N/A	N/A	MTBI	2	Memory problem
		157 Striking	Male	N/A	N/A	no injury	0	N/A
		157 Struck	Male	N/A	N/A	MTBI	2	Loss of consciousness
		162 Striking	Male	N/A	N/A	no injury	0	N/A
		162 Struck	Male	N/A	N/A	MTBI	2	Memory problem
		164 Striking	Male	N/A	N/A	no injury	0	N/A
		164 Struck	Male	N/A	N/A	MTBI	1	Somatic complaints
		175 Striking	Male	N/A	N/A	no injury	0	N/A
		175 Striking	Male	N/A	N/A	no injury	0	N/A
		181 Striking	Male	N/A	N/A	no injury	0	N/A
		181 Struck	Male	N/A	N/A	MTBI	1	N/A
		182 Striking	Male	N/A	N/A	no injury	0	N/A
		182 Striking	Male	N/A	N/A	no injury	0	N/A
NBDL	Human	LX3779 - LX4119 (335 cases)[a]	Male	20	N/A	no injury	0	N/A[c]

[a] Detailed information of the NDBL are listed in B.2.2.

[b] In the Sanchez's NFL data, the reconstructed concussion cases in the laboratory were independently verified as mild traumatic brain injuries (MTBIs) by two members of the MTBI committee (NFL team physicians) who reviewed the clinical information. The clinical information reviewed originated from three sources, i.e. team physician forms, athletic trainer forms, and through a direct contact with the member of the MTBI committee along with the medical staff of the injured player (independent verification).

[c] In the NBDL volunteer data, original medical reports were reviewed (non-blinded) by a clinician (JSM) specifically looking for evidence related to the current state of concussion and mild traumatic brain injury symptomatology. Pre- and post-test medical evaluations showed no clinical evidence of injury for any of the volunteers. Some volunteers had minor pre-existing orthopaedic issues identified during the entrance examination, none of which were affected by their participation in the research study. Following testing, participants returned to their daily jobs and did not seem to be affected by participation in the study.

B.3.2 Human head kinematic data set for analysing correlations between tissue-level and kinematics-based brain injury metrics

To investigate the relationship between tissue-level and kinematics-based brain injury metrics, a previously developed data set (Reference [17]) was used. The data set consists of 1 595 head kinematics data taken from ATDs, PMHSs and human volunteers subjected to various loading conditions. A breakdown of the test conditions is presented in Table B.6. Detailed lists of the data set are presented in Tables B.7 to B.12.

Table B.6 — Summary of the human head kinematic data set

Impact category (sample size)	Impact condition (sample size)	Test details (sample size)	Reference	Surrogates
Automotive (491)	Frontal (258)	UVA driver side universal gold standard (13)	(Reference [8])	THOR, M50 (13)
		UVA rear seat occupant (7)	(Reference [14])	H-III, M50 (4) H-III, F05 (3)
		NHTSA NCAP driver (46)	NHTSA	H-III, M50 (73) H-III, F05 (14)
		NHTSA NCAP front passenger (35)	NHTSA	
		NHTSA RSVT driver and rear passenger (6)	NHTSA	
		IIHS small & moderate overlap impact driver (151)	IIHS	H-III, M50 (151)
	Oblique (97)	UVA 20° & 60° far side oblique (31)	(References [9], [14])	PMHS (24) H-III, M50 (7)
		UVA rear seat occupant (12)	(Reference [14])	THOR, M50 (12)
		NHTSA R&D driver near side (31)	NHTSA	THOR, M50 (31)
		NHTSA R&D rear passenger near side (23)	NHTSA	H-III, F05 (23)
	Side (104)	UVA 90° far side pure lateral (14)	(Reference [14])	PMHS (14)
		UVA rear seat occupant (1)	(Reference [14])	H-III, M50 (1)
		NHTSA NCAP driver near side (33)	NHTSA	ES-2RE, M50 (59) SID-IIS, F05 (9)
		NHTSA NCAP rear passenger near side (10)	NHTSA	
		NHTSA RSVT driver and rear passenger near side (25)	NHTSA	
		IIHS driver and rear passenger near side (21)	IIHS	SID-IIS, F05 (21)
	Rear (4)	UVA rear seat occupant	(Reference [14])	H-III, F05 (3) THOR, M50 (1)
	Pedestrian (28)	UVA vehicle buck laterally into a pedestrian	(References [33], [34], [78])	PMHS (16) POLAR II, M50 (12)
Volunteer (335)	Frontal (132)	NBDL volunteer 0° rearward acceleration	(References [13], [74])	Human volunteer (20 subjects, repeated tests)
	Oblique (97)	NBDL volunteer 45° oblique acceleration		
	Side (106)	NBDL volunteer 90° lateral acceleration		
		NHTSA 0° pendulum into head CG/Forehead (74)		ES-2RE, M50 (20) H-III, F05 (23)

Table B.6 *(continued)*

Impact category (sample size)	Impact condition (sample size)	Test details (sample size)	Reference	Surrogates
Impactor tests (193)	TohHead (193)	NHTSA 30°/60° pendulum into head CG/Forehead (78)	(Reference [81])	THOR, M50 (25) WSID, F05 (41) H-III, M50 (63) SID-IIS, F05 (21)
		NHTSA 90° pendulum into head CG (41)		
Football (576)	To helmet (576)	Biokinetics oblique face-mask (72)	(Reference [90])	H-III, M50 (576)
		Biokinetics upper oblique facemask (72)		
		Biokinetics side of face-mask (72)		
		Biokinetics rear boss of shell (72)		
		Biokinetics front of shell (72)		
		Biokinetics rear of shell (72)		
		Biokinetics side of shell (72)		
		Biokinetics lower central facemask (72)		

Table B.7 — List of UVA sled tests (n=110) from the human head kinematic data set

Impact condition	Test details (sample size)	Surrogate	Source #
Frontal	Universal / gold standard 1	H-III, 50TH, M	S0171
		THOR, 50TH, M	S0156 - S0158 (3 cases)
	Universal / gold standard 2	THOR, 50TH, M	S0159 - S0161 (3 cases)
	Universal / gold standard driver side	H-III, 50TH, M	S0169, S0170
		THOR, 50TH, M	S0163, S0164, S0166, S0167
	Rear seat frontal sled test	H-III, 50TH, M	1210 - 1212 (3 cases) 1215 - 1217 (3 cases)
		H-III, 5TH, F	1218 - 1223 (6 cases)
		THOR, 50TH, M	1247 - 1252 (6 cases) 1256 - 1261 (6 cases)
Oblique	20° far side oblique sled	PMHS, 605, M	S0244
		PMHS, 642, M	S0243
		PMHS, 659, M	S0245
		H-III, 50TH, M	S0238, S0239, S0246
		THOR, 50TH, M	S0248 - S0251 (4 cases)

Table B.7 *(continued)*

Impact condition	Test details (sample size)	Surrogate	Source #
	60° far side oblique sled	PMHS, 587, M	S0126 - S0130 (5 cases)
		PMHS, 591, M	S0120 - S0125 (6 cases)
		PMHS, 602, M	S0131 - S0135 (5 cases)
		PMHS, 608, M	S0136 - S0140 (5 cases)
Side	90° far side pure lateral sled	PMHS, 551, M	S0082 - S0086 (5 cases)
		PMHS, 557, M	S0077 - S0080 (4 cases)
		PMHS, 559, M	S0087 - S0091 (5 cases)
Pedestrian	Vehicle sled laterally into pedestrian	PMHS, 326, M	1137
		PMHS, 328, M	1138
		PMHS, 352, M	1140
		PMHS, 353, M	1141
		PMHS, ID (N/A), F	M4
		PMHS, ID (N/A), F	M5
		PMHS, ID (N/A), F	S1
		PMHS, ID (N/A), F	S2
		PMHS, ID (N/A), F	S3
		PMHS, ID (N/A), F	Sed P1
		PMHS, ID (N/A), F	SUV P1
		PMHS, ID (N/A), M	Sed P2
		PMHS, ID (N/A), M	Sed P3
		PMHS, ID (N/A), M	SUV P3
		PMHS, ID (N/A), M	T6
		PMHS, ID (N/A), M	T7
		POLAR II, 50TH, M	1134, 1136
			Sed D1, Sed D2, Sed D3,
			Sed DA1, Sed DA1
			SUV D1, SUV D2, SUV D3
			SUV DA1, SUV DA2

Table B.8 — List of NHTSA Crash Tests (n=209) from the human head kinematic data set

Impact condition	Test details[a]	Surrogate[b]	Source #
Frontal	NCAP; vehicle into barrier (0˚, 1 %)	H-III, 50TH, M	3897, 3901 (2), 3915, 3916, 3952, 3987, 4080, 4090 (2), 4198 (2), 4205, 4215 (2), 4223, 4235 (2), 4237 (2)4240, 4241, 4242 (2), 4247, 4249, 4250, 4251, 4252, 4255, 4259 (2), 4264 (2), 4265, 4266, 4267, 4273, 43035287, 5301, 5567, 5594, 5595 (2),5609, 5613, 7966, 7977, 7978, 7989, 80008024, 8035, 8045, 8048, 8055, 8064, 80688071, 8077, 8081, 8091, 8106, 8151, 8153, 8156
	NCAP; vehicle into barrier (0˚, 1 %)	H-III, 5TH, F	7977, 7989, 8024, 8035, 8045, 8055, 8064, 8068, 8080, 8081, 8104, 8106, 8153, 8156
	RSVT; vehicle into barrier (0˚, 1 %)	H-III, 50TH, M	5711, 5713, 5714, 5715 (2),
	RSVT; vehicle into barrier (0˚, 50 %)	H-III, 50TH, M	6370
Oblique	RD; impactor into vehicle (7˚, 20 %)	THOR, 50TH, M	7426, 7427, 7430, 7432, 7444, 7456, 7468
	RD; impactor into vehicle (15˚, 35 %)	THOR, 50TH, M	7428, 7431, 7441, 7457, 7458, 7467, 7476
	RSVT; impactor into vehicle (9˚, 50 %)	THOR, 50TH, M	7144
	RSVT; impactor into vehicle (15˚, 18 %)	THOR, 50TH, M	6855
	RSVT; impactor into vehicle (15˚, 50 %)	THOR, 50TH, M	6852, 6937
	RSVT; vehicle into impactor (4˚, 26 %)	THOR, 50TH, M	6872
	RSVT; vehicle into impactor (6˚, 26 %)	THOR, 50TH, M	6873
	RSVT; vehicle into pole (7˚, 10 %)	THOR, 50TH, M	7145
	RSVT; vehicle into vehicle (7˚, 1 %)	THOR, 50TH, M	7292, 7293
	RSVT; vehicle into vehicle (15˚, 50 %)	THOR, 50TH, M	6830, 6831, 7371
	TPD; impactor into vehicle (7˚, 20 %)	THOR, 50TH, M	7368, 7434
	TPD; impactor into vehicle (15˚, 35 %)	THOR, 50TH, M	7366, 7429, 7433
	RD; impactor into vehicle (7˚, 20 %)	H-III, 5TH, F	7426, 7427, 7432, 7434, 7444, 7456, 7468
	RD; impactor into vehicle (15˚, 35 %),	H-III, 5TH, F	7428, 7429, 7431, 7433, 7441, 7457, 7467, 7476
	RSVT; impactor into vehicle (15˚, 10 %)	H-III, 5TH, F	6925
	RSVT; impactor into vehicle (15˚, 18 %)	H-III, 5TH, F	6855
	RSVT; impactor into vehicle (15˚, 50 %)	H-III, 5TH, F	6852, 6937
	RSVT; vehicle into impactor (4˚, 26 %)	H-III, 5TH, F	6872
	RSVT; vehicle into vehicle (15˚, 50 %)	H-III, 5TH, F	6865
	TPD; impactor into vehicle (7˚, 20 %)	H-III, 5TH, F	7368
	TPD; impactor into vehicle (15˚, 35 %)	H-III, 5TH, F	7366

[a] (##, ##) indicates impact parameters (degree offset, percent overlap).

[b] Kinematics scaled to 50TH male using the equal-stress-equal-velocity scaling technique.

Table B.8 *(continued)*

Impact condition	Test details[a]	Surrogate[b]	Source #
Side	NCAP; impactor into vehicle (90˚, 1 %)	ES-2RE, 50TH, M	3799 (2), 3800 (2), 3803 (2), 3819 (2), 3875, 3899, 4380 (2), 4456 (2), 5461, 7967, 7984, 7990, 7998, 8033, 8047, 8053, 8054, 8069, 8072, 8078, 8079, 8082, 8092, 8102, 8108, 8149, 8150, 8157
	RSVT; impactor into vehicle (90˚, 1 %)	ES-2RE, 50TH, M	4547 (2), 4551 (2)
	RSVT; vehicle into barrier (75˚, 1 %)	ES-2RE, 50TH, M	3802, 3818, 3820, 3845, 3898
	RSVT; vehicle into vehicle (90˚, 1 %)	ES-2RE, 50TH, M	4482
	TPD; vehicle into vehicle (90˚, 1 %)	ES-2RE, 50TH, M	4292 (2)
	NCAP; impactor into vehicle (90˚, 1 %)	SID-IIS, 5TH, F	8069, 8078, 8092, 8150
	NCAP; vehicle into pole (90˚, 1 %)	SID-IIS, 5TH, F	7955, 7979, 7988, 7997, 8052

[a] (##, ##) indicates impact parameters (degree offset, percent overlap).

[b] Kinematics scaled to 50TH male using the equal-stress-equal-velocity scaling technique.

Table B.9 — List of NHTSA pendulum impact tests (n=193) from the human head kinematic data set

Impact condition	Test details[a]	Surrogate[b]	Source #
Frontal	Padded pendulum impactor at 0˚ into forehead	H-III, 50TH, M	H3-50-1, H3-50-14, H3-50-17, H3-50-26, H3-50-29, H3-50-38, H3-50-45, H3-50-54, H3-50-60, H3-50-63
		THOR, 50TH, M	THOR-2 - THOR-6 (5 cases), THOR-13
	Padded pendulum impactor at 0˚ into head CG	H-III, 50TH, M	H3-50-2, H3-50-5, H3-50-13, H3-50-22, H3-50-33, H3-50-41, H3-50-42, H3-50-49, H3-50-62
		H-III, 5TH, F	H3.5.1 - H3.5.5 (5 cases), H3.5.22
		THOR, 50TH, M	THOR-1
	Unpadded pendulum impactor at 0˚ into forehead	H-III, 50TH, M	H3-50-4, H3-50-8, H3-50-10, H3-50-12, H3-50-16, H3-50-20, H3-50-24, H3-50-25, H3-50-28, H3-50-32, H3-50-34, H3-50-36, H3-50-40, H3-50-44, H3-50-48, H3-50-50, H3-50-52, H3-50-56, H3-50-57, H3-50-59, H3-50-61,
		THOR, 50TH, M	THOR-14, THOR-16, THOR-18, THOR-20, THOR-22, THOR-24
	Unpadded pendulum impactor at 0˚ into head CG	H-III, 50TH, M	H3-50-6, H3-50-9, H3-50-18, H3-50-21, H3-50-30, H3-50-37, H3-50-46, H3-50-53, H3-50-58
		H-III, 5TH, F	H3.5.11 - H3.5.16 (6 cases)

[a] (##, ##) indicates the impact parameters (degree offset, percent overlap).

[b] Kinematics scaled to 50TH male using the equal-stress-equal-velocity scaling technique.

Table B.9 *(continued)*

Impact condition	Test details[a]	Surrogate[b]	Source #
Oblique	Padded pendulum impactor at 30° into forehead	THOR, 50TH, M	THOR-7 - THOR-12 (6 cases)
	Padded pendulum impactor at 30° into head CG	H-III, 50TH, M	H3-50-7, H3-50-15, H3-50-23, H3-50-31, H3-50-39, H3-50-43, H3-50-47, H3-50-55
		H-III, 5TH, F	H3.5.7 - H3.5.10 (5 cases), H3.5.23
	Padded pendulum impactor at 60° into head CG	ES-2RE, 50TH, M	ES2-7, ES2-10, ES2-14, ES2-17, ES2-20
		SID-IIS, 5TH, F	SID2S-4, SID2S-10, SID2S-12, SID2S-17, SID2S-20
		WSID, 50TH, M	W50-6 - W50-10 (5 cases)
		WSID, 5TH, F	WS5-4, WS5-6, WS5-13, WS5-17, WS5-21
	Unpadded pendulum impactor at 30° into forehead	THOR, 50TH, M	THOR-15, THOR-17, THOR-19, THOR-21, THOR-23, THOR-25
	Unpadded pendulum impactor at 30° into head CG	H-III, 50TH, M	H3-50-3, H3-50-11, H3-50-19, H3-50-27, H3-50-35, H3-50-51
		H-III, 5TH, F	H3.5.17 - H3.5.21 (5 cases)
	Unpadded pendulum impactor at 60° into head CG	ES-2RE, 50TH, M	ES2-3, ES2-4, ES2-5, ES2-8, ES2-13
		SID-IIS, 5TH, F	SID2S-3, SID2S-7, SID2S-9, SID2S-14, SID2S-19
		WSID, 50TH, M	W50-16 - W50-21 (6 cases)
		WSID, 5TH, F	WS5-5, WS5-7, WS5-8, WS5-15, WS5-19
Side	Padded pendulum impactor at 90° into head CG	ES-2RE, 50TH, M	ES2-6, ES2-9, ES2-12, ES2-16, ES2-19
		SID-IIS, 5TH, F	SID2S-2, SID2S-6, SID2S-11, SID2S-15, SID2S-16, SID2S-21
		WSID, 50TH, M	W50-1 - W50-5 (5 cases)
		WSID, 5TH, F	WS5-2, WS5-9, WS5-11, WS5-16, WS5-20
	Unpadded pendulum impactor at 90° into head CG	ES-2RE, 50TH, M	ES2-1, ES2-2, ES2-11, ES2-15, ES2-18
		SID-IIS, 5TH, F	SID2S-1, SID2S-5, SID2S-8, SID2S-13, SID2S-18
		WSID, 50TH, M	W50-11 - W50-15 (5 cases)
		WSID, 5TH, F	WS5-1, WS5-3, WS5-10, WS5-14, WS5-18

[a] (##, ##) indicates the impact parameters (degree offset, percent overlap).

[b] Kinematics scaled to 50TH male using the equal-stress-equal-velocity scaling technique.

Table B.10 — List of IIHS crash tests (n=172) from the human head kinematic data set

Impact condition	Test details[a]	Surrogate[b]	Source #
Frontal	Vehicle into barrier (0˚, 25 %)	H-III, 50TH, M	CEN1219 - CEN1237 (19 cases) CEN1301 - CEN1349 (49 cases) CEN1401 - CEN1416 (16 cases) CEN1418 - CEN1440 (23 cases) CEN1442 - CEN1450 (9 cases) CEN1452, CEN1453 CEN1501 - CEN1512 (12 cases) CEN1514, CEN1515 CEN1518 CEN1539
	Vehicle into barrier (0˚, 40 %)	H-III, 50TH, M	CEF1206 - CEF1208 (3 cases) CEF1301 - CEF1308 (8 cases) CEF1402 - CEF1406 (5 cases) CEF1501
Side	Side impact, 1 500 kg IIHS MDB	SID-IIS, 5TH, F	CES1308 - CES1311 (4 cases) CES1401 (2) - CES1404 (2) (8 cases) CES1405 CES1406 (2) (2 cases) CES1502 CES1308 - CES1311 (4 cases)

[a] (##, ##) indicates the impact parameters (degree offset, percent overlap).

[b] Kinematics scaled to 50TH male using the equal-stress-equal-velocity scaling technique.

Table B.11 — List of biokinetics helmet impactor tests (n=576) from the human head kinematic data set

Impact condition	Test details	Surrogate	Source #
	Padded impact, front of shell	H-III, 50TH, M	H01-55-F, H01-74-F, H01-93-F, H02-55-F, H02-74-F, H02-93-F, H03-55-F, H03-74-F, H03-93-F, H04-55-F, H04-74-F, H04-93-F, H05-55-F, H05-74-F, H05-93-F, H06-55-F, H06-74-F, H06-93-F, H07-55-F, H07-74-F, H07-93-F, H08-55-F, H08-74-F, H08-93-F, H09-55-F, H09-74-F, H09-93-F, H10-55-F, H10-74-F, H10-93-F, H11-55-F, H11-74-F, H11-93-F, H12-55-F, H12-74-F, H12-93-F, H13-55-F, H13-74-F, H13-93-F, H14-55-F, H14-74-F, H14-93-F, H15-55-F, H15-74-F, H15-93-F, H16-55-F, H16-74-F, H16-93-F, H17-55-F, H17-74-F, H17-93-F, H18-55-F, H18-74-F, H18-93-F, H19-55-F, H19-74-F, H19-93-F, H20-55-F-R1-VN1, H20-74-F-R1-VN1, H20-93-F-R1-VN1, H21-55-F-R1-VN1, H21-74-F-R1-VN1, H21-93-F-R1-VN1, H22-55-F-R1-VN1, H22-74-F-R1-VN1, H22-93-F-R1-VN1, H23-55-F-R1-VN1, H23-74-F-R1-VN1, H23-93-F-R1-VN1, H24-55-F-R1-VN1, H24-74-F-R1-VN1, H24-93-F-R1-VN1

Table B.11 *(continued)*

Impact condition	Test details	Surrogate	Source #
Front	Padded impact, lower central face-mask	H-III, 50TH, M	H01-55-AP, H01-74-AP, H01-93-AP, H02-55-AP, H02-74-AP, H02-93-AP, H03-55-AP, H03-74-AP, H03-93-AP, H04-55-AP, H04-74-AP, H04-93-AP, H05-55-AP, H05-74-AP, H05-93-AP, H06-55-AP, H06-74-AP, H06-93-AP, H07-55-AP, H07-74-AP, H07-93-AP, H08-55-AP, H08-74-AP, H08-93-AP, H09-55-AP, H09-74-AP, H09-93-AP, H10-55-AP, H10-74-AP, H10-93-AP, H11-55-AP, H11-74-AP, H11-93-AP, H12-55-AP, H12-74-AP, H12-93-AP, H13-55-AP, H13-74-AP, H13-93-AP, H14-55-AP, H14-74-AP, H14-93-AP, H15-55-AP, H15-74-AP, H15-93-AP, H16-55-AP, H16-74-AP, H16-93-AP, H17-55-AP, H17-74-AP, H17-93-AP, H18-55-AP, H18-74-AP, H18-93-AP, H19-55-AP, H19-74-AP, H19-93-AP, H20-55-AP-R1-VN3, H20-74-AP-R1-VN3, H20-93-AP-R1-VN3, H21-55-AP-R1-VN3, H21-74-AP-R1-VN3, H21-93-AP-R1-VN3, H22-55-AP-R1-VN3, H22-74-AP-R1-VN3, H22-93-AP-R1-VN3, H23-55-AP-R1-VN3, H23-74-AP-R1-VN3, H23-93-AP-R1-VN3, H24-55-AP-R1-VN3, H24-74-AP-R1-VN3, H24-93-AP-R1-VN3
	Padded impact, oblique facemask	H-III, 50TH, M	H01-55-A, H01-74-A, H01-93-A, H02-55-A, H02-74-A, H02-93-A, H03-55-A, H03-74-A, H03-93-A, H04-55-A, H04-74-A, H04-93-A, H05-55-A, H05-74-A, H05-93-A, H06-55-A, H06-74-A, H06-93-A, H07-55-A, H07-74-A, H07-93-A, H08-55-A, H08-74-A, H08-93-A, H09-55-A, H09-74-A, H09-93-A, H10-55-A, H10-74-A, H10-93-A, H11-55-A, H11-74-A, H11-93-A, H12-55-A, H12-74-A, H12-93-A, H13-55-A, H13-74-A, H13-93-A, H14-55-A, H14-74-A, H14-93-A, H15-55-A, H15-74-A, H15-93-A, H16-55-A, H16-74-A, H16-93-A, H17-55-A, H17-74-A, H17-93-A, H18-55-A, H18-74-A, H18-93-A, H19-55-A, H19-74-A, H19-93-A, H20-55-A-R1-VN3, H20-74-A-R1-VN3, H20-93-A-R1-VN3, H21-55-A-R1-VN3, H21-74-A-R1-VN3, H21-93-A-R1-VN3, H22-55-A-R1-VN3, H22-74-A-R1-VN3, H22-93-A-R1-VN3, H23-55-A-R1-VN3, H23-74-A-R1-VN3, H23-93-A-R1-VN3, H24-55-A-R1-VN3, H24-74-A-R1-VN3, H24-93-A-R1-VN3

Table B.11 *(continued)*

Impact condition	Test details	Surrogate	Source #
Oblique	Padded impact, rear boss of shell	H-III, 50TH, M	H01-55-D, H01-74-D, H01-93-D, H02-55-D, H02-74-D, H02-93-D, H03-55-D, H03-74-D, H03-93-D, H04-55-D, H04-74-D, H04-93-D, H05-55-D, H05-74-D, H05-93-D, H06-55-D, H06-74-D, H06-93-D, H07-55-D, H07-74-D, H07-93-D, H08-55-D, H08-74-D, H08-93-D, H09-55-D, H09-74-D, H09-93-D, H10-55-D, H10-74-D, H10-93-D, H11-55-D, H11-74-D, H11-93-D, H12-55-D, H12-74-D, H12-93-D, H13-55-D, H13-74-D, H13-93-D, H14-55-D, H14-74-D, H14-93-D, H15-55-D, H15-74-D, H15-93-D, H16-55-D, H16-74-D, H16-93-D, H17-55-D, H17-74-D, H17-93-D, H18-55-D, H18-74-D, H18-93-D, H19-55-D, H19-74-D, H19-93-D, H20-55-D-R1-VN2, H20-74-D-R1-VN2, H20-93-D-R1-VN2, H21-55-D-R1-VN2, H21-74-D-R1-VN2, H21-93-D-R1-VN2, H22-55-D-R1-VN2, H22-74-D-R1-VN2, H22-93-D-R1-VN2, H23-55-D-R1-VN2, H23-74-D-R1-VN2, H23-93-D-R1-VN2, H24-55-D-R1-VN2, H24-74-D-R1-VN2, H24-93-D-R1-VN2
	Padded impact, side of facemask	H-III, 50TH, M	H01-55-UT, H01-74-UT, H01-93-UT, H02-55-UT, H02-74-UT, H02-93-UT, H03-55-UT, H03-74-UT, H03-93-UT, H04-55-UT, H04-74-UT, H04-93-UT, H05-55-UT, H05-74-UT, H05-93-UT, H06-55-UT, H06-74-UT, H06-93-UT, H07-55-UT, H07-74-UT, H07-93-UT, H08-55-UT, H08-74-UT, H08-93-UT, H09-55-UT, H09-74-UT, H09-93-UT, H10-55-UT, H10-74-UT, H10-93-UT, H11-55-UT, H11-74-UT, H11-93-UT, H12-55-UT, H12-74-UT, H12-93-UT, H13-55-UT, H13-74-UT, H13-93-UT, H14-55-UT, H14-74-UT, H14-93-UT, H15-55-UT, H15-74-UT, H15-93-UT, H16-55-UT, H16-74-UT, H16-93-UT, H17-55-UT, H17-74-UT, H17-93-UT, H18-55-UT, H18-74-UT, H18-93-UT, H19-55-UT, H19-74-UT, H19-93-UT, H20-55-UT-R1-VN4, H20-74-UT-R1-VN4, H20-93-UT-R1-VN4, H21-55-UT-R1-VN4, H21-74-UT-R1-VN4, H21-93-UT-R1-VN4, H22-55-UT-R1-VN4, H22-74-UT-R1-VN4, H22-93-UT-R1-VN4, H23-55-UT-R1-VN4, H23-74-UT-R1-VN4, H23-93-UT-R1-VN4, H24-55-UT-R1-VN4, H24-74-UT-R1-VN4, H24-93-UT-R1-VN4
	Padded impact, upper oblique face-mask	H-III, 50TH, M	H01-55-B, H01-74-B, H01-93-B, H02-55-B, H02-74-B, H02-93-B, H03-55-B, H03-74-B, H03-93-B, H04-55-B, H04-74-B, H04-93-B, H05-55-B, H05-74-B, H05-93-B, H06-55-B, H06-74-B, H06-93-B, H07-55-B, H07-74-B, H07-93-B, H08-55-B, H08-74-B, H08-93-B, H09-55-B, H09-74-B, H09-93-B, H10-55-B, H10-74-B, H10-93-B, H11-55-B, H11-74-B, H11-93-B, H12-55-B, H12-74-B, H12-93-B, H13-55-B, H13-74-B, H13-93-B, H14-55-B, H14-74-B, H14-93-B, H15-55-B, H15-74-B, H15-93-B, H16-55-B, H16-74-B, H16-93-B, H17-55-B, H17-74-B, H17-93-B, H18-55-B, H18-74-B, H18-93-B, H19-55-B, H19-74-B, H19-93-B, H20-55-B-R1-VN4, H20-74-B-R1-VN4, H20-93-B-R1-VN4, H21-55-B-R1-VN4, H21-74-B-R1-VN4, H21-93-B-R1-VN4, H22-55-B-R1-VN4, H22-74-B-R1-VN4, H22-93-B-R1-VN4, H23-55-B-R1-VN4, H23-74-B-R1-VN4, H23-93-B-R1-VN4, H24-55-B-R1-VN4, H24-74-B-R1-VN4, H24-93-B-R1-VN4

Table B.11 *(continued)*

Impact condition	Test details	Surrogate	Source #
Rear	Padded impact, rear of shell	H-III, 50TH, M	H01-55-R, H01-74-R, H01-93-R, H02-55-R, H02-74-R, H02-93-R, H03-55-R, H03-74-R, H03-93-R, H04-55-R, H04-74-R, H04-93-R, H05-55-R, H05-74-R, H05-93-R, H06-55-R, H06-74-R, H06-93-R, H07-55-R, H07-74-R, H07-93-R, H08-55-R, H08-74-R, H08-93-R, H09-55-R, H09-74-R, H09-93-R, H10-55-R, H10-74-R, H10-93-R, H11-55-R, H11-74-R, H11-93-R, H12-55-R, H12-74-R, H12-93-R, H13-55-R, H13-74-R, H13-93-R, H14-55-R, H14-74-R, H14-93-R, H15-55-R, H15-74-R, H15-93-R, H16-55-R, H16-74-R, H16-93-R, H17-55-R, H17-74-R, H17-93-R, H18-55-R, H18-74-R, H18-93-R, H19-55-R, H19-74-R, H19-93-R, H20-55-R-R1-VN2, H20-74-R-R1-VN2, H20-93-R-R1-VN2, H21-55-R-R1-VN2, H21-74-R-R1-VN2, H21-93-R-R1-VN2, H22-55-R-R1-VN2, H22-74-R-R1-VN2, H22-93-R-R1-VN2, H23-55-R-R1-VN2, H23-74-R-R1-VN2, H23-93-R-R1-VN2, H24-55-R-R1-VN2, H24-74-R-R1-VN2, H24-93-R-R1-VN2
Side	Padded impact, side of shell, oblique	H-III, 50TH, M	H01-55-C, H01-74-C, H01-93-C, H02-55-C, H02-74-C, H02-93-C, H03-55-C, H03-74-C, H03-93-C, H04-55-C, H04-74-C, H04-93-C, H05-55-C, H05-74-C, H05-93-C, H06-55-C, H06-74-C, H06-93-C, H07-55-C, H07-74-C, H07-93-C, H08-55-C, H08-74-C, H08-93-C, H09-55-C, H09-74-C, H09-93-C, H10-55-C, H10-74-C, H10-93-C, H11-55-C, H11-74-C, H11-93-C, H12-55-C, H12-74-C, H12-93-C, H13-55-C, H13-74-C, H13-93-C, H14-55-C, H14-74-C, H14-93-C, H15-55-C, H15-74-C, H15-93-C, H16-55-C, H16-74-C, H16-93-C, H17-55-C, H17-74-C, H17-93-C, H18-55-C, H18-74-C, H18-93-C, H19-55-C, H19-74-C, H19-93-C, H20-55-C-R1-VN1, H20-74-C-R1-VN1, H20-93-C-R1-VN1, H21-55-C-R1-VN1, H21-74-C-R1-VN1, H21-93-C-R1-VN1, H22-55-C-R1-VN1, H22-74-C-R1-VN1, H22-93-C-R1-VN1, H23-55-C-R1-VN1, H23-74-C-R1-VN1, H23-93-C-R1-VN1, H24-55-C-R1-VN1, H24-74-C-R1-VN1, H24-93-C-R1-VN1

Table B.12 — List of NBDL human volunteer sled tests (n=335) from the human head kinematic data set

Impact condition	Test details	Surrogate	Source #
		Human volunteer, 118, M	LX3782, LX3796, LX3833, LX3837, LX3856, LX3875, LX3880, LX3886, LX3903, LX3920, LX3945, LX3958, LX3969, LX3985
		Human volunteer, 119, M	LX3785, LX3797, LX3821
		Human volunteer, 120, M	LX3779, LX3793, LX3814, LX3851, LX3878, LX3882, LX3906, LX3921, LX3946, LX3954, LX3972, LX3995
		Human volunteer, 127, M	LX3780, LX3794, LX3812, LX3852, LX3883, LX3893, LX3904, LX3924, LX3949, LX3959
		Human volunteer, 130, M	LX3789, LX3803, LX3839, LX3854, LX3876, LX3889, LX3928, LX3944, LX3991
		Human volunteer, 131, M	LX3783, LX3804, LX3817, LX3840, LX3857, LX3885, LX3894, LX3908, LX3926, LX3948, LX3987, LX3990, LX3999

Table B.12 *(continued)*

Impact condition	Test details	Surrogate	Source #
Frontal	0° Rearward (-GX) sled acc.	Human volunteer, 132, M	LX3788, LX3805, LX3858, LX3887, LX3900, LX3909, LX3927, LX3950, LX3957, LX3982, LX3989, LX3997
		Human volunteer, 133, M	LX3791, LX3798, LX3819, LX3841, LX3869, LX3895, LX3913, LX3939, LX3951, LX3963, LX3986, LX3998
		Human volunteer, 134, M	LX3786, LX3807, LX3822, LX3842, LX3870, LX3890, LX3914, LX3940, LX3961, LX3968, LX3983, LX3993
		Human volunteer, 135, M	LX3800, LX3808, LX3871, LX3898, LX3916, LX3941, LX3955, LX3965, LX3970, LX3994
		Human volunteer, 136, M	LX3801, LX3809, LX3824, LX3872, LX3901, LX3918, LX3942, LX3953, LX3962
		Human volunteer, N/A, M	LX3524, LX3525, LX3530, LX3531, LX3536, LX3537, LX3544, LX3548, LX3550, LX3558, LX3573, LX3578, LX3583, LX3616, LX3815, LX3818
Oblique	45° oblique (-GX, +GY) sled acc.	Human volunteer, 130, M	LX4159, LX4235, LX4260, LX4286, LX4301, LX4309
		Human volunteer, 131, M	LX4161, LX4242, LX4246, LX4251
		Human volunteer, 132, M	LX4162, LX4244, LX4261, LX4287, LX4297, LX4306
		Human volunteer, 133, M	LX4163, LX4236, LX4240
		Human volunteer, 134, M	LX4164, LX4237, LX4264, LX4290, LX4298, LX4307
		Human volunteer, 135, M	LX4166, LX4238, LX4266, LX4314, LX4316
		Human volunteer, 136, M	LX4167, LX4247, LX4263
		Human volunteer, 138, M	LX4168, LX4241, LX4265, LX4284, LX4296, LX4305
		Human volunteer, 139, M	LX4170, LX4243, LX4268, LX4291, LX4303, LX4313
		Human volunteer, 140, M	LX4234, LX4259, LX4269, LX4281, LX4293, LX4302, LX4310
		Human volunteer, 141, M	LX4171, LX4248, LX4270, LX4282, LX4292
		Human volunteer, 142, M	LX4172, LX4249, LX4271, LX4288, LX4295
		Human volunteer, N/A, M	LX2784, LX2786, LX2799, LX2801, LX2813, LX2815, LX2827, LX2843, LX2872, LX2973, LX2979, LX2982, LX2985, LX2988, LX3061, LX3065, LX3077, LX3085, LX3089, LX3093, LX3097, LX3100, LX3102, LX3106, LX3122, LX3129, LX3133, LX3145, LX3148, LX3153, LX3417, LX2763, LX2770, LX2772, LX3049
		Human volunteer, 130, M	LX4050, LX4070, LX4088, LX4107, LX4123, LX4137
		Human volunteer, 131, M	LX4052, LX4071, LX4089, LX4109, LX4124, LX4138
		Human volunteer, 132, M	LX4053, LX4074, LX4090, LX4110, LX4128, LX4143, LX4155
		Human volunteer, 133, M	LX4057, LX4075, LX4093, LX4111, LX4125, LX4151

Table B.12 *(continued)*

Impact condition	Test details	Surrogate	Source #
Side	90° lateral (+GY) sled acc.	Human volunteer, 134, M	LX4054, LX4076, LX4097, LX4112, LX4126, LX4139
		Human volunteer, 135, M	LX4055, LX4078, LX4095, LX4114, LX4131, LX4140
		Human volunteer, 136, M	LX4058, LX4079, LX4098, LX4142, LX4153
		Human volunteer, 138, M	LX4059, LX4080, LX4092, LX4115, LX4129, LX4147
		Human volunteer, 139, M	LX4069, LX4085, LX4100, LX4118, LX4133, LX414
		Human volunteer, 140, M	LX4060, LX4081, LX4099, LX4116, LX4130, LX4145
		Human volunteer, 141, M	LX4068, LX4083, LX4094, LX4134, LX4148
		Human volunteer, 142, M	LX4073, LX4084, LX4104, LX4120, LX4135, LX4149
		Human volunteer, N/A, M	LX1456, LX1504, LX1505, LX1507, LX1509, LX1510, LX1512, LX1513, LX1525, LX1528, LX1785, LX1831, LX1874, LX1916, LX1960, LX1998, LX2010, LX2013, LX2027, LX2032, LX2072, LX2090, LX2102, LX2124, LX2148, LX2151, LX2182, LX2282, LX2302, LX2313, LX2326, LX2338, LX2341, LX2355, LX4119

B.3.3 Crash test data set for the field data evaluation

In order to evaluate the developed tissue-level IRCs, a total of 538 crash tests were used. The crash test data set comprises full engagement, moderate overlap, small overlap and oblique crash tests conducted by NHTSA, IIHS and TC. A break-down of the test conditions is presented in Table B.13. Detailed lists of the data set are presented in Tables B.14 to B.16.

Table B.13 — Summary of the crash test data set

Crash configuration	Driver/ frontal passenger	Test details	Sample size (n=534)
Full engagement	D	NHTSA, full engagement, 56 km/h, H-III	46
	FP	NHTSA, full engagement, 56 km/h, H-III	35
Moderate overlap	D	IIHS, moderate overlap, 64 km/h, H-III	17
	D	TC, moderate overlap, 48-56 km/h, THOR	124
	FP	TC, moderate overlap, 48-56 km/h, THOR	10
Small overlap	D	IIHS, small overlap, 64 km/h, H-III	134
Oblique	D	NHTSA, oblique, 90 km/h, THOR	109
	FP	NHTSA, oblique, 90 km/h, THOR	59

Table B.14 — List of NHTSA crash tests (n=249) from the crash test data set

Crash configuration	Driver/ frontal passenger	Test details	Source #
Full engagement	Driver	Vehicle into barrier (0, 100 %), 56 km/h	3901,3916,3987,4090,4198,4215, 4235,4237,4240,4241,4242,4247, 4250,4251,4252,4259,4264,4273, 4303,5287,5567,5595,5609,5613, 5711,5715, 7966,7977,7978, 7989,8000,8024,8035,8045,8048, 8055,8064,8068,8071,8077,8081, 8091,8106,8151,8153,8156
	Frontal passenger	Vehicle into barrier (0, 100 %), 56 km/h	3901,3915,3952,4090,4198,4205, 4215,4223,4235,4237,4242,4249, 4255,4259,4264,4265,4266,4267, 5301,5594,5595,7977,7989,8024, 8035,8045,8055,8064,8068,8080, 8081,8104,8106,8153,8156
Oblique	Driver	Impactor into vehicle (7, 20 %), (90-98) km/h	7368,7426,7427,7430,7432,7434, 7444,7456,7468
		Impactor into vehicle (15, 18 %), 110 km/h	6855
		Impactor into vehicle (15, 35 %), (90-100) km/h	7366,7428,7429,7431,7433,7441, 7457,7458,7467,7476,7851,7852
		Impactor into vehicle (15, 50 %), (115-126) km/h	6852,6937
		Vehicle into vehicle (15, 50 %), 113 km/h	6830,6831
		Vehicle into vehicle (7, 1), 113 km/h	7292,7293
		RMDB impactor into vehicle (7,20 %), 90 km/h	8510,9207,9209,9210,9213,9216, 9218,9219,9220,9221,9222
		RMDB impactor into vehicle (15,35 %), 90 km/h	8085,8099,8475,8476,8477,8478, 8488,8512,8591,8787,8788,8789, 8791,8998,8999,9042,9043,9110, 9122,9123,9124,9125,9126,9127, 9137,9138,9139,9140,9142,9143, 9144,9145,9146,9148,9149,9150, 9151,9152,9155,9206,9208,9211, 9212,9214,9223,9228,9354,9476, 9477,9478,9479,9480,9481,9482, 9483,9499,9500,9501,9572,9573, 9574,9585,9586,9587,9699,9726, 9727,9802,9804,9806

Table B.14 *(continued)*

Crash configuration	Driver/ frontal passenger	Test details	Source #
	Frontal passenger	RMDB impactor into vehicle (15,35 %), 90 km/h	8085,8099,8478,8488,8787,8788, 8789,8791,8998,8999,9042,9043, 9110,9122,9123,9124,9125,9126, 9127,9135,9137,9138,9139,9140, 9143,9144,9146,9147,9148,9149, 9150,9151,9152,9155,9223,9354, 9476,9477,9478,9479,9480,9481, 9482,9483,9499,9500,9501,9572, 9573,9574,9585,9586,9587,9699, 9726,9727,9802,9804,9806

Table B.15 — List of IIHS crash tests (n=151) from the crash test data set

Crash configuration	Driver/ frontal passenger	Test details	Source #
Moderate overlap	Driver	Vehicle into barrier (0, 40 %), 64 km/h	CEF1206,CEF1207,CEF1208,CEF1301, CEF1302,CEF1303,CEF1304,CEF1305, CEF1306,CEF1307,CEF1308,CEF1402, CEF1403,CEF1404,CEF1405,CEF1406, CEF1501

Table B.15 *(continued)*

Crash configuration	Driver/ frontal passenger	Test details	Source #
Small overlap	Driver	Vehicle into barrier (0, 25 %), 64 km/h	CEN1219,CEN1220,CEN1221,CEN1222,CEN1223,CEN1224,CEN1225,CEN1226,CEN1227,CEN1228,CEN1229,CEN1230, CEN1231,CEN1232,CEN1233,CEN1234, CEN1235,CEN1236,CEN1237,CEN1301, CEN1302,CEN1303,CEN1304,CEN1305, CEN1306,CEN1307,CEN1308,CEN1309, CEN1310,CEN1311,CEN1312,CEN1313, CEN1314,CEN1315,CEN1316,CEN1317, CEN1318,CEN1319,CEN1320,CEN1321, CEN1322,CEN1323,CEN1324,CEN1325, CEN1326,CEN1327,CEN1328,CEN1329, CEN1330,CEN1331,CEN1332,CEN1333, CEN1334,CEN1335,CEN1336,CEN1337, CEN1338,CEN1339,CEN1340,CEN1341, CEN1342,CEN1343,CEN1344,CEN1345, CEN1346,CEN1347,CEN1348,CEN1349, CEN1401,CEN1402,CEN1403,CEN1404, CEN1405,CEN1406,CEN1407,CEN1408, CEN1409,CEN1410,CEN1411,CEN1412, CEN1413,CEN1414,CEN1415,CEN1416, CEN1418,CEN1419,CEN1420,CEN1421, CEN1422,CEN1423,CEN1424,CEN1425, CEN1426,CEN1427,CEN1428,CEN1429, CEN1430,CEN1431,CEN1432,CEN1433, CEN1434,CEN1435,CEN1436,CEN1437, CEN1438,CEN1439,CEN1440,CEN1442, CEN1443,CEN1444,CEN1445,CEN1446, CEN1447,CEN1448,CEN1449,CEN1450, CEN1452,CEN1453,CEN1501,CEN1502, CEN1503,CEN1504,CEN1505,CEN1506, CEN1507,CEN1508,CEN1509,CEN1510, CEN1511,CEN1512,CEN1514,CEN1515, CEN1518,CEN1539

Table B.16 — List of TC crash tests (n=134) from the crash test data set

Crash configuration	Driver/ frontal passenger	Test details	Source #
Moderate overlap	Driver	Vehicle into vehicle (0, 40 %), (48-56) km/h	TC05-254, TC08-107, TC09-027, TC11-008, TC11-225, TC11-233, TC11-234, TC11-239, TC11-501, TC11-504, TC12-002, TC12-003, TC12-005, TC12-006, TC12-009, TC12-209, TC12-209, TC12-218, TC13-007, TC13-024, TC13-035, TC13-036, TC13-110, TC13-119, TC13-202, TC13-223, TC13-301, TC14-003, TC14-012, TC14-015, TC14-035, TC14-140, TC14-141, TC14-143, TC14-144, TC14-174, TC14-214, TC14-216, TC14-218, TC14-220, TC14-228, TC14-229, TC14-231, TC14-232, TC14-235, TC14-237, TC14-502, TC14-504, TC14-507, TC15-024, TC15-034, TC15-035, TC15-108, TC15-120, TC15-123, TC15-127, TC15-138, TC15-155, TC15-159, TC15-162, TC15-163, TC15-208, TC15-210, TC15-504, TC16-001, TC16-003, TC16-016, TC16-017, TC16-018, TC16-019, TC16-020, TC16-021, TC16-125, TC16-152, TC16-204, TC16-205, TC17-001, TC17-012, TC17-013, TC17-017, TC17-025, TC17-028, TC17-029, TC17-030, TC17-031, TC17-032, TC17-033, TC17-034, TC17-035, TC17-201, TC17-202, TC17-203, TC17-206, TC17-208, TC17-209, TC17-210, TC17-211, TC17-212, TC17-505, TC18-014, TC18-017, TC18-018, TC18-019, TC18-030, TC18-031, TC18-034, TC18-036, TC18-201, TC18-204, TC18-206, TC18-207, TC18-208, TC18-209, TC18-211, TC18-212, TC18-214, TC18-215, TC18-216, TC18-217, TC19-004, TC19-005, TC19-006, TC19-007, TC19-008, TC19-010
	Frontal passenger	Vehicle into vehicle (0, 40 %), (48-56) km/h	TC12-209, TC12-218, TC14-174, TC14-216, TC14-231, TC14-235, TC16-002, TC18-036, TC19-006, TC19-010

Annex C
(informative)

Neck

C.1 N_{ij} – data from Reference [12]

Data were published in Reference [52] and reprocessed with different intercepts.

$$N_{ij} = \frac{F_z}{F_{zc}} + \frac{M_y}{M_{yc}}$$

Table C.1 — Data used in Reference [12]

Neck AIS	Peak tension force [N]	Peak extension moment [N·m]	N_{te} Mertz F_{zc} = 1587 N M_{yc} = 20 Nm	N_{te} Eppinger F_{zc} = 2120 N M_{yc} = 27 Nm
0	1 030	5,6	0,93	0,69
0	680	14	1,13	0,84
4	1 925	0	1,22	0,91
0	574	18	1,26	0,94
0	1 460	7,9	1,32	0,98
0	588	20	1,37	1,02
0	960	15,8	1,4	1,04
0	635	20	1,4	1,04
1	805	18	1,41	1,05
0	625	23	1,55	1,15
0	525	26	1,63	1,21
0	525	26	1,63	1,21
0	525	26	1,63	1,21
6	313	29,4	1,67	1,24
0	560	26,4	1,68	1,24
0	855	23	1,69	1,26
6	0	33,9	1,7	1,26
0	1 150	20	1,73	1,28
0	813	25	1,76	1,31
0	813	25	1,76	1,31
4	1 250	20	1,79	1,33
3	1 530	18	1,87	1,39
3	1 445	20	1,91	1,42
4	1 490	20	1,94	1,44
4	1 920	15	1,96	1,46
0	938	30	2,09	1,55
0	1 660	22,6	2,18	1,62
6	0	46,3	2,32	1,71

Table C.1 *(continued)*

Neck AIS	Peak tension force [N]	Peak extension moment [N·m]	N_{te} Mertz F_{zc} = 1587 N M_{yc}= 20 Nm	N_{te} Eppinger F_{zc} = 2120 N M_{yc}= 27 Nm
4	**1 164**	**37,3**	**2,6**	**1,93**
0	**1 254**	**37,8**	**2,68**	**1,99**
6	**760**	**47,5**	**2,86**	**2,12**
5	**1 260**	**46**	**3,1**	**2,30**
5	**3 040**	**24**	**3,12**	**2,32**
2	**943**	**67**	**3,95**	**2,93**
4	**2 960**	**42,4**	**3,99**	**2,97**
3	**1 500**	**66**	**4,25**	**3,15**
4	**1 500**	**66**	**4,25**	**3,15**
4	**2 270**	**64**	**4,63**	**3,44**
6	**2 270**	**64**	**4,63**	**3,44**
6	**2 270**	**64**	**4,63**	**3,44**
3	**2 680**	**63**	**4,84**	**3,60**
5	**4 100**	**80**	**6,59**	**4,90**

C.2 N_{te} – data from Reference [53]

Table C.2 — Data used in Reference [53]

Piglet test	Neck AIS	N_{te}
2 348	0	0,65
2 349	0	0,76
2 247	0	0,79
2 330	1	0,83
2 389	0	0,86
F6	0	0,87
2 296	0	0,89
2 309	0	0,90
2 346	0	0,91
2 255	3	1,01
2 326	0	1,01
2 340	0	1,01
2 344	2	1,01
F1	0	1,03
2 192	5	1,05
2 193	4	1,08
F3	0	1,12
F7	0	1,15
2 182	4	1,16
2 186	3	1,16
2 295	3	1,22
2 299	0	1,24

Table C.2 *(continued)*

Piglet test	Neck AIS	N_{te}
2 133	6	1,27
2 155	4	1,27
2 161	6	1,27
2 203	0	1,27
2 220	0	1,27
2 351	4	1,35
F14	6	1,36
2 343	3	1,38
F12	6	1,54
2 163	5	1,56
F9	4	1,61
F11	6	1,61
F2	0	1,62
2 181	3	1,63
2 162	5	1,90
F4	4	1,94
F8	0	1,96
F10	6	2,69
F5	4	2,76

Annex D
(informative)

Thorax

Table D.1 — Data for maximum deflection and PC-Score

Ref. #	Reference	Test#	Cad ID#	Age	Sex	Height	Mass	NFR	NSFR	UL	UR	LL	LR	Rmax	UP dif	LOW dif
10	Lopez-Valdes 2010	1397	393	59	F	167	80	0	0	3,6	12,6	3	6,6	12,6	10	4,8
		1404	422	60	M	191	81	0	0	3,6	12,6	3	6,6	12,6	10	4,8
		1401	462	69	M	178	84	0	0	3,6	12,6	3	6,6	12,6	10	4,8
11	Lopez-Valdes 2010	1398	393	59	F	167	80	11	NA	14	49,4	12,8	31	49,4	38,3	28,5
		1405	422	60	M	191	81	5	NA	14	49,4	12,8	31	49,4	38,3	28,5
		1402	462	69	M	178	84	13	NA	14	49,4	12,8	31	49,4	38,3	28,5
8	Shaw 2009	1295	403	47	M	177	68	17	8	47,7	16,1	47,4	14,7	47,7	32,3	35,6
		1294	411	76	M	178	70	6	1	47,7	16,1	47,4	14,7	47,7	32,3	35,6
		1358	425	54	M	177	79	10	NA	47,7	16,1	47,4	14,7	47,7	32,3	35,6
		1359	426	49	M	184	76	8	NA	47,7	16,1	47,4	14,7	47,7	32,3	35,6
		1360	428	57	M	175	64	5	NA	47,7	16,1	47,4	14,7	47,7	32,3	35,6
		1379	433	40	M	179	88	8	0	47,7	16,1	47,4	14,7	47,7	32,3	35,6
		1380	441	37	M	180	78	2	0	47,7	16,1	47,4	14,7	47,7	32,3	35,6
		1378	443	72	M	184	81	8	5	47,7	16,1	47,4	14,7	47,7	32,3	35,6
13	NA	S0029	492	66	M	179	70	0	0	26,8	13,4	19,4	14,7	26,8	20	13,9
		S0028	494	59	M	178	68	0	0	26,8	13,4	19,4	14,7	26,8	20	13,9
		S0302	674	67	M	178	72	4	0	26,8	13,4	19,4	14,7	26,8	20	13,9
		S0303	736	67	M	170	70	7	1	26,8	13,4	19,4	14,7	26,8	20	13,9
		S0304	695	74	M	178	73	0	0	26,8	13,4	19,4	14,7	26,8	20	13,9
14	NA	S0313	362	69	M	173	69	7	0	35,8	9,4	36,2	17,5	36,2	27,3	19,3
		S0314	750	66	M	172	76	5	2	35,8	9,4	36,2	17,5	36,2	27,3	19,3
		S0315	767	67	M	177	64	0	0	35,8	9,4	36,2	17,5	36,2	27,3	19,3
2	Kent 2001	580	105	57	M	177	57	0	0	51,3	23,9	39,4	13,5	51,3	33,5	36,8
		579	106	72	F	156	59	11	NA	51,3	23,9	39,4	13,5	51,3	33,5	36,8
		578	107	69	F	155	53	4	NA	51,3	23,9	39,4	13,5	51,3	33,5	36,8
		577	111	57	M	174	70	0	0	51,3	23,9	39,4	13,5	51,3	33,5	36,8
3	NA	652	118	46	M	175	74	0	0	27,2	30,1	19	16,9	30,1	5,4	7,2
		651	121	70	M	176	70	0	0	27,2	30,1	19	16,9	30,1	5,4	7,2
		650	124	40	M	150	47	4	NA	27,2	30,1	19	16,9	30,1	5,4	7,2
4	Kent 2001	665	112	55	M	176	85	3	NA	54,8	22,7	45,7	20	54,8	34,9	37,2
		666	115	69	M	176	84	3	NA	54,8	22,7	45,7	20	54,8	34,9	37,2
		667	120	59	F	161	79	12	NA	54,8	22,7	45,7	20	54,8	34,9	37,2
5	Forman 2006	1094	322	49	M	178	58	0	0	42,7	15,9	36,2	17,1	42,7	28,2	28,1
		1095	323	44	M	172	77	0	0	42,7	15,9	36,2	17,1	42,7	28,2	28,1
		1096	327	39	M	184	79	0	0	42,7	15,9	36,2	17,1	42,7	28,2	28,1
6	Forman 2006	1110	323	44	M	172	77	0	0	51,2	21,7	46,6	17,7	51,2	30,7	36,8

Table D.1 *(continued)*

Ref. #	Reference	Test#	Cad ID#	Age	Sex	Height	Mass	NFR	NSFR	UL	UR	LL	LR	Rmax	UP dif	LOW dif
7	Forman 2009	1262	362	51	M	175	55	9	0	58	28,3	43	14,5	58	41,8	40,7
		1264	367	57	M	179	59	9	0	58	28,3	43	14,5	58	41,8	40,7
		1263	394	57	F	165	109	18	8	58	28,3	43	14,5	58	41,8	40,7
9	Forman 2009	1386	429	67	M	175	71	8	NA	46,7	29	35,2	13,8	46,7	30,3	32,3
		1387	444	69	M	171	60	1	NA	46,7	29	35,2	13,8	46,7	30,3	32,3
		1389	457	72	M	175	73	10	NA	46,7	29	35,2	13,8	46,7	30,3	32,3
12	Kent 2011	1428	461	69	M	175	69	0	0	25,4	29,7	20,8	13,6	29,7	13,6	11,5
		1427	481	72	M	173	88	7	NA	25,4	29,7	20,8	13,6	29,7	13,6	11,5
		1429	482	40	M	186	83	2	NA	25,4	29,7	20,8	13,6	29,7	13,6	11,5

Table D.2 — Data to be added to Table D.1 for TIC

Ref. #	Ref.	Test#	Cad ID#	Age	Sex	Height	Mass	NFR	NSFR	UL	UR	LL	LR	Rmax	UP dif	LOW dif
LAB1	Uriot 2015	SubBIO22	683	55	M	177	92	16	15	32,2	81,7	36,2	52,1	81,7	53,3	30
		SubBIO23	679	86	M	168	67	17	15	32,2	81,7	36,2	52,1	81,7	53,3	30
		SubBIO24	681	87	M	175	77	15	12	32,2	81,7	36,2	52,1	81,7	53,3	30
		SubBIO25	682	87	M	171	64	17	14	32,2	81,7	36,2	52,1	81,7	53,3	30
LAB2	Uriot 2015	SubBIO26	678	85	M	165	79	20	19	33,7	63,9	30,5	84,5	84,5	30,9	58,01
		SubBIO27	677	84	M	170	57	13	8	33,7	63,9	30,5	84,5	84,5	30,9	58,01
		SubBIO28	676	84	M	170	64	13	11	33,7	63,9	30,5	84,5	84,5	30,9	58,01
		SubBIO29	680	89	M	175	77	18	18	33,7	63,9	30,5	84,5	84,5	30,9	58,01
LAB3	Luet 2012	IRIS09	631	67	M	171	59,5	15	3	25,5	53,2	14,7	51,9	53,2	47,2	38,3
		IRIS10	632	85	M	167	69,5	23	23	25,5	53,2	14,7	51,9	53,2	47,2	38,3
		IRIS11	633	76	M	163	54	10	2	25,5	53,2	14,7	51,9	53,2	47,2	38,3
LAB4	Luet 2012	IRIS12	636	77	M	171	61,5	15	9	26,8	63,7	NA	55,8	63,7	49,5	NA
		IRIS13	635	56	F	161	57	19	13	26,8	63,7	NA	56,8	63,7	50,5	NA
		IRIS14	634	68	M	170	79	15	10	26,8	63,7	NA	57,8	63,7	51,5	NA
LAB5	Luet 2012	IRIS15	639	90	M	162	71	21	21	29,9	56,1	21,9	48,6	56,1	46,3	41,9
		IRIS16	638	67	M	170	58	16	9	29,9	56,1	21,9	48,6	56,1	46,3	41,9
		IRIS17	637	79	M	161	57	22	15	29,9	56,1	21,9	48,6	56,1	46,3	41,9
LAB6	Uriot 2015	IRIS39	659	70	M	167	54	12	6	NA	69,7	17,4	54,2	69,7	NA	41,4
		IRIS40	657	88	M	178	90,5	14	12	NA	69,7	17,4	54,2	69,7	NA	41,4
		IRIS41	658	64	M	179	69	14	11	NA	69,7	17,4	54,2	69,7	NA	41,4
LAB7	Uriot 2015	IRIS29	653	75	M	168	57,5	19	18	20,0	58,2	41,2	47,7	58,2	54,4	39,3
		IRIS30	652	63	M	180	70	19	19	20,0	58,2	41,2	47,7	58,2	54,4	39,3
		IRIS31	651	68	M	176	80,5	20	20	20,0	58,2	41,2	47,7	58,2	54,4	39,3
LAB8	Uriot 2015	IRIS32	649	80	M	178	81,5	15	14	31,5	60,2	27,9	55,9	60,2	47,9	31,8
		IRIS33	650	60	M	176	68,5	11	3	31,5	60,2	27,9	55,9	60,2	47,9	31,8
		IRIS34	648	76	M	174	73	13	13	31,5	60,2	27,9	55,9	60,2	47,9	31,8

Table D.2 *(continued)*

Ref. #	Ref.	Test#	Cad ID#	Age	Sex	Height	Mass	NFR	NSFR	UL	UR	LL	LR	Rmax	UP dif	LOW dif
		SEB206	656	83	M	174	76	9	1	54,5	55,9	78,5	68,6	78,5	3,21	10,9
		SEB207	660	89	M	164	65	1	0	45,2	44,8	67,6	60,6	67,6	3,31	10,6
LAB9	Un-published	SEB210	672	83	M	167	67	7	0	39,6	37,4	54,7	52,8	54,7	4,35	6,36
		SEB220	674	81	M	165	79	8	5	44,7	42,5	63,5	56,6	63,5	2,85	8,22
		SEB221	675	91	M	150	54	16	9	49,7	50,2	64,3	61,8	64,3	2,41	3,77
LAB10	Trosseille 2008	SEB144	594	78	M	169	65	8	0	37,0	37,1	59	59,6	59,6	1,93	5,43
	Lebarbe 2005	PCH1624	559	73	M	174	67	11	3	37,0	37,1	59	59,6	59,6	1,93	5,43
		PCH1658	561	72	M	173	83	0	0	37,0	37,1	59	59,6	59,6	1,93	5,43
LAB11	Un-published	SEB159	607	84	M	175	56	18	15	34,7	35,3	63,5	60,0	63,5	2,00	4,70

Annex E
(informative)

Abdomen

Table E.1 — Original data for the abdomen (Reference [32], ramp release tests only)

Test	(dn)max	Abdomen AIS
PAC1.07	0,36	3
PAC1.08	0,37	4
PAC1.09	0,37	0
PAC1.10	0,55	2
PAC1.11	0,32	0
PAC1.12	0,32	2
PAC1.13	0,35	2
PAC1.15	0,4	2
PAC1.16	0,46	3
PAC1.17	0,23	0
PAC1.18	0,26	2
PAC1.20	0,43	3
PAC1.21	0,43	3
PAC1.22	0,39	3
PAC1.23	0,4	2
PAC1.24	0,4	2
PAC1.25	0,42	4
PAC1.26	0,4	3
PAC1.27	0,3	1
PAC1.28	0,42	3
PAC1.29	0,52	3
PAC1.30	0,23	0
PAC1.31	0,37	3
PAC1.32	0,36	0
PAC1.33	0,4	3
PAC1.34	0,45	3
PAC1.35	0,44	3
PAC1.36	0,27	0
PAC1.39	0,46	3
PAC1.41	0,43	3
PAC1.43	0,47	2
PAC1.44	0,56	3
PAC1.45	0,62	4

Annex F
(informative)

Knee-thigh-hip

F.1 Femur force

F.1.1 Objective

The objective of this study was to find the distribution of the biomechanical tolerance limit (the injury risk function) in the adult population for sustaining a AIS2+ KTH injury in a frontal impact (impact at the knee) as a function of individual-related characteristics (age, anthropometry) and specific impact conditions that can be used with the THOR 50th percentile male dummy in frontal impact testing.

The injury criterion used in the injury risk function is the impact force. This study doesn't prove or analyse if the impact force is the best criterion to be used for assessing KTH injuries in frontal impacts.

F.1.2 Data

The scientific literature was searched for publications regarding the injury tolerance of the human knee-thigh-hip complex in dynamic frontal impact tests. From the data found in these scientific publications a comprehensive data set was built that can be used as a basis for developing injury risk functions.

Although no specific selection procedure for the PMHS used in the impact tests was mentioned in the publications, it is obvious that the samples are no random samples from the whole adult population. Therefore, the injury risk function built upon these data includes some selection bias.

The data collected from the scientific literature included tests with embalmed cadavers. Reference [47] found a significant difference in the injury threshold of embalmed and unembalmed cadavers. That is why it was first checked if tests with embalmed cadavers might confound the resulting injury risk function of this study. This was done by calculating a preliminary prediction model and checking if the variable "embalmed" is a significant confounder in the model. The result of this check was that "embalmed" is a significant confounder. This led to the decision to remove all embalmed PMHS from the data set and all subsequent calculations are done on the data set without embalmed PMHS tests.

After excluding the tests with embalmed cadavers, the final data set included tests from the following publications:

1. Reference [48]
2. Reference [27]
3. Reference [88]
4. Reference [5]
5. Reference [58]
6. Reference [41]
7. Reference [6]
8. Reference [11]
9. Reference [55]
10. Reference [92]

Whenever the same tests were reported in multiple publications, only the results of the most recent publication were used (e.g. Reference [71] reanalysed the results of many tests).

Defective data were removed from the data set:

— data from tests with missing impact force data;

— when specimens were tested multiple times until an injury occurred (if no injury occurred in multiple tests the test with the highest impact force without injury was used as right censored observation);

— data from impacts on specimen with low bone quality (osteoporotic bone);

— data from tests were a PCL rupture was found (which shows that there was a substantial load on the tibia);

— data from tests that led to a tibia fracture (which shows that there was a substantial load on the tibia);

— data from tests with implanted load cell in the femur shaft were a femur shaft fracture occurred.

The information about the censoring of the impact force was added in the data set. Exact data was assumed for cases with only femur fractures because a femur fracture leads to a drop in the impact force and the measured maximum force is equal to the fracture force. The assumption of exact data for cases with femur fracture was not checked in this study. Left censoring was used for all cases where a patella fracture or soft tissue injury (cartilage, ligament) occurred and right censoring was used for cases with injury severities lower than AIS2+ or no injury. That is, if a femur fracture together with a patella fracture or soft tissue injury was observed, the data was defined as left censored.

For some of the variables in the data set, values are missing. Figure F.1 shows the number of missing values per variable as well as the combination of missing data, e.g. in three observations stature and mass are missing, in 35 tests only posture is missing.

Simple meaningful variable names were used to describe the variables in the data set. Explanations and units of the variables can be found in Table F.6.

There was no scientific basis for excluding observations from this data set. The resulting final data set (Table F.7) will be used in the modelling process. The final data set is summarized by:

— 175 observations;

— 10 possible predictors (covariates):

  — source, age, stature, mass, gender, side, velocity, configuration, rigid, posture;

— data set includes missing data.

It is important to note that studies mostly used both the left and right femurs. That is, the data set most probably shows less variability than expected from such a sample size. The fracture force of left and right femur from one PMHS differs less than one femur from each of two randomly selected PMHS. Consequently, the resulting confidence intervals will be biased and will indicate a better prediction reliability than there really is.

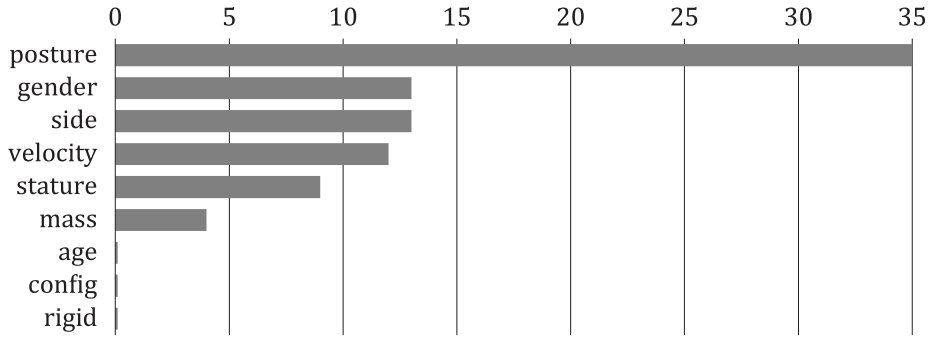

a) Histogram of missing data (count)

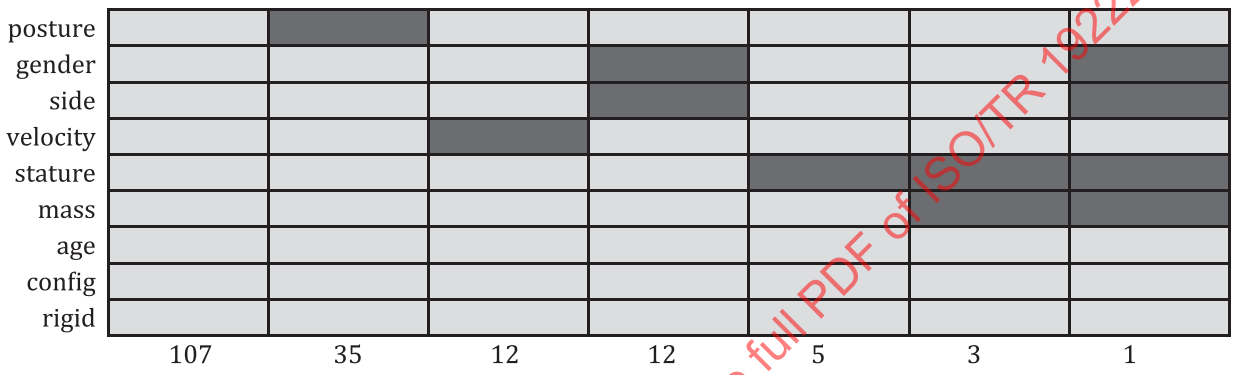

b) Pattern (count)

Figure F.1 — Pattern of missing data

F.1.3 Statistical modelling

For building the injury risk function or prediction model the method of model selection was used. Model selection is a widely used and proven method for finding a good prediction model.

Figure F.2 shows the typical procedure of model selection. This procedure was used in this study with some modifications:

— the distribution assumption was tested at the beginning (this can be justified, because only linear models were looked at);

— candidate models are not explicitly formulated, instead the global model, i.e. a model with all possible predictors was used;

— additivity was not checked because no interaction terms were included in the candidate models;

— predictive ability was not calculated;

— no validity check against field observations was performed.

The data set has missing data, that is why imputation of missing values was needed. For data imputation the method of multiple imputation (utilizing the mice package of R, a free software environment for statistical computing and graphics) was used, which is the preferred method to get unbiased results. The multiple imputation leads to multiple data sets and the modelling approach described in the Figure F.2 needs to be applied to all imputed data sets. Due to the multiple imputation multiple final models are calculated, one model for each imputed data set. To arrive at one final model the modelling results of the imputed data sets are pooled (i.e. averaged) according to the so-called Rubin's Rules.

Rubin's Rules use the law of total variance to calculate the total variance as the sum of a between and within imputation variance.

In a first step in the model selection procedure the best fitting distribution was calculated based on the AICc value for a log-normal, log-logistic and Weibull distribution. In addition, the distribution of the biomechanical tolerance limit was checked against the Non-Parametrical Maximum Likelihood Estimate (NPMLE) to see if the best fitting parametric distribution is a meaningful representation of the underlying data (see Figure F.3).

The log-normal distribution is the best fitting as well as a meaningful distribution for the data at hand. Consequently, all subsequent calculations were performed with the log-normal distribution assumption.

The best predicting model (for each imputed data set) was found by using all subset models from a global model definition, i.e. all combinations of candidate predictors were compared to each other. The prediction performance was evaluated by using the information criterion AICc.

The best model was defined as the model that shows the lowest AICc value and the lowest degree of freedom (lowest number of predictors). That is, first the model with the lowest AICc value and all models with an AICc value differing not more than by 2 from the model with the lowest AICc value were selected. From those models the model with the lowest degree of freedom (lowest number of predictors) was selected.

Candidate predictors of the global model definition were age, stature, mass, gender, velocity, config, rigid and posture.

The variables source and side were not used as candidate predictors because they make no sense in the prediction model.

For each imputed data set the best model was selected by the procedure described above and the overall best model was calculated by pooling the best models from different imputed data sets according to Rubin's Rules.

The effect of some of the covariates were found to be very small. That is, the risk function has been simplified without loss of information. A model with age and impact surface as predictors was found to be reasonable to predict the AIS2+ injury risk for KTH injuries.

Table F.1 shows the coefficients of the resulting model for a 60-year-old person in a padded impact. Figure F.4 is a plot of this injury risk curve.

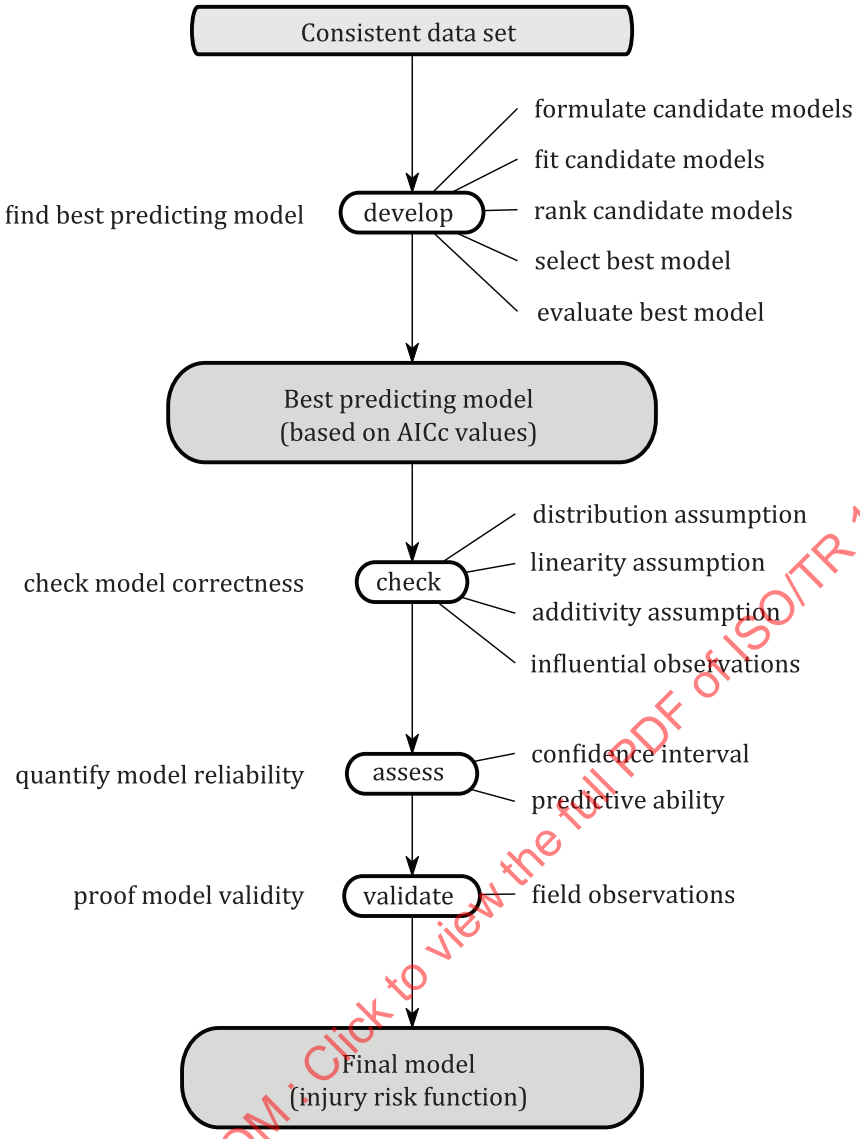

Figure F.2 — Statistical modeling approach

Table F.1 — Coefficients of the injury risk function

	coefs
(Intercept)	10,796 838 6
age	-0,016 166 2
Rigid (yes)	-0,414 277 5
scale	0,671 337 1

Table F.2 — Coefficients of the injury risk function for a 60 years old person in a padded impact

Meanlog	SDlog
9,826 86	0,671 34

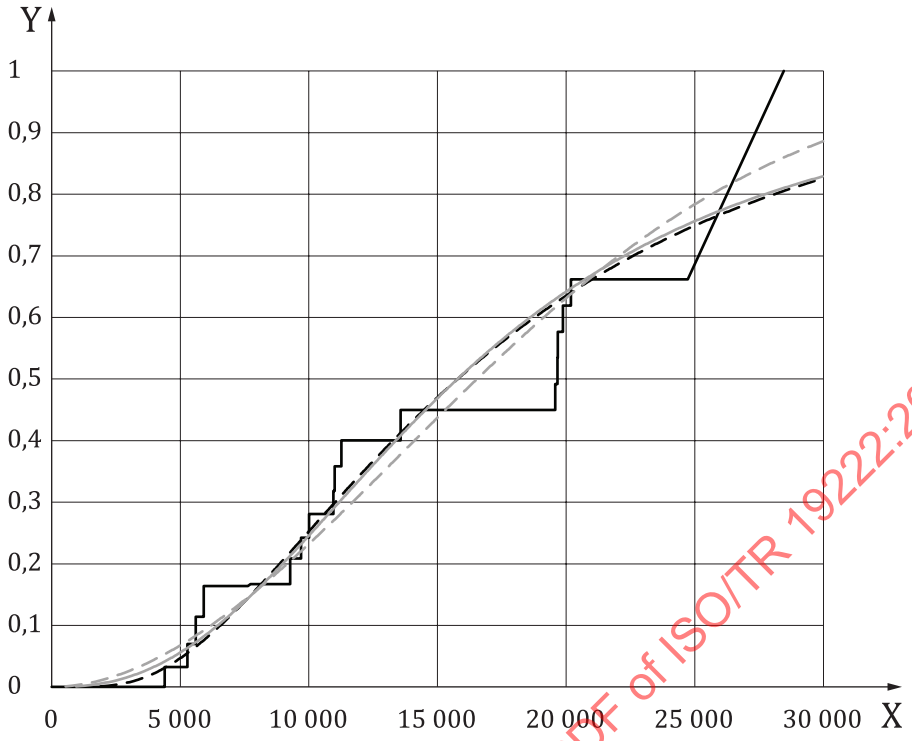

Key

X impact force (N)
Y risk of injury
IRF (NPMLE)
IRF (log-normal)
IRF (log-logistic)
IRF (Weibull)

Figure F.3 — Check of distribution assumption of the model

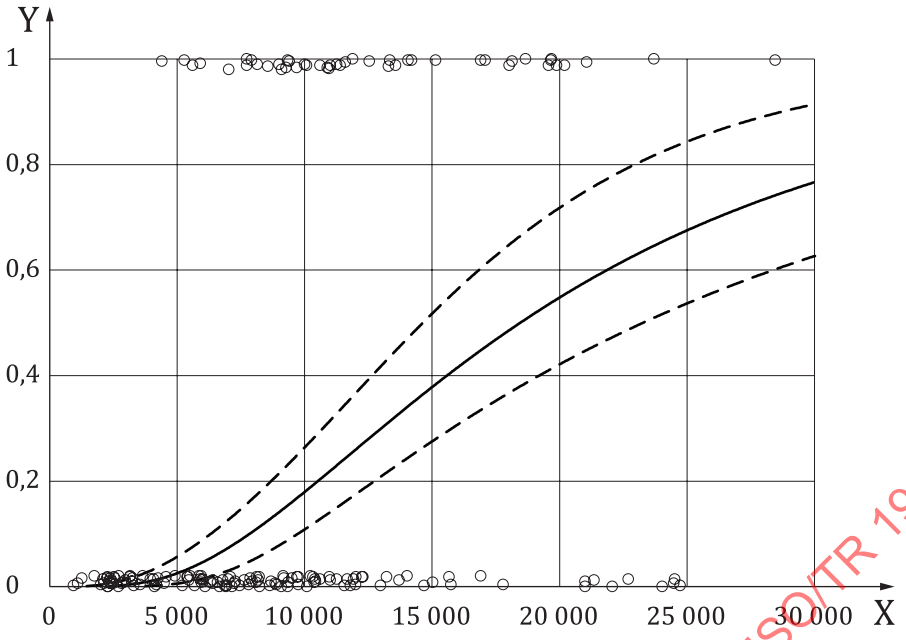

Key

X impact force (N)
Y risk of injury
——— IRF
- - - - CI
○ datapoints

Figure F.4 — Final injury risk curve with 95 % CI at 60 years old, for a padded impact

Table F.3 shows the threshold values for different risks of AIS2+ injury. In addition, the confidence interval bounds are given. The widths of the confidence interval as well as the ratio of the interval widths with respect to the threshold value are also shown.

The relative width is between 0,4 and 0,5. The injury risk curve shows a "good" quality for injury probabilities between 5 % and 50 %.

Table F.3 — Threshold, confidence bounds at specific injury probabilities for a 60 years old person and a padded impact

risk [%]	threshold [N]	lower [N]	upper [N]	width [N]	relative width
5	6 140,2	4 575,7	7 704,7	3 129	0,5
10	7 836,2	6 143,3	9 529,1	3 385,7	0,4
15	9 237,9	7 402,8	11 072,9	3 670,1	0,4
20	10 528,6	8 512,7	12 544,6	4 031,9	0,4
25	11 778,8	9 533,6	14 023,9	4 490,3	0,4
30	13 027,5	10 499,2	15 555,8	5 056,6	0,4
35	14 302,4	11 432,1	17 172,8	5 740,7	0,4
40	15 627,4	12 350,2	18 904,6	6 554,4	0,4
45	17 026,1	1 3269	20 783,2	7 514,2	0,4
50	18 524,8	14 203,1	22 846,5	8 643,4	0,5

The data set used to derive the AIS2+ KTH injury risk function includes some non-injury cases with very high loading. To understand the influence these tests have, non-injury observations with an impact